Characterization of a Putative *Triticum aestivum* Abscisic Acid Receptor and its Role in Fungal Pathogen Resistance

A Thesis Submitted to the College of Graduate Studies and Research in Partial Fulfillment of the Requirements for the Degree of Masters of Science in the Department of Biochemistry
University of Saskatchewan, Saskatoon

By

Cameron Gordon

PERMISSION TO USE

In presenting this thesis in partial fulfillment of the requirements for a Postgraduate degree from the University of Saskatchewan, I agree that the Libraries of this University may make it freely available for inspection. I further agree that permission for copying of this thesis in any manner, in whole or in part, for scholarly purposes may be granted by Dr. Michele Loewen who supervised my thesis work, or in her absence, by the Head of the Department or the Dean of the College in which my thesis work was done. It is understood that any copying or publication of this thesis or parts thereof for financial gain shall not be allowed without my written permission. It is also understood that due recognition shall be given to me and the University of Saskatchewan in any scholarly use which may be made of any materials in my thesis.

Request for permission to copy or make other use of material in this thesis in whole or part should be addressed to:

Head of the Department of Biochemistry

University of Saskatchewan

Saskatoon, Saskatchewan, S7N 5E5

ABSTRACT

Abscisic acid (ABA) has been well defined as an important stress hormone in plants. The signaling pathway of ABA involves a family of pyrabactin resistant-like-1 PYR/PYL/RCAR receptors (PYL receptors) that bind ABA and form a complex with a protein phosphatase 2C (PP2C) family member resulting in downstream signaling events. The ABA receptor family has been well characterized in the model dicot *Arabidopsis thaliana* and more recently this characterization has branched out into cereals *Oryza sativa* (rice) and *Hordeum vulgare* (barley), as well as the monocot model plant *Brachypodium distachyon* and *Fragaria vesca* (strawberry). The analysis of these characterized ABA receptors and the use of online databases has allowed the identification of multiple putative ABA receptors in *Triticum aestivum* (wheat).

ABA has been historically called a positive effector. Overexpression of proteins in the ABA signalling pathway or exogenous application of ABA is known to cause an increase in drought, cold, and salt tolerance. More recently ABA has been linked to increased fungal susceptibility in several plants. The role ABA plays in the biotic stress response is still largely unexplored.

The focus of this project was to identify and characterize a putative wheat ABA receptor through bioinformatics and an *in vitro* enzyme activity assay, and use virus induced gene silencing (VIGS) to test what role this receptor plays in fugal susceptibility. A total of 13 putative ABA receptors were located, nine of which are unique between the wheat subgenomes. One receptor TaPYL5.1 was recombinantly expressed, purified, and confirmed as an ABA receptor through a phosphatase based enzyme activity assay. A receptor with high sequence identity to TaPYL5.1, TaPYL5.2A, was targeted for plant trials because the TaPYL5.1 plasmid sequence was codon

optimized. A VIGS approach was used to knock down TaPYL5.2A *in planta*. The TaPYL5.2A knockdown plants were found to have an increased resistance to *Fusarium* Head Blight progression in the early stages of the disease.

In conclusion, wheat ABA receptors were successfully identified and an important correlation between decreased receptor levels and increased early *Fusarium* Head Blight resistance was found. This correlation however was not easily reproducible due to the severity of coupling VIGS with *Fusarium* Head Blight, and should be followed up with additional studies looking at the broader family of wheat ABA receptors.

ACKNOWLEDGMENTS

I would like to express my gratitude to my supervisor, Dr. Michele Loewen, for her guidance throughout this Master's project. Michele's vision, patience, and support made this project possible. I would like to thank my committee members Dr. Hong Wang, Dr. Chris Todd, and Dr. Stan Moore, for your time, comments, and input over the years. Thanks to my external reviewer Dr. Peta Bonham-Smith for taking the time to go through my research and provide valuable feedback from an outside perspective. A special thanks to past and present Loewen Lab members Dr. Kishore Rajagopalan, Dr. Shawn Clark, Mr. Enwu Liu, Dr. Pooja Choudary, Dr. Olesya Kharenko, Dr. Eddy Risseeuw, and Mr. Fraser Ball for your help and contributions to my project, and also for making my time in the lab a positive and fun experience. I would also like to thank Dr. Sue Abrams and Mr. Ken Nelson for the use of their ABA analogs and acknowledge the National Research Council in Saskatoon for providing me with the best possible facilities, equipment, and financial support to carry out my research.

DEDICATION

I dedicate this thesis to my father Bruce Gordon for all his support over the years and for always encouraging me to go for it.

TABLE OF CONTENTS

LIST OF TABLES

LIST OF FIGURES

LIST OF ABBREVIATIONS

ABA	Abscisic acid
ABF	ABA binding factor
ABI1	Abscisic acid insensitive 1
ABRE	ABA responsive promoter elements
Amp	Ampicillin
BSA	Bovine serum albumin
BSMV	*Barley Stripe Mosaic Virus*
bZIP	Basic leucine zipper
CaMV	*Cauliflower mosaic virus*
CMC	Carboxymethylcellulose
CWSWS	Canadian Western Soft White Spring
$_dH_2O$	Distilled water
DON	Deoxynivalenol
DTT	Dithiothreitol
EDTA	Ethylenediaminetetraacetic acid
ETI	Effector-triggered immunity
FDK	*Fusarium*-damaged kernels
FG	*Fusarium graminearum*
FHB	*Fusarium* Head Blight
GFP	Green fluorescent protein
IPTG	Isopropyl β-D-1-thiogalactopyranoside
IWGSC	International Wheat Genome Sequencing Consortium
JA	Jasmonic acid
LB	Luria Broth

LIC	Ligation independent cloning
MAMPs	Microbe associated molecular patterns
MCS	Multiple cloning site
MES	2-(N-morpholino)-ethanesulfonic acid
NCBI	National Center for Biotechnology Information
PAMPs	Pathogen associated molecular patterns
PDA	Potato dextrose agar
PDB	Protein Data Bank
PDS	Phytoene desaturase
PP2C	Protein Phosphatase 2C
PR	Pathogenesis-related
PTI	PAMP-triggered immunity
PYL	Pyrabactin resistant-like-1
QTL	Quantitative trait loci
ROS	Reactive oxygen species
Rz	Ribozyme sequence
SA	Salicylic acid
SAR	Systemic acquired resistance
SDS	Sodium dodecyl sulfate
SDS PAGE	SDS polyacrylamide gel electrophoresis
SnRK2	SNF1-related protein kinases 2
TBE	Tris/Borate/EDTA
TRSV	*Tobacco Ringspot Virus*
VIGS	Virus induced gene silencing
2X35S	Double 35S promoter

1.0 Introduction

1.1 *Triticum aestivum*

1.1.1 The Importance of Wheat

Triticum aestivum (Bread wheat, wheat) is one of the world's most important cereal grain crops that serves as the staple food source for 30% of the human population (International Wheat Genome Sequencing, 2014). Bread wheat provides approximately 20% of calories consumed by humans (Pfeifer *et al*., 2014). Hexaploid bread wheat accounts for 95% of the wheat grown in the world with the other 5% being tetraploid durum wheat for pasta (Godfray *et al*., 2010). In 2013 wheat accounted for 28.2% of seeded acres in Canadian fields and of that 74% was bread wheat (Statistics Canada, 2014). Wheat is therefore a very important crop for export and the Canadian economy.

1.1.2 Wheat Genomics

The hexaploid bread wheat genome consists of three closely related subgenomes (A, B, and D) that arose from hybridizations of three diploid ancestor species. A clear understanding of their phylogenetic history has been lacking due to *Triticeae* containing at least 80% repetitive DNA (Pfeifer *et al*., 2014; Wicker *et al*., 2011). Having access to the complete wheat genome will be key in allowing researchers to develop high quality feed and food that meet increasing worldwide demand during times of increasing biotic and abiotic stressors. Many of the standard genetic analysis techniques become more difficult when used with bread wheat due to its hexaploid genome. Recently an ordered and structured draft sequence of the bread wheat genome was published, and that study is a major milestone in facilitating the location of important genes, providing a reference for future integration into the more holistic approach of systems biology,

and improving wheat breeding efficiency (International Wheat Genome Sequencing, 2014). Obtaining genomic sequence is the first step in a genomics-oriented approach to biology because genes can be compared to model plants like *Arabidopsis thaliana* (Rensink and Buell, 2004). *Arabidopsis thaliana* is well studied and has been used as the starting point for studies in cereal crops (Zhang *et al*., 2004). The recent genome-wide sequencing of wheat will allow a more in depth look at the major signaling pathways by comparing genetic sequences that are closely related and well characterized in *Arabidopsis*.

1.2 *Fusarium* Head Blight

Fusarium Head Blight (FHB) has been a major factor in worldwide crop loss since the late 1800's and remains one of the most destructive diseases of North American wheat in the last 20 years (De Wolf *et al*., 2003; McMullen *et al*., 1997). FHB is caused by several ascomycete fungi of the genus *Fusarium*, the most common of which in North America being *Fusarium graminearum* (also known as *Gibberella zeae*) (De Wolf *et al*., 2003).

1.2.1 FHB Life Cycle

The life cycle of *Fusarium graminearum* as it interacts with wheat is shown in Figure 1.1. *F. graminearum* is a haploid homothallic ascomycete type fungus. Ascospores originate from perithecium which grow on the mycelium and develop from crop residue through sexual reproduction. Macroconidia are developed through asexual reproduction after one life cycle of the ascospore and will remain on crop residue, producing a mycelium. The airborne ascospores are considered the primary inoculum for the disease; however the relative contributions of conidia versus ascospores is not known (Trail, 2009).

Once inside the spikelet the spores require a period of high humidity for at least 12 hours for spore germination and infection. Temperatures favoring infection range from 16 to 30°C, with the optimum range for *F. graminearum* being 25 to 28°C. If conditions remain warm and moist after seed set, the pathogen may spread to other kernels or heads. FHB infection is most likely to occur when the florets are open during flowering, which allows the spore to come in close proximity to the lemma and palea. The fungus can also enter through wounds caused by hail, birds or insects (Government of Saskatchewan, 2007). When mycelia grow into the host rachis xylem there is a disruption in the water supply to the distal and above areas causing necrosis. The fungus spreads downwards with the help of the virulence factor deoxynivalenol (DON), which also causes necrosis (Jansen *et al*., 2005; Trail, 2009) (Section 1.2.2).

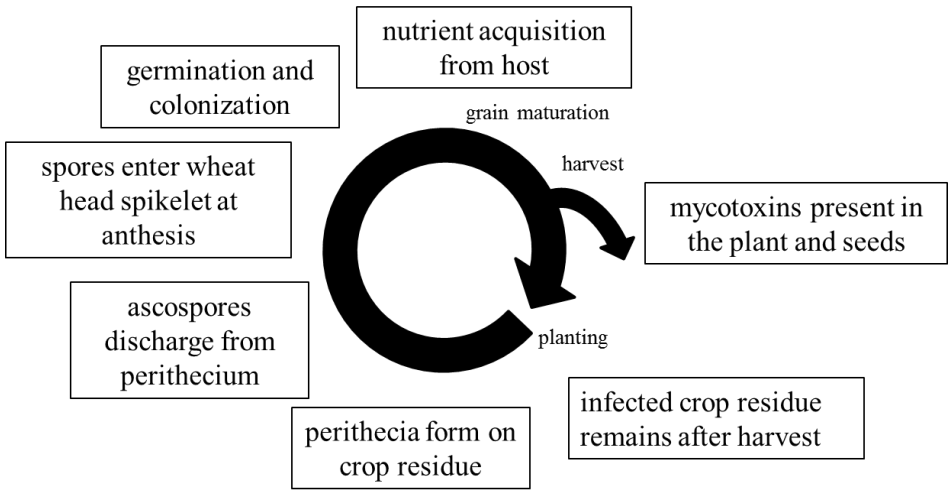

Figure 1.1: The Life Cycle of *Fusarium graminearum*, the Main Agent of *Fusarium* Head Blight of Wheat. FHB is initiated when *F. graminearum* spores enter the wheat head spikelet during anthesis. The spores will germinate during a period of high humidity and colonize the host. *F. graminearum*, a necrotroph, will acquire water and nutrients from the host during spread. The mycotoxin DON which is biosynthesized after the initial infection causes host cell necrosis and remains in infected plants and seed after harvest. Perithecia form on infected crop residue and produce ascospores which are the main inoculum for the disease and complete the cycle (Trail, 2009).

1.2.2 Deoxynivalenol (DON)

After *F. graminearum* spores infect a wheat head, a mycotoxin called DON (Figure 1.2), a sesquiterpenoid fungal metabolite, is produced (McMullen *et al*., 1997; Plattner and Maragos, 2003). As FHB causes a decrease in wheat yield, the accumulation of DON in the soil or plant can also have adverse effects on livestock and human health (Plattner and Maragos, 2003). DON is known to cause vomiting and feed refusal in non-ruminant animals and is a major health risk for humans as well if exposed to levels over 1-2 ppm (Snijders, 1990). DON is important for the spread of FHB as *Fusarium* lines with knocked-out DON biosynthesis can infect the initial spikelet but fail to progress and instead remain contained at point-inoculated sites (Foroud and Eudes, 2009; Jansen *et al*., 2005). There are other mycotoxins produced during infection but the level of DON provides a more precise measurement of mycotoxin contamination in grain (Gautam and Macky, 2011).

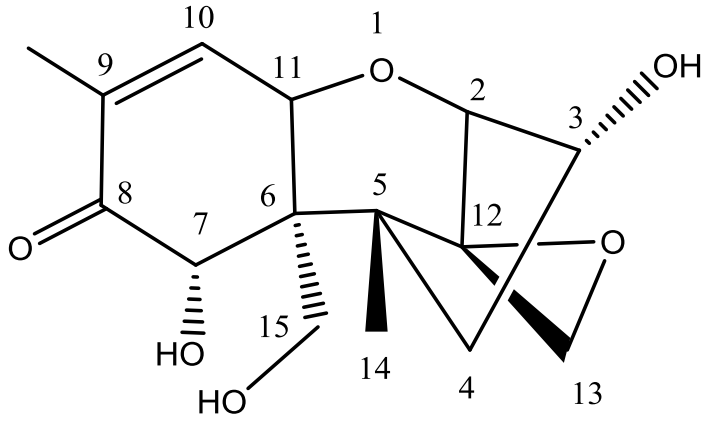

Figure 1.2: The Chemical Structure of the Mycotoxin DON. DON is a naturally occurring mycotoxin and the main toxin produced by *F. graminearum* during FHB infection of wheat. The three hydroxyl groups, the 9-10 double bond, and 12-13 epoxide are all known to be associated with the toxicity of the compound (Kushiro, 2008; Sobrova *et al*., 2010).

1.2.3 Impact of FHB on Wheat

FHB reduces yields and seed quality because of shriveled "tombstone" kernels, contamination with mycotoxins, resulting in reduced market value due to lower grade and test weight (McMullen *et al*., 1997). In Canada, the Canadian Grain Commission measures the percentage of *Fusarium*-damaged kernels (FDK) and DON levels from crop samples across the country and every year publishes its findings (Canadian Grain Commission, 2014). The infection and colonization of wheat by *F. graminearum* is favored by warm temperature and extended periods of moisture around anthesis (Gautam and Macky, 2011), therefore the Grain Commission data can be correlated with Agroclimate data and inferences can be made about cause and severity of FHB outbreaks (Figure 1.3). In spring and early summer 2013, there was a higher than average amount of precipitation recorded in the Canadian prairies (Figure 1.3 D). This precipitation is correlated with higher than average levels of FDK, and DON in samples of Canadian Western Soft White Spring wheat (Figure 1.3 A-C).

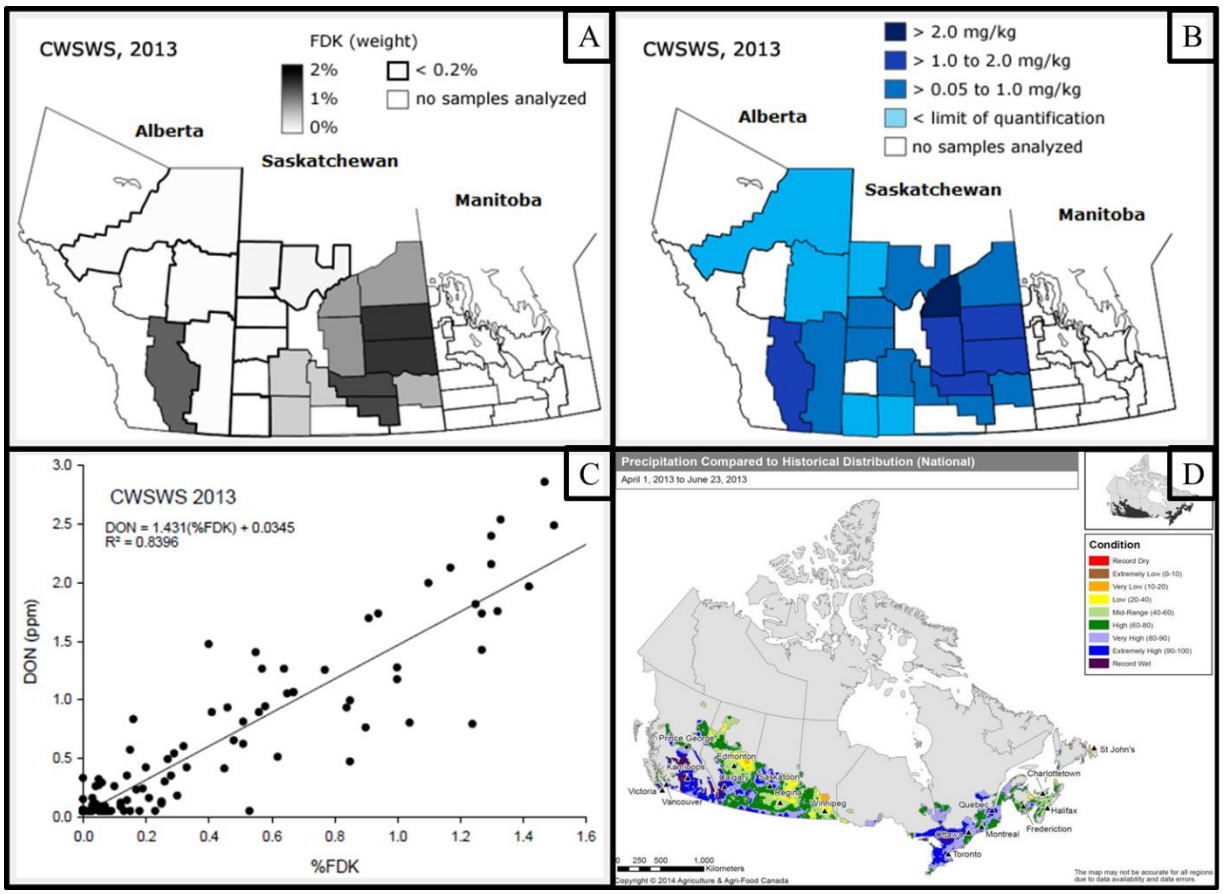

Figure 1.3: FHB Sampling and Precipitation Levels in Western Canada in 2013. (A) Average concentrations of FDK in Canadian Western Soft White Spring (CWSWS). Levels ranged between 0 and 20% FDK by weight with highest levels found in samples from crop districts in southwestern and central Saskatchewan. (B) Average concentrations of DON (mg/kg) in CWSWS collected in Saskatchewan and Alberta prairie crop districts during the 2013 Harvest Sample Program. (C) DON concentrations increased linearly with % FDK for CWSWS samples collected in the 2013 Harvest Sample Program. (D) The 2013 Annual Review of Agroclimate Conditions Across Canada reported High (Green) to Very High (Light Blue) precipitation throughout the Prairie region, and Extremely High (Blue) to Record Wet (Purple) precipitation throughout all of British Columbia, in western Alberta stretching into Saskatchewan from April 13th 2013 to June 23rd, 2013. (AAFC, 2013) (Canadian Grain Commission, 2014). Permission to reproduce from the Canadian Grain Commission.

1.2.4 Plant Disease Responses & Wheat FHB Resistance

Plants face a wide variety of pathogens and their response will depend on the specific pathogen. Accordingly, plants have evolved complex pathogen responses that are both host and non-host specific. Host resistance and non-host resistance are differentiated based on pathogen

adaptation to a specific species and the lack of adaptation to other species. A plant species susceptible to a given pathogen is the host for that pathogen and most pathogens exhibit narrow host specificity and will not infect non-host species. The resistance of plants to the vast majority of potential pathogens is termed non-host resistance (Oh *et al*., 2006). A host specific resistance is the less durable of the two types and involves resistance (R) genes within a single cultivar (Gill *et al*., 2015). Conversely, in non-host resistance the resistance is found across all cultivars and is effective against all races of a particular pathogen. For these reasons, non-host resistance is the more durable of the two. Non-host resistance is further characterized into two types; Type I, which does not result in visible cell death, and Type II, in which a hypersensitive response occurs, resulting in cell death at the site of infection (Oh *et al*., 2006).

Plants possess an immune system that is composed of two branches that are interconnected; PAMP-triggered immunity (PTI), and effector-triggered immunity (ETI) (De Vleesschauwer *et al*., 2014). PTI is triggered by perception of pathogen or microbe associated molecular patterns (PAMPs/MAMPs) and in most cases, PTI is sufficient to impede pathogen colonization. These molecules are present on the surface of the pathogen, or secreted, but absent from the plant and are therefore selected as "non-self" recognition determinants and recognized by Pathogen Recognition Receptors (PRRs) (Deller *et al*., 2011; Schoonbeek *et al*., 2015). Information on *F. graminearum* PAMPs is lacking, however, researchers recently developed a successful bioinformatics approach to locate novel effectors (Sperschneider *et al*., 2013). A transgenic wheat line expressing *Arabidopsis* PRR AtEFR was able to recognize bacterial PAMP elongation factor Tu (EF-Tu) and resist fungal infection highlighting that PTI can be transferred from one non-host plant species to another, even dicot to monocot (Schoonbeek *et al*., 2015).

When successful pathogens bypass the PTI-based response by delivering small effector proteins to the apoplast or the cytosol of host cells, plants have adapted to recognize these pathogen-specific effectors by means of transmembrane or intracellular resistance proteins, triggering the superimposed layer of ETI (De Vleesschauwer *et al*., 2014). Pathogen response often begins with protein-to-protein recognition of the pathogen wherein there is a production of virulence effector proteins, which leads to a reduction of the resistance response from the plant. Recognition of the pathogen will often lead to reactive oxygen species (ROS) production, and the hypersensitive response (Glazebrook, 2005). R gene–mediated resistance is also associated with activation of a salicylic acid (SA)-dependent hormone signaling pathway that leads to expression of certain pathogenesis-related (PR) proteins thought to contribute to resistance (Glazebrook, 2005). During PTI and ETI responses, SA and its conjugates increase, preceding the induction of PR proteins and the onset of systemic acquired resistance (SAR) (De Vleesschauwer *et al*., 2014). SAR is a non-specific, whole plant response, which protects against secondary infection by a pathogen (Fu and Dong, 2013). SAR is a broad spectrum response that can last weeks or months (Fu and Dong, 2013). *F. graminearum* infection has been found to result in systemic PR expression and accumulation of SA in wheat spikes (Makandar *et al*., 2012).

Jasmonic acid (JA) is the key defense hormone against necrotrophic pathogens and in general, defense induction relies on the combined action of JA and ethylene (Browse, 2009). Combinations of ethylene and JA have been found to induce the PR gene superfamily of defense genes (Xu *et al*., 1994). There is evidence showing that many members of the PR superfamily have antifungal activity (Bol *et al*., 1990). Recent studies suggest that JA signaling plays a role in FHB infection in wheat (Makandar *et al*., 2012). FHB resistance has been enhanced when wheat spikes

were sprayed with methyl-JA suggesting that JA contributes to wheat defense against *F. graminearum* (Li and Yen, 2008; Makandar *et al*., 2012).

Various studies have investigated the role of the plant hormone abscisic acid (ABA) (Section 1.3) during plant-pathogen interactions and the results of these studies largely support a negative role to the plant (Cao *et al*., 2011). These include the use of mutants with altered ABA biosynthesis or signaling, as well as exogenous application of ABA. One study found that ABA, whether endogenously synthesized or exogenously applied, could play a role in antagonizing JA-ethylene responsive defense gene expression in *Arabidopsis* (Anderson *et al*., 2004). Other researchers were able to show that ABA signaling negatively regulates resistance to the fungus *Plectosphaerella cucumerina* in *Arabidopsis* (Sanchez-Vallet *et al*., 2012). Sacnhez-Vallet *et al*., (2012) showed that *Arabidopsis* plants impaired in ABA signaling, or biosynthesis were more resistant to the fungus than wild type plants showing a link between ABA signaling and fungal susceptibility. Spraying ABA on rice plants increased the severity of rice blast fungus *M. grisea* infection (Koga *et al.*, 2004). Results from these studies suggest targeting the ABA signaling pathway will modulate FHB resistance in wheat. Likely, there is a lot of hormone cross-talk during plant disease infection, and whether one hormone negatively or positively regulates another depends on the invading pathogen and plant species (De Vleesschauwer *et al*., 2014) such that plant-hormone-pathogen relationships should be studied one at a time.

Wheat resistance to FHB is categorized into five types. Resistance to the initial infection by *F. graminearum* (type I resistance) and resistance to the spread of the fungus within the host head tissue (type II resistance) are accepted as the two main types of resistance (Schroeder and Christensen, 1963). Type I resistance is attributed to morphological traits and is harder to study while Type II resistance is controlled by genes and therefore the easier to study of the two (Zhuang

et al., 2012). Type III is resistance to kernel infection, Type IV is tolerance to infection, and Type V is resistance to DON and other toxin accumulation (Mesterhazy, 1995). FHB resistance has been linked to 100 quantitative trait loci (QTL) in the FHB resistant wheat cultivar Sumai 3 (Nussbaumer et al., 2015). The major FHB resistance QTL *Fhb1* is the most studied with a link to Type II FHB resistance in multiple studies (Buerstmayr *et al*., 2009).

Current understanding of the signaling pathways in wheat that regulate plant defenses to FHB is limited (Makandar *et al*., 2012). An improved understanding of the mechanisms that govern susceptibility and resistance has the potential to provide new tools in the development of FHB-resistant wheat (Foroud *et al*., 2012).

1.3 Abscisic Acid (ABA)

Abscisic acid (ABA; Figure 1.4) is a hormone found in plants that mediates responses to environmental stresses through regulation of signaling events (Christmann *et al*., 2006). ABA is biosynthesized in plant cells through the rate limiting cleavage of C40 epoxy-carotenoid compounds into C25 and C15 products, where the C15 xanthoxins are further processed into ABA (Nambara and Marion-Poll, 2005). The stress-induced biosynthesis of ABA allows plants to survive through periods of drought, cold, and salt stress (Christmann *et al*., 2006; Finkelstein *et al*., 2002). At the same time, ABA also plays important roles in the development of plants, such as seed oil deposition, germination, and dormancy (Finkelstein *et al*., 2002). As well, one of its main functions is the regulation of water and salt levels (Zhu *et al*., 2011). The role of ABA in stress responses was originally demonstrated when reduction of ABA biosynthesis *in planta* was shown to lead to decreased stress tolerance (i.e. decreased growth under stress conditions), which was restored through the addition of exogenous ABA (Zeevaart & Creelman, 1988).

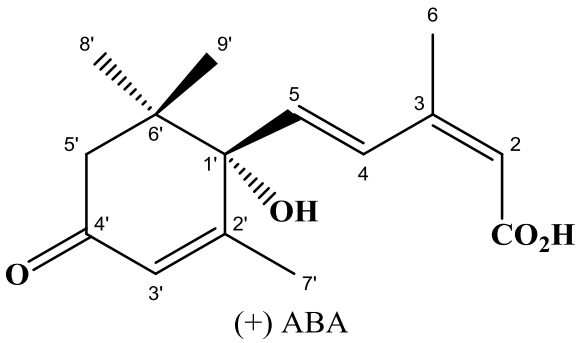

Figure 1.4: The Chemical Structure of (+) Abscisic acid ((+)-ABA).

While it is known that ABA is biosynthesized in plant cells, whether it acts directly in the biosynthetic cells or is secreted and transported and taken up in other locations in the plant remains a question of debate. ABA, a weak acid (pKa = 4.8), is able to permeate through membranes when protonated. Thus movement of ABA into different compartments was therefore thought to be dependent on the pH difference between cellular compartments (Zeevaart & Creelman, 1988)(Finkelstein and Rock, 2002). However more recently, studies have identified three plant ABA transporters, including two ABC transporters and a mitochondrial adenine nucleotide translocator, highlighting protein controlled import and export of ABA across cell membranes (Kang *et al*., 2010; Kharenko *et al*., 2011; Kuromori *et al*., 2010).

1.3.1 ABA Signaling

To date as many as three different types of ABA receptors have been identified (Cutler et al., 2010). This study will focus on the best characterized and soluble family of pyrabactin resistant-like-1 PYR/PYL/RCAR receptors (PYL receptors). PYL receptors are proteins that bind ABA and form a complex with Protein Phosphatase 2C (PP2C) family phosphatases thereby

inhibiting the latter (Figure 1.5). Inhibition of the PP2C allows subsequent autophosphorylation of SnRK2 kinases, which in turn phosphorylate transcription factor ABA Binding Factor (ABF) and leads to transcription from ABA-responsive promoter elements (ABRE) (Figure 1.5). If ABA is absent then the PP2Cs are free to dephosphorylate the SnRK2 kinases, which inhibits the activation of downstream ABA signaling.

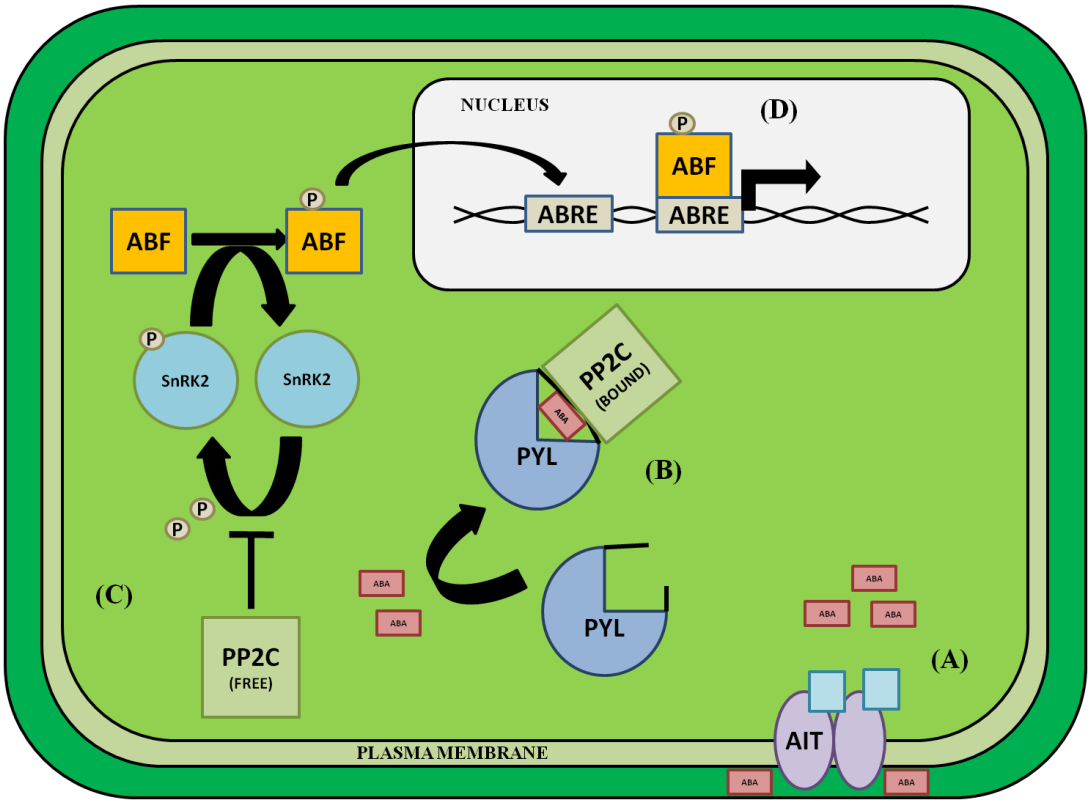

Figure 1.5: ABA Signaling Pathway. (A) ABC transporter ABA-Importing Transporter (AIT) mediates cellular ABA uptake and transports ABA across the plasma membrane. (B) ABA binds the free receptor causing the gating loop to close and expose a hydrophobic binding site where the Protein Phosphatase 2C (PP2C) binds through its active site. (C) In the absence of ABA, PP2C is free to inhibit the autophosphorylation of SnRK2 kinases and no downstream signaling occurs. (D) In the presence of ABA, PP2C binds the receptor/ABA complex which allows SnRK2 kinases to autophosphorylate and subsequently activate downstream basic leucine zipper (bZIP) transcription factors (ABF) by phosphorylation. The transcription factors will bind transcription ABA responsive promoter elements (ABRE) and promote downstream signaling (Boursiac *et al*., 2013; Kanno *et al*., 2012; Lackman *et al*., 2011; Sheard and Zheng, 2009).

The 14-member PYL receptor family has been well characterized in *Arabidopsis*, and reports are now emerging about members of this family of receptors in other species. Thirteen ABA receptors have been identified in rice and are shown to be involved in ABA signaling pathways (He *et al*., 2014; Kim *et al*., 2012). As well, one ABA receptor has been characterized in strawberry (Chai *et al*., 2011), and eight in grape (Boneh *et al*., 2012; Li *et al*., 2012). The PP2C phosphatase family includes six members in *Arabidopsis*: Abscisic Acid Insensitive 1 (ABI1), ABI2, PP2CA/AHG3, AHG1, HAB1, and HAB2, where this family inhibits SnRK2 subclass III kinase activity through dephosphorylation (Umezawa *et al*., 2009). There are also nine PP2C phosphatases that have been identified in grape (Boneh *et al*., 2012) and one in wheat (Nakamura *et al.*, 2007).

1.3.2 ABA Receptor Structure

Researchers have published several different *Arabidopsis* ABA receptor and PP2C structures that are available in the Protein Data Bank. Analysis and comparison of these structures with predicted structures could give insights into structure-function relationships. An ABA bound PYL9 structure has been published (Figure 1.6) along with an Apo-PYL5 structure (Zhang *et al*., 2013).

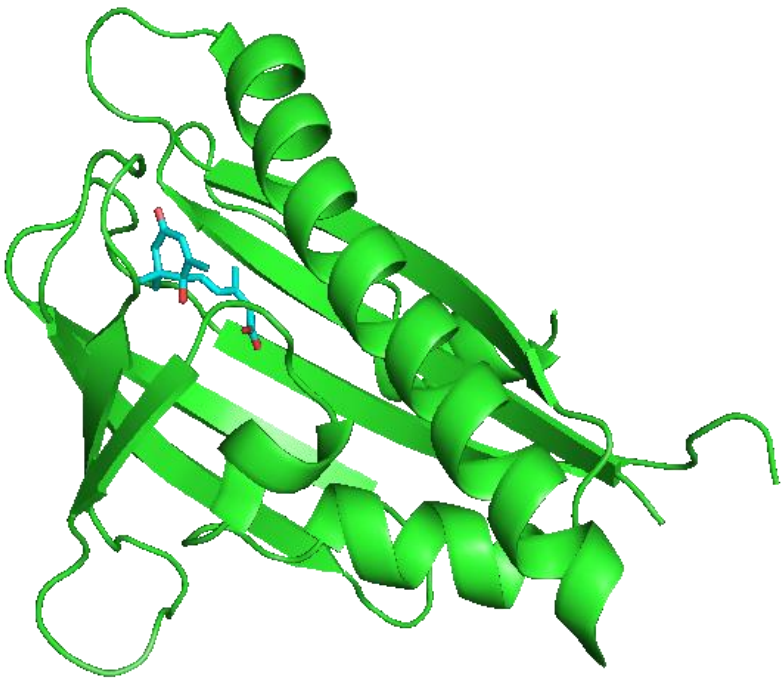

Figure 1.6: Structure of ABA Receptor PYL9 Bound with ABA. The structure of *Arabidopsis* ABA receptor (green) with ABA (blue) in the docking site. Protein data bank accession number 3OQU. Picture generated with PyMOL software and viewer (The PyMOL Molecular Graphics System, Version 1.2r3pre, Schrödinger, LLC) (Zhang *et al*., 2013).

1.3.3 ABA Analogs

Recent studies have shown the potential for screening small molecule libraries for ABA agonists that could be used as treatments during stress as well as a way to characterize the receptors (Cao *et al*., 2013; Okamoto *et al*., 2013). The use of ABA in agriculture is limited due to its instability therefore a synthetic compound that mimics ABA but retains bioactivity for a longer period of time would have commercial value (Ng *et al*., 2014). The discovery of new ABA analogs that mimic ABA actions could lead to important agricultural applications (Cao *et al*., 2013). A new targeted approach that uses ABA analogs has been used to probe the structural elements of *Arabidopsis* ABA receptors (Benson *et al*., 2014). Benson *et al.* (2014) used ABA as a "lead'

molecule to develop potential analogs through structural modifications to the ABA ring (Figure 3.10) and then used the analogs to characterize the multiple ABA receptors and PP2Cs. Another group developed ABA antagonists that were able to block multiple stress-induced *Arabidopsis* ABA responses in vivo (Takeuchi *et al*., 2015; Takeuchi *et al*., 2014). Takeuchi *et al*. (2014) developed a potent ABA antagonist that was validated through physiological, biochemical, and structural analysis.

1.4 Virus Induced Gene Silencing (VIGS)

Gene silencing is a useful tool for functional analysis in hexaploid wheat (Scofield *et al*., 2005). Virus induced gene silencing (VIGS) involves the application of endogenous RNA which invokes an RNA-mediated defense mechanism in plants termed RNA interference. When double stranded RNA is recognized by Dicer-like endonuclease it is cleaved into small interfering RNAs which are then incorporated into the RNA-induced Silencing Complex (RISC) resulting in the targeting of the viral RNA (Lacomme, 2015). In VIGS, a target cDNA sequence fragment is inserted into the viral RNA redirecting the degradation machinery to target the plants own genes resulting in a targeted decrease of gene expression (Figure 1.7) (Purkayastha and Dasgupta, 2009).

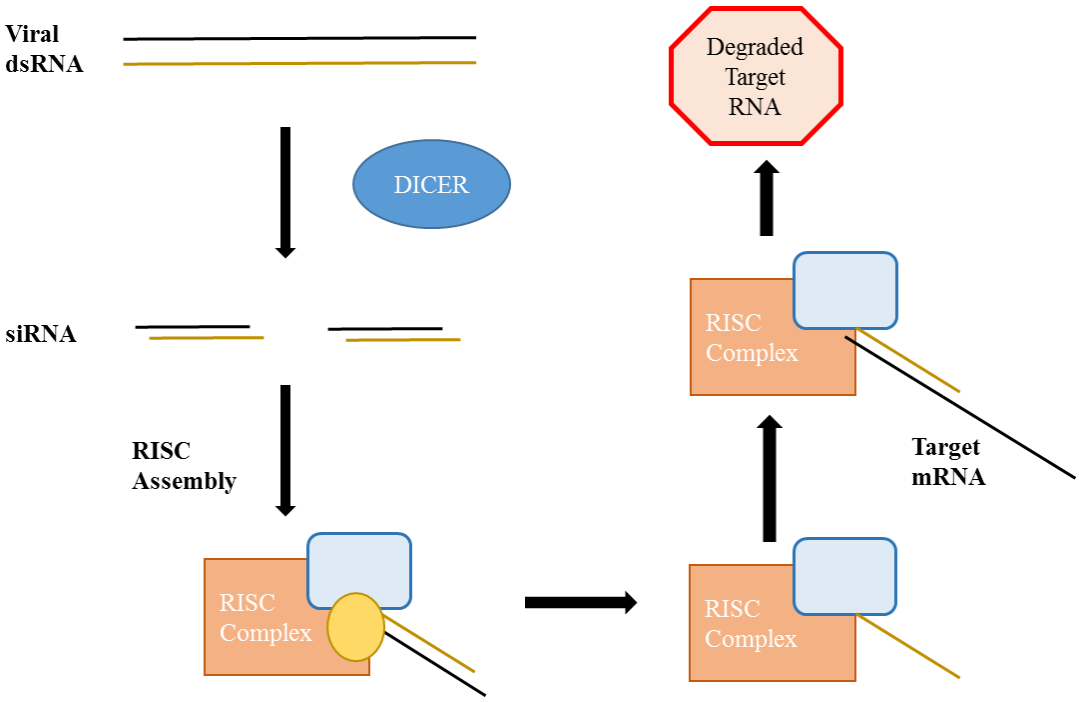

Figure 1.7: Plant Degradation of Viral RNA. Double stranded viral RNA are cleaved into small interfering RNAs (siRNA) by Dicer, which are then incorporated into the RISC. The RISC will unwind the siRNA and become activated. The RISC containing a single strand RNA will then target complementary mRNAs promoting RNA degradation, and translational inhibition. (Lacomme, 2015; Lu *et al*., 2003; Purkayastha and Dasgupta, 2009).

Barley Stripe Mosaic Virus (BSMV) is a positive-sense RNA virus from the *Hordeivirus* genus that has been successfully used to apply VIGS to cereals such as barley and wheat (Scofield *et al*., 2005; Yuan *et al*., 2011). In BSMV-VIGS a 120 to 200 base pair fragment representative of a transcribed sequence from a target plant gene is inserted into the γRNA plasmid (Figure 1.8) (Holzberg *et al*., 2002). An effective use of BSMV-VIGS for functional genomic experiments was developed for wheat (Yuan *et al*., 2011). It relies on an *Agrobacterium tumefaciens* delivery system for BSMV coupled with ligation independent cloning (LIC). The *Agrobacterium* mediated BSMV VIGS vectors were engineered by inserting BSMV cDNA in between a double *Cauliflower mosaic virus* (CaMV) 35S promoter and a ribozyme (Rz) sequence from *Tobacco ringspot virus* (TRSV) satellite RNA (Figure 1.8 B). The LIC site was inserted into BSMV in order to facilitate efficient

cloning of desired gene fragments. The 35S promoter and Rz sites along with the LIC site allows for rapid VIGS analysis of many different gene targets in *N. bethamiana* plants. The pCa-γbLIC vector along with vectors pCaBS-α and pCaBS-β which encode the BSMV α and β genomes, are used to transform *Agrobacterium* which is subsequently used to infect tobacco to elicit VIGS. The high accumulation of the BSMV engineered genome in *N. bethamiana* leaves provides a source for secondary inoculations to elicit VIGS in wheat, which cannot be transformed directly by *Agrobacterium* (Yuan *et al*., 2011).

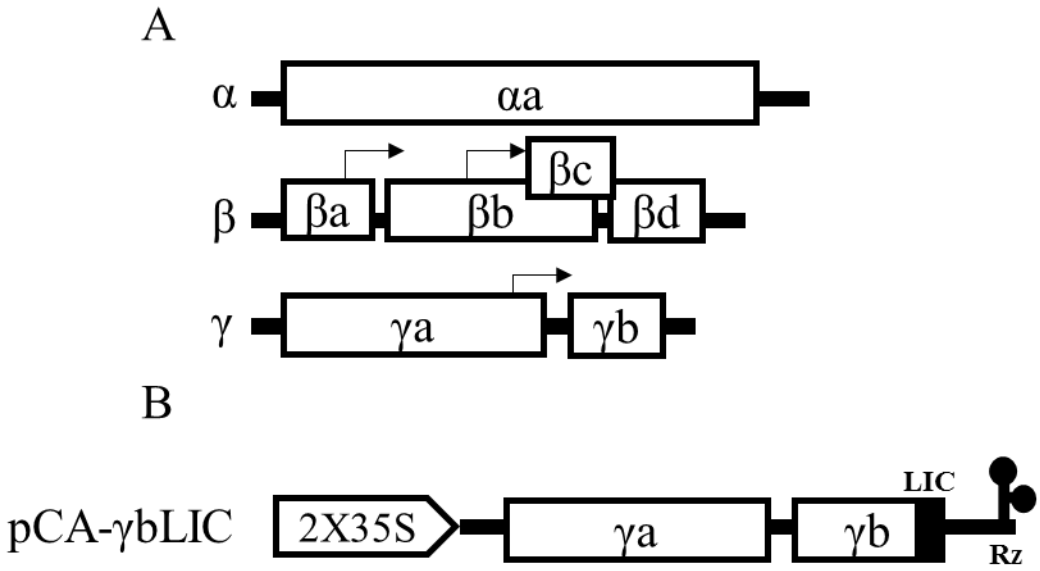

Figure 1.8: A Schematic Representation of the BSMV-VIGS System. (A) A graphic representation of the tripartite BSMV genome organization (Holzberg et al., 2002). (B) The modified pCA-γbLIC construct with the γ BSMV genome inserted between a double *Cauliflower mosaic virus* (CaMV) 35S promoter (2X35S) and the *Tobacco ringspot virus* satellite RNA ribozyme sequence (Rz). The LIC site is inserted downstream of the γb gene keeping the γb intact for proper viral mobility within *N. benthamina* cells (Yuan *et al*., 2011).

1.5 Hypothesis & Objectives

When reviewing studies relating hormone and defense pathways to pathogens it becomes apparent that ABA could play a role either directly or indirectly in the FHB infection of wheat. The ABA signaling pathway in wheat has not been extensively investigated therefore to look at this pathogen-plant relationship it will be necessary to first characterize members of the ABA signaling pathway in order to find targets for future experiments.

1.5.1 Hypothesis

There are ABA receptors in wheat and the knock-down of these ABA receptors will promote FHB disease resistance.

1.5.2 Objectives

(1) Identify a new member of the wheat ABA receptor gene family.

A. Identify the putative ABA receptor family in wheat

B. Characterize one of these receptors for ABA receptor activity *in vitro*.

C. Analyze the ABA binding pocket for differences and similarities between wheat and *Arabidopsis* receptors.

(2) Demonstrate that this family of wheat ABA receptors mediates FHB susceptibility through a targeted gene knock-down approach.

2.0 MATERIALS & METHODS

2.1 Reagents

A list of all reagents and the respective suppliers can found in Table 2.1. A list of all suppliers with location can be found in Table 2.2.

Table 2.1: List of Reagents & Suppliers

2-(N-morpholino)-ethanesulfonic acid (MES)	Sigma Aldrich
4-Methylumbelliferyl phosphate	Sigma Aldrich
ABA Analog PBI352	National Research Council
ABA Analog PBI354	National Research Council
ABA Analog PBI413	National Research Council
ABA Analog PBI414	National Research Council
ABA Analog PBI425	National Research Council
ABA Analog PBI426	National Research Council
ABA Analog PBI514	National Research Council
ABA Analog PBI515	National Research Council
ABA Analog PBI694	National Research Council
ABA Analog PBI695	National Research Council
Absisic Acid (-)	National Research Council
Absisic Acid (+)	Sigma Aldrich
Acetic Acid	Sigma Aldrich
Acetonitrile	Sigma Aldrich
Acetosyringone	Sigma Aldrich
Acrylamide	Bio Rad
Agarose	Bio Shop
Agrobaterium tumeferins	Life Technologies
Ammonium Persulfate	Sigma Aldrich
Ampicillin	Sigma Aldrich
ApaI	Sigma Aldrich
Bacto Tryptone	BD
Batco Yeast Extract	BD
Bio Rad Protein Assay Kit	Bio Rad
Boric Acid	Sigma Aldrich
Bromophenol Blue	Sigma Aldrich
Bovine Serum Albumin	Sigma Aldrich

BSMVγLIC-ccdB	National Research Council (Dr. Clark)
Calcium Chloride	Sigma Aldrich
Carboxymethylcellulose sodium salt	Sigma Aldrich
Chloroform	Fisher Scientific
Coomassie Brilliant Blue R-250	Sigma Aldrich
Deoxynivalenol	Sigma Aldrich
Difco Agar Granulated	BD
Dimethyl Sulfoxide (DMSO)	Sigma Aldrich
Dithiothreitol (DTT)	Life Technologies
Ethylenediaminetetraacetic acid (EDTA)	Sigma Aldrich
Ethanol	Sigma Aldrich
Fast SYBR Green Kit	Life Technologies
Fusarium graminearum Z3639	Agriculture and Agri-Food Canada (Dr. Foroud)
Gel Red	VWR
Glycerol	Sigma Aldrich
Hydrochloric Acid	Sigma Aldrich
Imidazole	Sigma Aldrich
Intercept 60 WP	Bayer Crop Science
Isopropyl β-D-thiogalactopyranoside (IPTG)	BioShop
Isoamyl alcohol	Sigma Aldrich
Kanamycin	Sigma Aldrich
Magnesium Chloride	Sigma Aldrich
Methanol	Fisher Scientific
NEB buffer 2	New England Biolabs
Nickel-NTA resin	Qiagen
pEX-N-His vector PS10030	Origene/Blue Heron
Pfu PCR amplification kit	Thermo Scientific
Phenol	Sigma Aldrich
Piperazine-N,N′-bis(2-ethanesulfonic acid)	Sigma Aldrich
Potato dextrose agar	Sigma Aldrich
Potassium chloride	Fisher Scientific
QIAquick Gel Extraction Kit	Qiagen
QuantiTect Reverse Transcription Kit	Qiagen
Rhapsody	Bayer Crop Science
Rifamycin	Sigma Aldrich
Rnase-Free Dnase Kit	Qiagen
Rneasy Plant Mini Kit	Qiagen
Rosetta (DE3)	Novagen
Sodium dodecyl sulfate (SDS)	Sigma Aldrich

SeeBlue® Plus2 Pre-stained Standard	Invitrogen
Senator 70 WP	Direct Solutions
Seranade	Bayer Crop Science
Silica sand	Sigma Aldrich
Silicon carbide	Sigma Aldrich
Sodium Acetate	Sigma Aldrich
Sodium Chloride	Sigma Aldrich
Sodium Hydroxide	Sigma Aldrich
Sodium phosphate monobasic hydrate	Sigma Aldrich
Streptomycin sulfate	Life Technologies
T4 DNA ligase	Invitrogen
N,N,N',N'-tetramethylethylenediamine	Sigma Aldrich
Tris-HCl	Fisher Scientific
Tris Base	Fisher Scientific
β-mercaptoethanol	Sigma Aldrich

Table 2.2: List of Names & Addresses of Suppliers.

Agriculture and Agri-Food Canada	Lethbridge, Alberta, Canada
Bayer Crop Science	Regina, Saskatchewan, Canada
BD	Mountain View, CA (Clontech)
Bio Rad	Mississauga, Ontario, Canada
Bio Shop	Burlington, Ontario, Canada
Direct Solutions	Calgary, Alberta, Canada
EMD	Toronto, Ontario, Canada
Fisher Scientific	Ottawa, Ontario Canada
Invitrogen/Life Technologies	Carlsbad, California, USA
National Research Council	Saskatoon, Saskatchewan, Canada
New England Biolabs	Whitby, Ontario, Canada
Novagen	Edmonton, Alberta, Canada (VWR)
Origene/Blue Heron	Bothell, Washington, USA
Qiagen	Mississauga, Ontario, Canada
Sigma-Aldrich	Oakville, Ontario, Canada
Stratagene	La Jolla, California, USA
VWR	Edmonton, Alberta, Canada

2.2 Molecular Biology & Protein Analysis

2.2.1 TaPYL5.1/TaABI1

2.2.1.1 Preliminary Bioinformatics

An NCBI BLAST search using the DNA sequence for *Arabidopsis* ABA receptor PYL5 identified a Chinese Spring cDNA clone (>gi|241988461|dbj|AK335719.1| *Triticum aestivum* cDNA, clone: WT013_J18, cultivar: Chinese Spring) encoding a putative wheat ABA receptor TaPYL5.1 (Altschul *et al*., 1990; Coordinators, 2014). A wheat PP2C phosphatase sequence TaABI1 (>gi|147225200|dbj|AB238930.1| *Triticum aestivum* TaABI1 mRNA for protein phosphatase 2C, complete cds) was already annotated and available from NCBI. The TaPYL5.1 sequence was optimized at nine different arginine (R) codons in order to increase the probability of efficient and high yield recombinant expression from *E. coli* without lowering the probability of the same in wheat (Table 2.3). The sequence for TaABI1 was not codon optimized.

Table 2.3: TaPYL5.1 Codon Optimization Table. Columns *E. coli* and *T. aestivum* (1) are the frequencies of the existing codon in their genome. *E. coli* and *T. aestivum* (2) are the frequencies of the optimized R codon that was incorporated into the synthetic TaPYL5.1 gene.

Residue	Codon	*E. coli (1)*	*T. aestivum (1)*	Optimized	*E. coli (2)*	*T. aestivum (2)*
R30	AGG	0.03	0.13	CGC	0.44	0.43
R44	CGG	0.07	0.13	CGC	0.44	0.43
R76	CGG	0.07	0.13	CGC	0.44	0.43
R118	CGG	0.07	0.13	CGC	0.44	0.43
R120	CGG	0.07	0.13	CGC	0.44	0.43
R128	CGG	0.07	0.13	CGC	0.44	0.43
R141	CGG	0.07	0.13	CGC	0.44	0.43
R146	CGG	0.07	0.13	CGC	0.44	0.43
R206	CGG	0.07	0.13	CGC	0.44	0.43

2.2.1.2 Gene Cloning

The putative ABA receptor and PP2C phosphatase genes were synthesized and cloned into the MSC site of the bacterial expression vector pEX-N-His (PS100030, Origene/BlueHeron) (Figure 2.1).

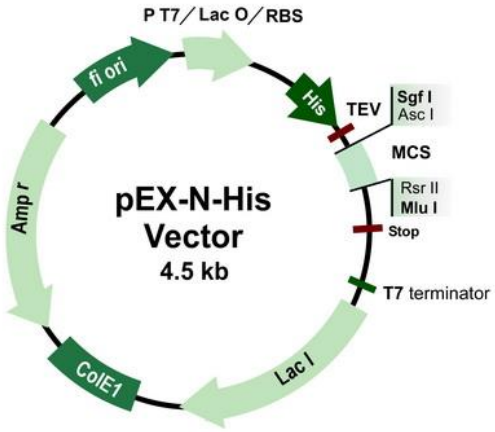

Figure 2.1: The pEX-N-His Vector from BlueHeron/Origene. Genes of interest were cloned into the multiple cloning site (MCS) downstream of the His-tag (His), and TEV protease site (TEV). Gene expression was regulated by the T7 promoter (P T7) under control of the Lac Operon (Lac O) and Ribozome Binding Site (RBS). Included is the ampicillin resistance gene (Amp^r) for positive selection of transformants. The vector catalogue number is PS100020.

2.2.1.3 Competent Cell Preparation

Rosetta (DE3) *E. coli* (Novagen) competent cells were prepared by first inoculating 2 mL of overnight culture in 250 mL Luria Broth (LB) and incubating at 22°C with moderate shaking until the OD_{600} was ~ 0.550 then put on ice for 10 min and then centrifuged at 4000 rpm for 10 min at 4°C. The cells were resuspended in 80 mL ice-cold Inoue buffer (55 mM $MnCl_2$, 15 mM $CaCl_2$, 10 mM KCl, and 10 mM PIPES pH 6.7), and centrifuged at 4000 rpm for 10 min at 4°C. Cells were resuspended in 10 mL ice-cold Inoue buffer by swirling and 1.5 mL of DMSO was slowly added then left on ice for 10 min. Fifty µL aliquots were dispensed into 1.5 µL micro centrifuge tubes, snap frozen in liquid nitrogen, and stored for future transformations (Inoue et al., 1990).

2.2.1.4 Cell Transformation & Protein Expression

Rosetta (DE3) competent cells were thawed on ice and 100 ng of pEX-N-His-TaPYL5.1 was added. The mixture was incubated on ice for 30 minutes and heat shocked at 42°C for 30 seconds. The reaction mix was incubated on ice for 10 minutes and 100 µL were plated on Luria Broth (LB) plates containing 100 µg/mL Ampicillin (Amp) and incubated overnight at 37°C. Overnight starter cultures of LB media with 100 µg/mL Amp were inoculated from single colonies and incubated overnight at 37°C at 120 rpm. These starter cultures were used to inoculate (1:50) fresh cultures in 250 mL Erlenmeyer flasks, which were incubated at 37°C to an OD_{600} of 0.4-0.6 and induced with 1 mM IPTG (or 1% arabinose in certain expression systems, see Section 2.2.2). Induced cultures were further grown for 12 hours at 16°C. Cells were harvested by centrifugation at 4000 rpm for 15 min at 4°C and resuspended in SDS loading buffer for SDS PAGE or protein purification lysis buffer for purification, or stored at -80°C until further analysis.

2.2.1.5 SDS Polyacrylamide Gel Electrophoresis (SDS PAGE) Analysis of Proteins

Over expressed target proteins were visualized with an SDS PAGE method from Molecular Cloning: a laboratory manual (A8.42-A8.47) (Sambrook, 2001). Sample pellets were re-suspended in 2 X SDS gel loading buffer (200 mM β-mercaptoethanol, 100 mM tris-HCl (pH 6.8), 4% SDS, 0.2% bromophenol blue, and 20% glycerol) and incubated at 100°C for 5 minutes. Proteins were resolved on a 5% stacking gel (5% acrylamide, 125 mM tris (pH 6.8), 0.1% SDS, 0.1% ammonium persulfate, 0.1% N,N,N',N-tetramethylethylenediamine) and a 15% resolving gel (15% acrylamide mix, 375 mM tris (pH 8.8), 0.1% SDS, 0.1% ammonium persulfate, 0.04% N,N,N',N'-tetramethylethylenediamine) using a Bio-Rad apparatus and power supply (Bio-Rad) at a constant voltage of 100 volts through the stacking gel and 200 volts through the resolving gel along with a SeeBlue® Plus2 Pre-stained Standard (Invitrogen). The running buffer was composed of 25 mM Tris-HCl, 250 mM glycine (pH 8.3) and 0.1% SDS. Gels were stained with coomassie brilliant blue R-250 0.05% (2.5 g in 450 mL methanol, 100 mL of acetic acid, and 450 mL of distilled water - filtered through a Whatman No 1 filter) and de-stained with a 30% methanol, 10% acetic acid, 60% $_{d}H_2O$ solution.

2.2.1.6 Bradford Protein Concentration Assay

All protein concentrations were determined using the Bio-Rad Protein Assay kit following manufacturer's instructions (Bio-Rad) (Bradford, 1976).

2.2.1.7 Protein Purification with Ni-NTA Column

A Ni-NTA resin column (Invitrogen) was used to purify proteins through His tag affinity. Cell pellets from large 1.5 L induction cultures were re-suspended in 20-30 mL of protein

purification and lysis buffer (100 mM tris-HCl (pH 7.9), 100 mM NaCl, 0.3 mM $MnCl_2$, 4 mM DTT (or 1.4 mM 2-Me)) containing 10 mM imidazole (note that both imidazole and DTT or 2-Me were made and used the same day). Cells were lysed by French Press and the cell lysate was centrifuged at 39,800 x g for 30 minutes at 4°C. Ni NTA resin (50% suspension) was poured into a plastic column and the storage solution was allowed to flow through. The resin was washed three times with 5 mL of lysis buffer containing 10 mM imidazole. The cell lysate supernatant was used to resuspend the washed resin and then incubated at 4°C for 45 minutes with gentle shaking to facilitate protein binding to the column. The flow through was collected, and the column was washed three times with 5 mL lysis buffer containing 20 mM imidazole and collected. Proteins were eluted with lysis buffer containing 150 mM imidazole (two 5 mL elutions).

2.2.1.8 PP2C/Receptor Activity Assays

Proteins were tested for activity using a phosphatase based enzyme assay that relies on fluorescence to determine activity levels (Ma *et al*., 2009). ABA or ABA analogs were available in the lab as a gift from Dr. Suzanne Abrams (University of Saskatchewan; Table 2.1). TaPYL5.1 receptor (0.024 µg/µL final concentration), and TaABI1 phosphatase (0.004 µg/µL final concentration), in a molar ratio of 10:1 receptor to phosphatase, were mixed together in a 50 µL final volume with ABA or ABA analog (0.1 µM) and buffer containing 100 mM Tris pH 7.9, 100 mM NaCl, 0.3 mM $MnCl_2$ and 4 mM DTT. The mixture was incubated for 15 min at 30°C. Fifty µL of substrate (1 mM 4-Methylumbelliferyl phosphate) were added to start the reaction and the assay mix was incubated for 15 min at 30°C. The intensity of the fluorescent product was measured using a Perkin Elmer Victor 3 V 1420 fluorescent plate reader at 15, 30, and 60 min after initiation

of the assay. The excitation wavelength was 355 nm, the emission wavelength was 460 nm, and the measurement time was 0.1 s.

2.2.2 *Arabidopsis* ABA Receptors & PP2C Phosphatases

Various *Arabidopsis* ABA receptor and PP2C phosphatase expression constructs were available for use in the Loewen Lab. Thus, AtPYL5, AtPYL6, AtPYR1, AtABI1, AtABI2, and AtHAB1 were expressed and purified as described in section 2.2.1 with some modifications (Table 2.4).

Table 2.4: Recombinantly Expressed Target Proteins. The eight proteins in this study were expressed with a variety of vectors and *E. coli* strains. Vectors expressed in *E. coli* strains Rosetta (DE3) and BL21 Star (DE3) were induced with 1 mM IPTG and vectors expressed in *E. coli* strain BL21-AI were induced with 1% arabinose. All proteins were purified with the Ni-NTA purification column described in section 2.2.1.7.

Protein	Vector	Strain	Induction
TaPYL5.1	pEX-N-His	ROSETTA (DE3)	IPTG
TaABI1	pEX-N-His	ROSETTA (DE3)	IPTG
AtPYL5	pET 100	BL21 STAR (DE3)	IPTG
AtPYL6	pET 100	BL21 STAR (DE3)	IPTG
AtPYR1	pDEST17	BL21 STAR (DE3)	IPTG
AtABI1	pDEST17	BL21-AI	Arabinose
AtABI2	pDEST17	BL21 STAR (DE3)	IPTG
AtHAB1	pDEST17	BL21-AI	Arabinose

2.3 In Depth Bioinformatics: Online Database Receptor Mining

TaPYL5.1 and all other additional putative wheat ABA receptors were identified using a combination of the National Center for Biotechnology Information database (Benson *et al.*, 2010; Coordinators, 2014), the CerealsDB database (Wilkinson *et al.*, 2012), and the International Wheat Genome Sequencing Consortium database (International Wheat Genome Sequencing, 2014). All DNA sequence was translated to protein using the ExPASy protein translator tool (Artimo *et al*., 2012).

2.4 ABA Receptor Alignments

Multiple DNA and protein sequences were aligned with Clustal Omega using the default settings (Goujon *et al*., 2010; McWilliam *et al*., 2013; Sievers *et al*., 2011).

2.5 ABA Receptor Phylogenetics

Phylogenetic analyses were carried out and tree diagrams produced using Mega 6.0 (Tamura *et al*., 2013)

2.6 Virus Induced Gene Silencing

An ABA receptor target and a control gene were selected to test for physiological relevance using a wheat VIGS knock-down system. Details of the ABA receptor target and its preparation for knockdown can be found below in section 2.6.2 and the following sections. A control VIGS construct was also produced that contained a fragment of the Green Fluorescent Protein (GFP) gene with no relation to wheat.

2.6.1 ABA Receptor Target Gene Selection

Since the original expression vector designed for recombinant expression in *E. coli* was codon optimized, it was necessary to amplify the VIGS gene target sequences from a cDNA library. A cDNA library was prepared using a spikelet from a wild type wheat head, Fielder cultivar (see section 2.10.3 and 2.10.4 for methods). The TaPYL5.2A gene (chromosome 4A) was used as the VIGS knock-down target (Appendix 6.1). TaPYL5.2A has paralogs on chromosomes 4B and 4D that code for proteins with 96.5% and 97.4% identity to TaPYL5.2A respectively. At the gene level these two proteins are 96% and 96.3% identical respectively, so it was expected that the levels of these proteins would be affected similarly to the TaPYL5.2A target during VIGS knockdown. A nucleotide sequence alignment of the three TaPYL5.2 paralogs, and the VIGS insert can be found in the Appendix (6.3).

2.6.2 Primer Selection

Primers were designed using the online Primer3 software (Koressaar and Remm, 2007; Untergasser *et al*., 2012). Primers were found by imputing the TaPYL5.2A gene into the platform with an output length between 180 and 220 base pairs and using the recommended default settings with optimum Tm of 60°C and GC content between 40-60%. Ligation Independent Cloning (LIC) sites had to be manually added to the primer sequences afterwards (5'-AAGGAAGTTTAA-3' onto forward primer and 5'AACCACCACCACCGT-3' onto the reverse primer). The full sequences of the primers including the LIC sequence (underlined) are TaPYL5.2A-F: 5'-AAGGAAGTTTAAGCTGGAGATCCTGGACGAC-3' and TaPYL5.2A-R: 5'-AACCACCACCACCGTGTTGCACTTGACGATGGTGT-3'. All primers were synthesized at the DNA synthesis lab at the National Research Council in Saskatoon.

2.6.3 PCR Amplification of Targets

PCR amplifications were set up with 2.5 µL of each 100 µM primer, 2.5 µL of 10X Pfu turbo buffer, 0.5 µL (~ 50 ng) of cDNA, 0.5 µL of Pfu turbo (2.5 U/µL), 0.3 µL of 2 mM dNTPs mix, and up to 25 µL with sterile $_dH_2O$ (Kit from Thermo Scientific). The PCR steps can be found in Table 2.5.

Table 2.5: PCR amplification steps for VIGS targets. PCR amplifications were completed with a Peltier Thermal Cycler-200.

Step	**Temp**	**Time**
1	95°C	4 min
2	95°C	25 sec
3	58°C	15 sec
4	72°C	25 sec
5	Back to step 2	30 cycles
6	72°C	7 min
7	4°C	Storage

2.6.4 DNA Visualization with Agarose Gels

PCR products were visualized on a 2% Agarose gel prepared with 1 X TBE buffer (5 X; 54 g tris base, 27.5 g boric acid, and 20 mL of 0.5 M EDTA (pH 8.0) up to 1 L) and stained with Gel Red (diluted 20,000X). Gel extractions were carried out with a QIAquick Gel Extraction Kit (Qiagen) according to manufacturer's instructions. A second round of PCR amplification using the same procedure was carried out for the TaPYL5.2A fragment due to a low intensity band after the first round of amplification.

2.6.5 Ligation Independent Cloning

The BSMVγLIC constructs were produced by Shawn Clark at NRC Saskatoon, by following the protocol described in Yuan *et al.* (2011), with some modifications (Figure 2.2). Essentially, a BSMVγLIC plasmid was modified to carry a ccdB cassette that would be lethal to the cell if left intact during un-successful cloning. The first step was the digestion of the BSMVγLIC-ccdB plasmid by adding 5 µg plasmid DNA, 5 µL ApaI buffer, 5 µL ApaI, 0.5 µL BSA into 50 µL (total volume) sterile water and incubating overnight at 25^0C. The overnight digestion was mixed with an equal volume of phenol:chloroform:isoamyl alcohol (25:24:1) and centrifuged at 4500 rpm for 5 min at room temperature. The top layer was transferred to a new tube and extracted with an equal volume of chloroform:isoamyl alcohol (24:1) and centrifuged at 4500 rpm for 5 min at room temperature. The top layer was again transferred to a new tube and 1/10 of a volume 3 M sodium acetate (pH 5.2) and two volumes ice cold ethanol were added and then the mix was incubated on ice for 2 hours. The sample was centrifuged 4500 rpm for 20 min at 4^0C and liquid was carefully removed leaving a DNA pellet in the bottom of the tube. The pellet was washed with 1 mL ice cold 70% ethanol and centrifuged at 4500 rpm for 15 min at 4 ^{0}C. All

traces of ethanol were removed and pellet was air dried at room temperature and resuspended in water. The T4 DNA polymerase treatment of the vector was carried out by adding together 4 µL digested BSMVγLIC plasmid, 2 µL NEB buffer 2, 1 µL dTTP (100 mM), 1 µL DTT (100 mM), 0.2 µL BSA (1000 x), 11.4 µL water, and 0.4 µL T4 DNA polymerase, incubating at room temperature for 30 min and then transferring to 75^{0}C for 20 min to inactivate the enzyme. The PCR product treatment was carried out by adding 4 µL PCR product, 2 µL NEB buffer 2, 1 µL $_d$ATP (100 mM), 1 µL DTT (100 mM), 0.2 µL BSA (1000 x), 11.4 µL water, and 0.4 µL T4 DNA polymerase together and incubating at room temperature for 30 min and then inactivating the polymerase with a 20 min incubation at 75 ^{0}C. The LIC cloning reaction was performed by mixing 1 µL vector DNA, 1 µL insert DNA, and 3 µL water together then incubating the tube at 66 ^{0}C for 2 min and then leaving the reaction at room temperature to cool for 20 min. After bacterial transformation colonies were selected on 50 µg/mL kanamycin LB selection media.

Following receipt of the constructs from Dr. Shawn Clark, the BSMVγLIC-PYL5.2A plasmid was used to transform *Agrobacterium* using an electroporation method. One hundred ng of BSMVγLIC-PYL5.2A was pipetted into 60 µL of electrocompetent *Agrobacterium* and transferred to an electroporation cuvette (0.2 cm). The vial was inserted into a Bio Rad Gene Pulser and pulsed at 2.50 kV for one second. One mL of LB media was added to cells and incubated at 28°C for 4 hours at 200 rpm. Fifty µL of the culture was plated on LB plates containing 50 µg/mL kanamycin and 10 µg/mL rifamycin for selection.

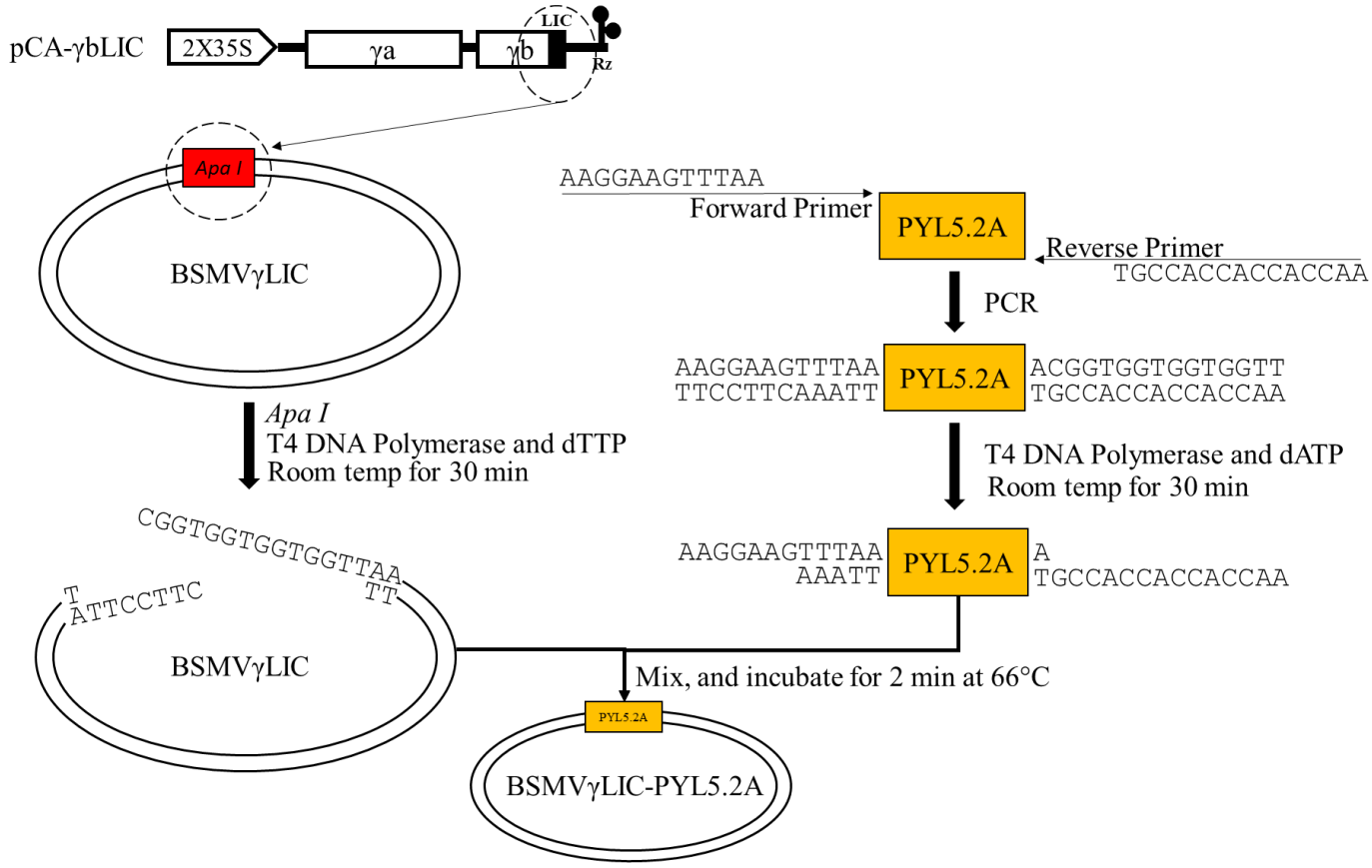

Figure 2.2: Overview of Ligation Independent Cloning Protocol. A 217 bp fragment of *TaPYL5.2A* was amplified from wheat head cDNA and cloned into the BSMVγLIC vector. Protocol and figure based on Yuan *et al*. (2011).

2.6.6 Sequencing

All sequencing was completed by the sequencing facility at the National Research Council of Canada in Saskatoon.

2.6.7 *Nicotiana benthamiana*

The VIGS construct was not directly used to inoculate wheat but instead passed through a *Nicotiana benthamiana* intermediate for amplification. *N. benthamiana* plants are grown under the same conditions as wheat plants (see section 2.7.1) with watering only when the soil was dry.

BSMVγLIC-PYL5.2A, BSMVγLIC-GFP, BSMVβ, BSMVα, and P19 *Agrobacterium* cell lines were used to inoculate 5 mL of LB media and incubated overnight at 28°C. Cultures were centrifuged at 4500 x g for 10 minutes and pellets were resuspended to an OD_{600} of 0.700 in infiltration buffer (10 mM $MgCl_2$, 10 mM 2-(N-morpholino)-ethanesulfonic acid (MES) (pH 5.2), and 0.1 mM acetosyringone). Equal volumes of α, β, γPYL5.2A/γGFP, and P19 were added together and incubated at room temperature for 4 hours. A 1 mL needleless syringe was used to push the assay mix into the abaxial surface of the leaves of 4 week old *N. benthamiana* plants in order to infiltrate them. The *N. benthamiana* plants were left to accumulate the virus in the leaves for 1 week.

2.6.8 VIGS Rub Preparation & Application

Leaves from VIGS TaPYL5.2A and GFP infected *N. benthamiana* plants were ground up with an autoclaved mortar and pestle in phosphate buffer (20 mM sodium phosphate monobasic hydrate (pH 7.2)), silica sand purified by acid, and silicon carbide. Wheat plants were inoculated by pinching and rubbing the *N. benthamiana* VIGS construct preparation on the flag leaf of each tiller 3-5 days before the emergence of the head.

2.7 Wheat Growth

The cultivar Fielder was used for all plant trials. Plants were kept in growth chambers until *Fusarium* trials were initiated. For *Fusarium* trials plants were transported to a high humidity growth chamber capable of >95% humidity. A normal plant trial consisted of 72 plants.

2.7.1 Growth Conditions

Normal growing conditions were 16/8 hour photoperiod, full light; 25 °C day/20 °C night, and relative humidity set at 45%. Plants were watered every day that the soil was observed to be dry (which ranged from every third day as seedlings to every day for adult plants), from the top, including a 20-20-20 NPK fertilizer mix once every week.

2.7.2 Growth Timeline

The overall progression of a plant trial followed a basic timeline (Table 2.6). The plants needed to be closely monitored for deviations from this timeline and adjustments made accordingly.

Table 2.6: Timeline with respective thesis sections for wheat FHB plants trials.

Day	Task	Section Description
1	Wheat Planting	2.7, 2.7.1
33	*N. benthamiana* Seedling Transplant	2.6.7
53	*N. benthamiana* Infiltrations	2.6.8
60	VIGS Rub Inoculation	2.6.8
61	Culture *Fusarium* from Plate	2.8.2
65	Collect and Count *Fusarium* Spores	2.8.3, 2.8.4
67	*Fusarium* Inoculation	2.8.5
67	High Humidity Treatment	2.7
70-99	Phenotyping and Sampling	2.9, 2.9.1, 2.9.2, 2.9.3

2.7.3 Non-target Disease Treatments

To control the spread of *Blumeria graminis* (Powdery Mildew) there could be no standing water in the chambers. Leaves showing colonies of powdery mildew were trimmed and treated with F-mix (20% canola oil, 10% baking soda, and 10% Safer's soap in water) to help control the spread of infection. Senator 70 WP (Direct Solutions) was used for powdery mildew infections (0.65 g/L water) and was applied at the three leaf stage. Also for powdery mildew, Rhapsody (Bayer Crop Science) was used during early stages of disease development at a dilution of 1:100 in water. Seranade ready to spray (Bayer Crop Science) was used with Rhapsody treatments as together they target a larger spectrum of plant diseases. Intercept 60 WP (Bayer Crop Science) was used as a systemic treatment for aphids (0.40 g/L water). Intercept was applied at the two-leaf stage and worked for the life of the plant.

2.8 *Fusarium graminearum* (FG)

2.8.1 FG Strain Z3639

The *F. graminearum* strain used in the plant trials was Z3639 (Bowden and Leslie, 1992).

2.8.2 FG Growth

Mycelium were grown on potato dextrose agar (PDA) plates (Sigma Aldrich) with 50 µg/mL streptomycin-sulfate by placing some mycelium or spores at the center of the plate and incubating at room temperature for 4-7 days (until mycelium covered 2/3 of the plate). The plates were exposed to light for at least 8-12 hours a day. In order to produce liquid spore cultures for wheat head treatments and glycerol stocks a carboxymethylcellulose (CMC) media with 50 µg/mL streptomycin-sulfate was used (1.0 g NH_4NO_3, 1.0 g KH_2PO_4, 0.5 g $MgSO_4$-$7H_2O$, 1.0 g yeast

extract, 15.0 g CMC up to 1 L water, and autoclaved). A 5 mm plug or 100,000 spores was used to inoculate 100 mL of CMC media in a sterile 250 mL flask. The culture was incubated at 27°C at 180 rpm for 4-7 days. The culture was cloudy and a brownish red when ready.

2.8.3 FG Spore Purification

The cultures were shaken aggressively to release macroconidia from the mycelia, and then filtered through four layers of cheese cloth. Spores were collected by centrifugation at 4400 rpm for 10 minutes (removed the supernatant with a pipette or vacuum filtration, washed three times with sterile water). Spores were resuspended in 5 mL of sterile water.

2.8.4 FG Spore Counting

FG spore concentrations were measured using a Burker Turk hemocytometer (In Cyto, Fisher Scientific) according to manufacturer's instructions. Suspensions of spores were diluted to 40,000 – 50,000 macroconida per mL in sterile water. Glycerol stocks were prepared using 0.5 mL of 10^5 FG spore culture in 0.5 mL autoclaved water/glycerol (50/50) mix and stored at -80°C for no longer than 3 months.

2.8.5 FG Inoculations

Wheat heads were inoculated at two different spikelets with 10 µL each of 0.5 x 10^5 spores/mL FG solution. Plants were transferred to a high humidity (> 95 %) chamber for three days to initiate FG infection.

2.9 Wheat Phenotyping

2.9.1 Disease Progression Monitoring

The progression of the FHB disease in knock-down and control plants was monitored at 0, 3, 5, 7, 9, and 13 days past the initial spore inoculation which is also 7, 10, 12, 14, 16, and 20 days past the VIGS knock-down. The number of infected spikelets per head as well as the number of infected rachis nodes per head was monitored. There were 72 plants grown for each plant trial and each plant developed 3-6 tillers. Any tillers that developed late or beyond the six maximum were trimmed to help control powdery mildew infections. Plants were divided evenly into treatment groups and control groups consisting of wild type, wild type-FG, TaPYL5.2A, TaPYL5.2A-FG, GFP, and GFP-FG. The number of infected spikelets per head was measured using all available heads in the respective treatment or control group (n).

2.9.2 Spikelet & Head Sample Selection

Whole heads were collected for DON analysis. Spikelets immediately underneath the initial FG inoculation site were collected for Q-PCR and RNA SEQ analysis. All samples were snap frozen in liquid nitrogen and stored at -80°C until further analysis.

2.10 Quantitative Real Time PCR (Q-PCR)

2.10.1 Sample Preparation

Plant samples were taken at 3, 5, 7, 9 and 13 days past the infection of *Fusarium graminearum* spores which is also 10, 12, 14, 16, and 20 days past the VIGS treatment. Target gene transcript *TaPYL5.2A* levels were measured in TaPYL5.2A, TaPYL5.2A-FG, GFP, and GFP-FG plants.

2.10.2 Gene Target & Control Primers

Primers for visualizing relative expression levels of the target gene *TaPYL5.2A* were chosen by using the basic parameters set by the Step One instrument guide. Primers were designed using the online Primer3 software (Koressaar and Remm, 2007; Untergasser *et al*., 2012). The primer set used for the target was TaPYL5.2A-UTR4_F: CCGTGTCGTGACTCCAGTC, and TaPYL5.2A-UTR4_R: CGCCGAAGAAACACACATCC. This primer set was chosen because it fell outside of the VIGS construct region which is crucial for proper visualization of transcript levels due to the presence of the BSMV virus that contains a fragment of the same gene. The primers were also chosen to target the 3' un-translated region of the gene to decrease the level of non-specific amplification. The endogenous control gene used was *ACTII* (Actin) with the primer set EW412: CAAATCATGTTTGAGACCTTCAATG and EW413: ACCAGAATCCAACACGATACCTG. All primers were synthesized at the DNA synthesis lab at the National Research Council of Canada in Saskatoon.

2.10.3 RNA Preparation

To extract total RNA, the RNeasy Plant Mini Kit was used with the RNase-Free DNase kit following the manufacturer's instruction (Qiagen). DNase was applied to columns between the two RW1 wash steps. After DNase application the column stood for 15 minutes at room temp then the second RW1 wash step carried out. Once RNA was eluted off the column, samples were immediately transferred to ice and the concentration measured with a NanoDrop 8000 (Thermo Scientific) measuring for RNA at 260 nm in 2 µL. The concentration of each sample was taken three times and the average value was used as the actual concentration. RNA was reverse transcribed into cDNA, or stored at -80°C until further analysis.

2.10.4 cDNA Preparation

RNA was reverse transcribed into cDNA using the QuantiTect Reverse Transcription Kit (Qiagen) following manufacturer's instructions complete with a second DNase treatment.

2.10.5 Q-PCR on a Step One Instrument

The Q-PCR analyses were carried out using a StepOnePlus Real Time PCR instrument and accompanying software (Applied Biosystems). cDNA samples were prepared for analysis using the Fast SYBR Green kit (Applied Biosystems) following manufacturer's instructions. SYBR Green reaction mix comprised 1 µL of template, 10 µL 2 X SYBR green master mix, 2 µL forward primer (10 µM), 2 µL reverse primer (10 µM), and 5 µL double distilled nucleotide-free water. The PCR program used was as follows; an initial denaturing step at 95.0°C for 5 minutes followed by 40 amplification cycles at 95.0°C for 20 s and 60°C for 30 s. After completion, a melting curve was constructed as follows; an initial step of 95.0°C for 30 s, 60°C for 1 minute, then 95.0°C for 15 s. To monitor contamination, negative controls using water as a template were performed for each experiment. Each experiment included three biological replicates for each pair of primers.

2.11 Deoxynivalenol Quantification

2.11.1 Sample Preparation

TaPYL5.2A, TaPYL5.2A-FG, GFP, and GFP-FG whole head samples (n=3) were harvested at five and thirteen days past FG infection and ground in liquid nitrogen with an autoclaved mortar and pestle. DON was extracted with 4 mL/g 84% acetonitrile-water extraction solvent by incubating at 1000 rpm for 2 hours at room temperature. Samples are filtered through Whatman No 2 filters and stored in capped brown vials at 4°C until analysis.

2.11.2 Quantification with LC-MS

An aliquot of the extract is diluted 10 fold with 84% acetonitrile-water and DON levels were measured using a Waters LC/MS (Plattner and Maragos, 2003).

2.12 Protein Structure Modeling

A predicted structure of TaPYL5.1 was created using Phyre2 (Jefferys *et al*., 2010; Kelley and Sternberg, 2009; Soding, 2005) and PyMOL (The PyMOL Molecular Graphics System, Version 1.2r3pre, Schrödinger, LLC) software. The structures used for the modeling were all published structures from the Protein Data Bank (Berman *et al*., 2000). Pymol was used to align the different protein structures and overlay the PBI 352 analog on ABA. The protein structure was validated using the Phyre2 validation software and RAMPAGE online software (Kelley and Sternberg, 2009; Lovell *et al*., 2003).

3.0 RESULTS

3.1 Identification of a Putative *T. aestivum* ABA Receptor Gene

The 14 *Arabidopsis* PYL cDNA sequences were used as blast queries against all available wheat sequences in the NCBI database. Only a single putative wheat PYL cDNA was identified from *T. aestivum* (bread wheat; uncharacterized gene, gi 241988461 (accession AK335719)). The coding region of the cDNA was predicted to be 645 base pairs long, encoding a protein of 215 amino acids (Figure 3.1). ClustalW alignments and phylogenetic analyses of the translated amino acid sequence indicated that it is similar to the *Arabidopsis* AtPYL5 receptor (85% coverage and 58% amino acid identity) and was subsequently named TaPYL5.1. Further analyses demonstrate that TaPYL5.1 is most similar to a PYL5-like protein (91% amino acid identity) in the monocot cereal model plant *Brachypodium distachyon*.

```
1  ATGCCGACGCCGTACAGCGCGGCGGCGCTGCAGCAGCACCAGCGTCTGGTC
1  M  P  T  P  Y  S  A  A  A  L  Q  Q  H  Q  R  L  V

52  TCCTCCTCCGGCGGCCTGGCGGCGACGGGGGCCCACAGGTGCGGCGAGCAC
18  S  S  S  G  G  L  A  A  T  G  A  H  R  C  G  E  H

103  GACGGGACGGTGCCGCCGGAGGTGGCGCGGCACCACGAGCACGCGGCGCCG
35   D  G  T  V  P  P  E  V  A  R  H  H  E  H  A  A  P

154  GGGGGGCGCTGCTGCTGCTCGGCGGTGGTGCAGCGCGTGGCGGCGCCGGCG
52  G  G  R  C  C  C  S  A  V  V  Q  R  V  A  A  P  A

205  GCGGACGTGTGGGCCGTGGTCCGGCGCTTCGACCAGCCGCAGGCGTACAAG
69  A  D  V  W  A  V  V  R  R  F  D  Q  P  Q  A  Y  K

256  AGCTTCGTGCGCAGCTGCGCGCTGCTGGACGGCGACGGCGGCGTGGGCACG
86  S  F  V  R  S  C  A  L  L  D  G  D  G  G  V  G  T

307  CTGCGCGAGGTGCGCGTGGTGTCGGGCCTCCCCGCGGCGTCCAGCCGGGAG
103  L  R  E  V  R  V  V  S  G  L  P  A  A  S  S  R  E

358  CGGCTGGAGATCCTGGACGACGAGCGGCACGTGCTGAGCTTCAGCGTGGTG
120  R  L  E  I  L  D  D  E  R  H  V  L  S  F  S  V  V

409  GGCGGCGAGCACCGGCTCCGCAACTACCGGTCGGTGACCACGGTGCACCCG
137  G  G  E  H  R  L  R  N  Y  R  S  V  T  T  V  H  P

460  GCGCCGGGGGAGAGCGCGTCGGCGACGCTGGTGGTGGAGTCGTACGTGGTG
154  A  P  G  E  S  A  S  A  T  L  V  V  E  S  Y  V  V

511  GACGTGCCCCCCGGGAACACGCCCGAGGACACCCGCGTCTTCGTGGACACC
171  D  V  P  P  G  N  T  P  E  D  T  R  V  F  V  D  T

562  ATCGTCAAGTGCAACCTCCAGTCCCTCGCCCGCACCGCCGAGAAGCTCGCC
188  I  V  K  C  N  L  Q  S  L  A  R  T  A  E  K  L  A

613  GGCCGGGGGGCGGCCTACGGCGCGCTGCCGTGA        (645)
205  G  R  G  A  A  Y  G  A  L  P  *          (215)
```

Figure 3.1: TaPYL5.1 cDNA Sequence with Corresponding Protein Sequence. The cDNA coding sequence and predicted translated protein amino acid sequence were produced using NCBI and the EXPASY Translate tool (http://www.ncbi.nlm.nih.gov/protein) (Artimo *et al.*, 2012).

3.2 Analysis of the Wheat ABA Receptor Family

Multiple putative wheat ABA receptors were found using the BLAST tool accessible through the International Wheat Genome Sequencing Consortium website (http://www.wheatgenome.org) (Deng *et al.*, 2007). The genes and proteins were assigned names and numbers as follows. A putative protein was named by taking the name of the *Arabidopsis* receptor with the highest identity when a blastp was performed with the wheat protein sequence against all *Arabidopsis* proteins. Gene names included the wheat genome identifier A, B, or D on it if more information about its location is available. TaPYL5.1 has two homologous genes on chromosomes 2D and 2B, which are named TaPYL5.1D, and TaPYL5.1B respectively. The cDNA coding sequence for TaPYL5.1 was used as a template sequence in the IWGSC BLAST tool either directly or through a *Hordeum vulgare* gene contig intermediate (http://webblast.ipk-gatersleben.de/barley/viroblast.php) (Deng *et al*., 2007). To date, 13 putative wheat ABA receptor sequences have been identified (Appendix 6.1). A large protein sequence alignment of ABA receptors was constructed with Clustal Omega (Goujon *et al*., 2010; McWilliam *et al*., 2013; Sievers *et al*., 2011) (Data not shown). Two wheat receptors, TaPYL4.1 and TaPYL4.2, were omitted from the alignment due to having too low sequence identity and making future phylogenetic analysis problematic. A total of 77 ABA receptor sequences from various monocot and dicot plant species were used for the alignment, including 14 *Arabidopsis* (At), 10 Rice (Os), 11 wheat (Ta), 10 strawberry (Fv), nine chickpea (Ca), six soybean (Gm), six tomato (Sl), one potato (St), six grape (Vv), and four *Brachypodium* (Bd) sequences. The protein alignment was used to perform a phylogenetic analysis and construct a neighbor-joining tree (Figure 3.2). The phylogenetic tree highlights three different clades that receptors fall into based upon their sequence identity. The membership in a certain clade gives insights into potential activity levels, PP2C

preference, and preference for monomeric versus dimeric configuration. Most of the wheat ABA receptors located to date are contained within clade II (Ma *et al*., 2009; Szostkiewicz *et al*., 2010).

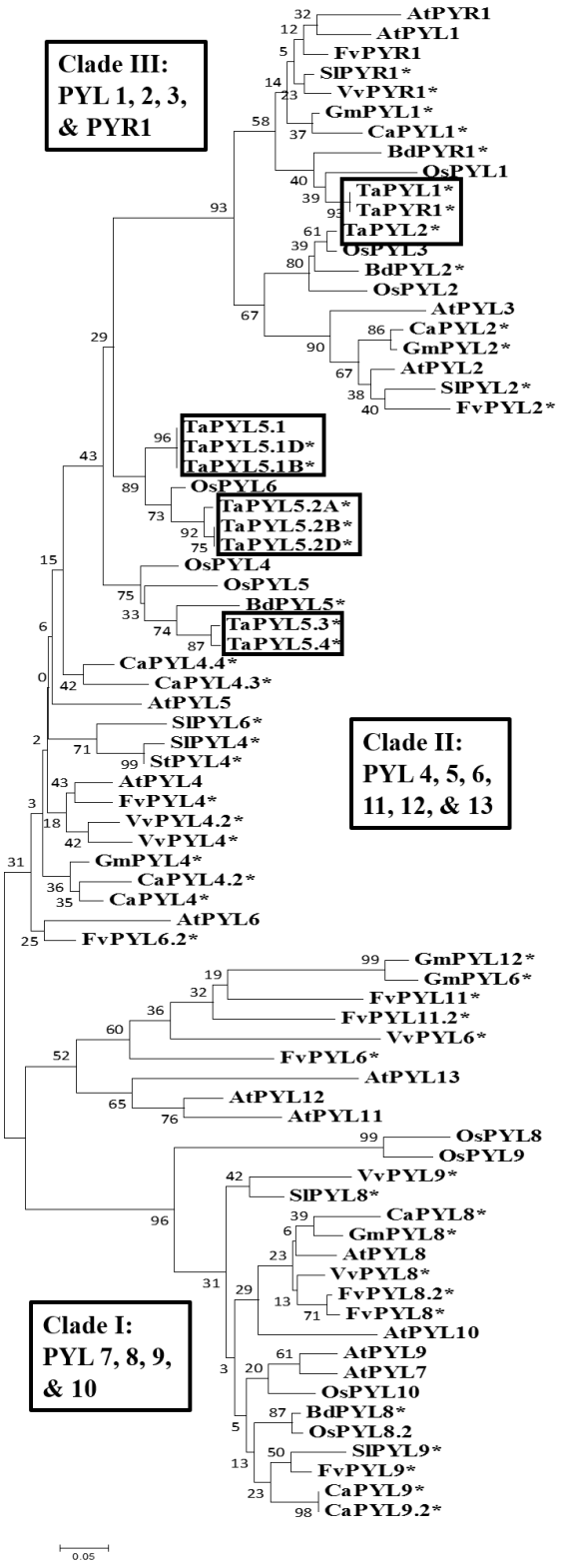

Figure 3.2: Phylogenetic Analysis of ABA Receptors. A protein alignment of 77 ABA receptors from various plant species was constructed with Clustal Omega (Goujon *et al*., 2010; McWilliam *et al*., 2013; Sievers *et al*., 2011) (Data not shown). The alignment was used to perform a phylogenetic analysis. The evolutionary history was inferred using the Neighbor-Joining method (Saitou and Nei, 1987). The optimal tree with the sum of branch length = 6.059444 is shown. The percentage of replicate trees in which the associated taxa clustered together in the bootstrap test (1000 replicates) are shown next to the branches. The evolutionary distances were computed using the Poisson method (Zuckerkandl and Pauling, 1965). All positions containing gaps were eliminated and there were a total of 53 positions in the final data set. Evolutionary analyses were conducted in MEGA6 (Tamura *et al*., 2013). Putative and NCBI PREDICTED proteins are marked with a *. Putative wheat receptors are boxed.

A protein alignment of the eight wheat clade II ABA receptors along with clade II members from *Arabidopsis* (At), rice (Os), strawberry (Fv), chickpea (Ca), soybean (Gm), grape (Vv), *Brachypodium* (Bd), tomato (Sl), and potato (St) are shown in Figure 3.3. The truncated TaPYL5.1D and TaPYL5.1B protein sequences have a 100% identity to TaPYL5.1. The TaPYL5.1D gene fragment has a 100% sequence identity to TaPYL5.1 at the nucleotide level as well. The alignment in Figure 3.3 highlights important sequence-function information including secondary structure and residues involved in the ABA binding pocket and/or PP2C interface. There is a high level of conservation throughout the clade II sequences especially in the loops that are involved in the ABA binding pocket (ABA pocket), the "gate", and the "latch". There is more conservation in the residues involved in ABA binding than the PP2C interaction, which probably contributes to PP2C promiscuity. A percent identity matrix was produced by Clustal Omega for the alignment in Figure 3.3 (Appendix 6.4). The matrix highlights the high percent of amino acid identities between Clade II receptors across different species.

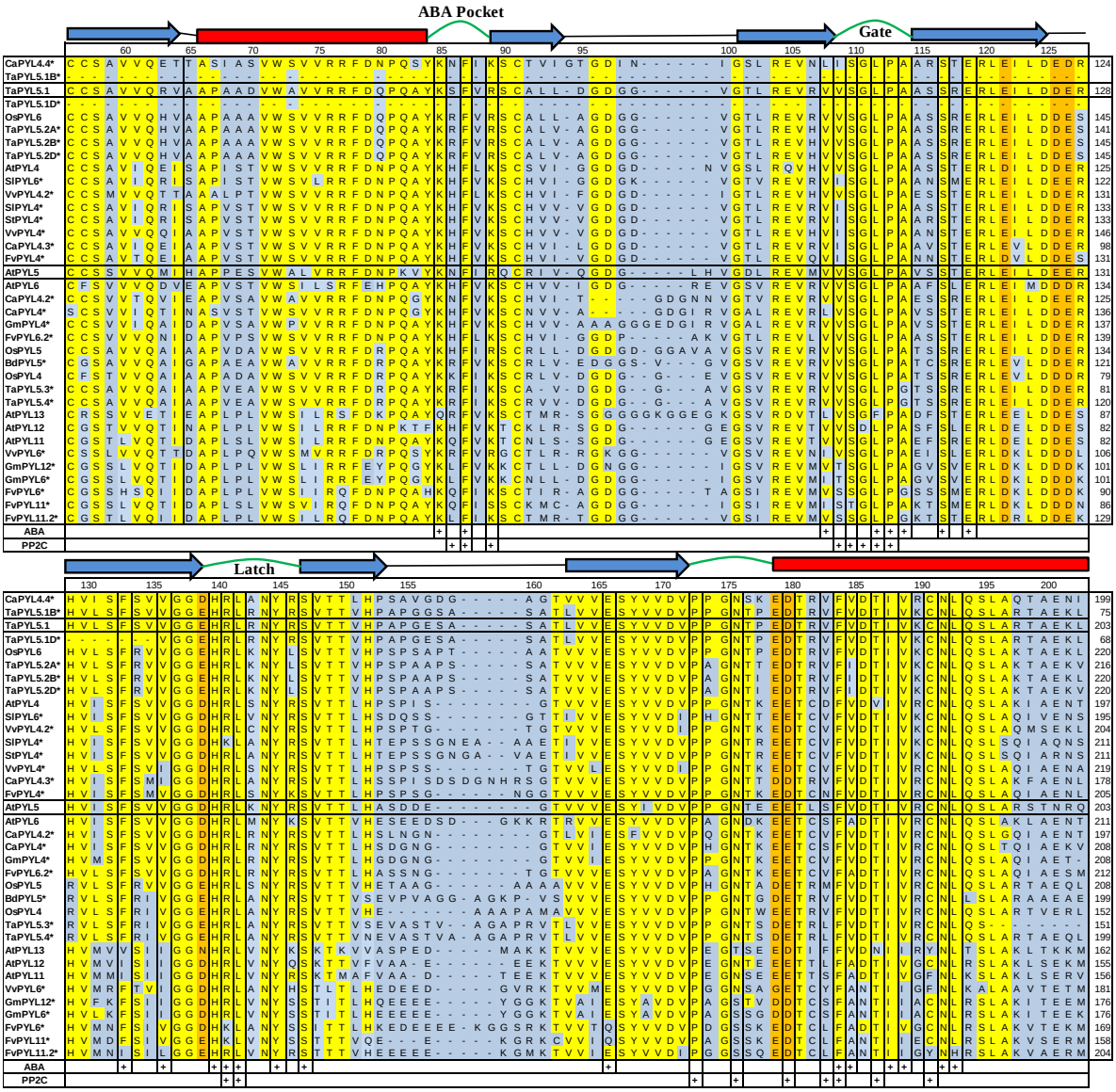

Figure 3.3: Protein Sequence Alignment of 36 Clade II ABA Receptors. Identical residues are shown in yellow and conserved acidic in orange while variable amino acids are shown in blue. Secondary structure is shown above the primary sequence. Blue arrows are representative of beta strands, and red rectangles are representative of alpha helices. The functional loops are represented by green curved lines. Below the primary sequence there will be a '+' symbol underneath a residue if it is involved in the binding of ABA or the PP2C interface respectively (Dorosh *et al*., 2013). The alignment was completed using Clustal Omega (Goujon et al., 2010; McWilliam et al., 2013; Sievers *et al*., 2011) and Mega6 (Tamura *et al*., 2013). The secondary structure was predicted with PredictProtein (Rost *et al*., 2004) and a recent study on the characterization of Rice ABA receptors (He *et al*., 2014). Residues are numbered by the wheat TaPYL5.1 amino acid sequence numbers.

3.3 Recombinant Expression & Purification of ABA Receptors & PP2Cs

3.3.1 Expression in *E. coli*

Both the putative ABA receptor TaPYL5.1 and PP2C phosphatase TaABI1 (gi|147225200|dbj|AB238930.1) genes were synthesized and cloned into the pEX-N-His bacterial expression vector by Origene/BlueHeron. The pEX-N-His vector produces a fusion protein with a HIS tag at the N terminus. TaPYL5.1 expression was confirmed in BL21 (DE3) cells although expression was low (data not shown). Although codon optimization was completed, there were still residues with lower than optimal scores (~12 %) in the sequence which could have been affecting expression in *E. coli*, so the pEX-N-His/TaPYL5.1 and pEX-N-His/TaABI1 plasmids were purified and used to transform Rosetta (DE3) cells in order to solve the potential codon usage problems. Over expression bands for the PP2C TaABI1 (49.8 kDa) and for the receptor TaPYL5.1 (25.3 kDa) were observed in the Rosetta (DE3) cell line (Figure 3.4).

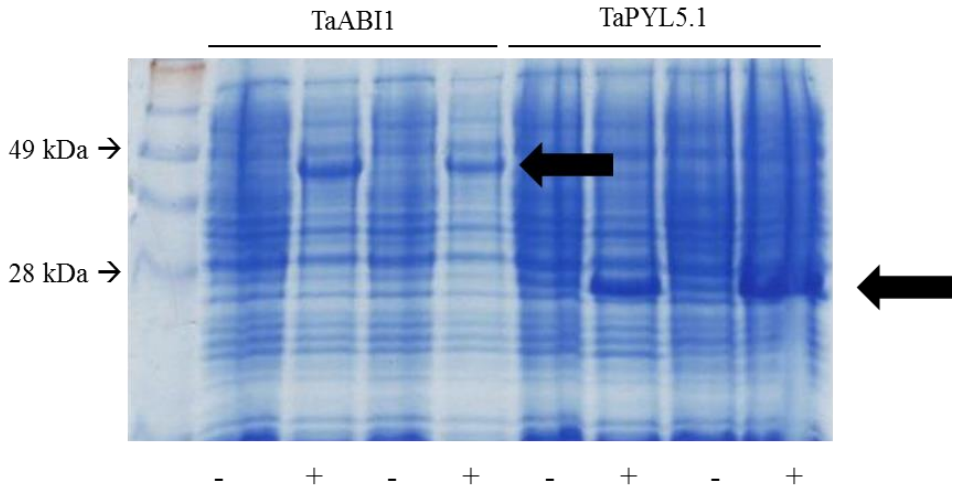

Figure 3.4: A 12% SDS-PAGE Gel Showing TaPYL5.1 & TaABI1 Protein Expression in the Rosetta (DE3) Cell Line. TaABI1 and TaPYL5.1 expression through the pEX-N-His and Rosetta (DE3) expression system. Total cell samples were subjected to 12% SDS-PAGE and stained with coomasie blue. Both protein expression assays were completed in duplicate as well as with non-induced (-) and induced (+) controls. The two upper bands are representative of the phosphatase TaABI1 at 49.8 kDa while the lower two bands are representative of the ABA receptor TaPYL5.1 at 25.3 kDa.

3.3.2 Purification

The TaPYL5 and TaABI1 proteins were purified using a Ni-NTA column to separate proteins with an attached His tag. The purification of both the receptor and the phosphatase was successful with small amounts of a few other proteins showing up on a 12% SDS-PAGE gel (Figure 3.5). The large 50 kDa band in the E1 TaPYL5.1 column is possibly a dimer of the TaPYL5.1 while the smaller fragments are probably proteolytically degraded segments, although this remains to be confirmed. In the TaABI1 E1 column the lower weaker bands may again be proteolytic cleavage products of the full length protein. These proteins were produced in bacteria so the small bands will not represent glycosylated forms of the proteins. However, the possibility that one or two of the bands might be a small amount of contaminating *E. coli* protein that co-eluted, cannot be strictly eliminated. For the purposes of looking at receptor activity, I moved ahead on the assumption that all protein in the eluted fraction, as detected by Bradford assay, was receptor or phosphatase for the purposes of quantifying proteins to add to assay reactions.

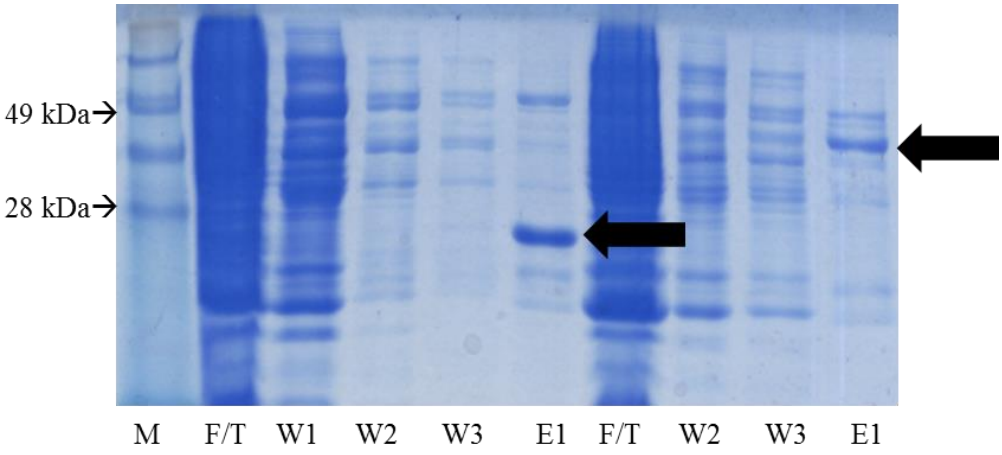

Figure 3.5: Ni-NTA Purification of TaPYL5.1 & TaABI1. *E. coli* cells transformed with a protein expression plasmid and induced by IPTG, were harvested by centrifugation and the cells lysed by sonication. Target proteins in the soluble fraction were enriched by Ni-NTA affinity column chromatography and the fraction analyzed by 12% SDS-PAGE. M: Marker; F/T: Flow Through; W1-W3: washes; E1: First elution fraction. The lower E1 band marked with an arrow is representative of purified TaPYL5.1 protein (25.3 kDa) while the upper E1 band marked with an arrow is representative of purified TaABI1 protein (49.8 kDa).

In order to perform the PP2C phosphatase activity assays discussed in the next section, three *Arabidopsis* PP2C's were expressed in *E. coli* and purified by a Ni-NTA affinity column; AtABI1, AtABI2 (Figure 3.6), and AtHAB1 (Figure 3.7). All three proteins were found to be expressed and purified with various levels of success.

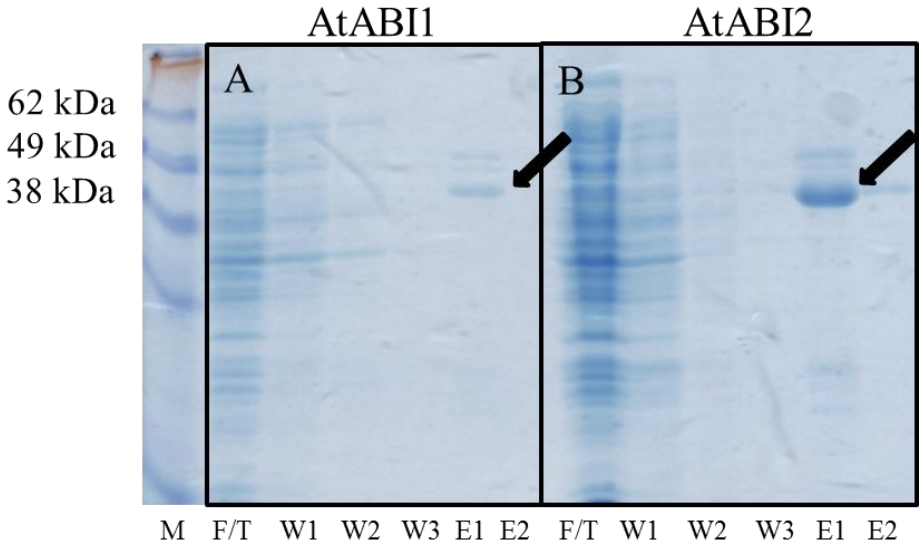

Figure 3.6: Ni-NTA Purification of *Arabidopsis* Phosphatases AtABI1 & AtABI2. *E. coli* cells transformed with protein expression plasmids and induced by Arabinose (AtABI1) and IPTG (AtABI2), were harvested by centrifugation and the cells lysed by sonication. Target proteins in the soluble fraction were enriched by Ni-NTA affinity column chromatography and the fraction analyzed by 12% SDS-PAGE. M: Marker; F/T: Flow Through; W1-W3: washes; E1-E2: Elution fractions. (A) The E1 band marked with an arrow is representative of purified AtABI1 protein at 47.5 kDa. (B) The E1 band marked with and arrow is representative of purified AtABI2 protein at 46.3 kDa.

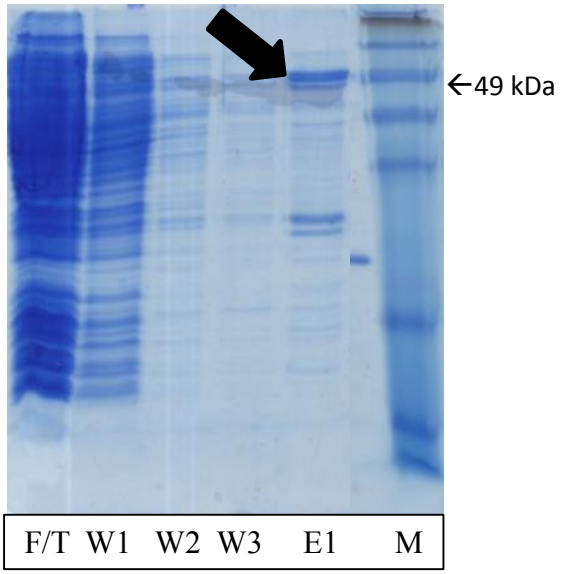

Figure 3.7: Ni-NTA Purification of *Arabidopsis* Phosphatase AtHAB1. *E. coli* cells transformed with protein expression plasmids and induced by Arabinose, were harvested by centrifugation and the cells lysed by sonication. Target proteins in the soluble fraction were enriched by Ni-NTA affinity column chromatography and the fraction analyzed by 12% SDS-PAGE. M: Marker; F/T: Flow Through; W1-W3: washes; E1: Elution fraction. The E1 band is representative of purified AtHAB1 protein at 56 kDa.

Protein expressions and Ni-NTA purifications of AtPYL5, AtPYL6, and AtPYR1 were completed and a 12% SDS-PAGE gel showing the Ni-NTA purified expression bands can be found in Figure 3.8. Protein concentrations varied so in order to ensure uniform protein concentrations for all assays (final concentrations of 0.024 µg/µL for receptors and 0.004 µg/µL for PP2Cs), a Bio Rad protein concentration assay kit was used to determine the protein concentration following manufacturer's instructions (Bio Rad). An important finding was that protein concentration would reduce over time even when stored in -80°C therefore it was essential to use the proteins as quickly as possible after purification and to avoid freeze-thaw cycles.

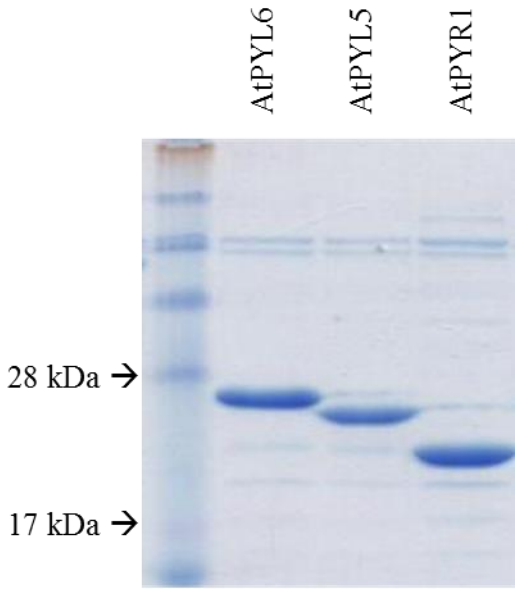

Figure 3.8: Purified *Arabidopsis* ABA Receptors. *E. coli* cells transformed with protein expression plasmids and induced by IPTG, were harvested by centrifugation and the cells lysed by sonication. Target proteins in the soluble fraction were enriched by Ni-NTA affinity column chromatography and the fraction analyzed by 12% SDS-PAGE. The bands are aliquots of E1 fractions. The molecular weights of AtPYL6, AtPYL5, and AtPYR1 are 25 kDa, 24 kDa, and 22 kDa respectively.

3.4 PP2C/Receptor Activity Assays

3.4.1 Phosphatase Inhibition by TaPYL5.1 in an ABA-dependent Manor

The recombinantly produced TaPYL5.1 was tested for its ability to inhibit TaABI1 in an ABA-dependent manner. The PP2C receptor TaABI1 was observed to have phosphatase activity and when the putative ABA receptor TaPYL5.1 was incubated with TaABI1 along with ABA the phosphatase activity was decreased by over 80 % (Figure 3.9A). A preliminary assay of TaPYL5.1 with *Arabidopsis* ABI2 was also completed (Figure 3.9B). These preliminary experiments involving only (+)-ABA found that TaPYL5.1 is a wheat ABA receptor that inhibits TaABI1, a wheat phosphatase, in an ABA dependent manner. Wheat PYL5.1 was shown to be able to interact with, and inhibit the *Arabidopsis* PP2C ABI2.

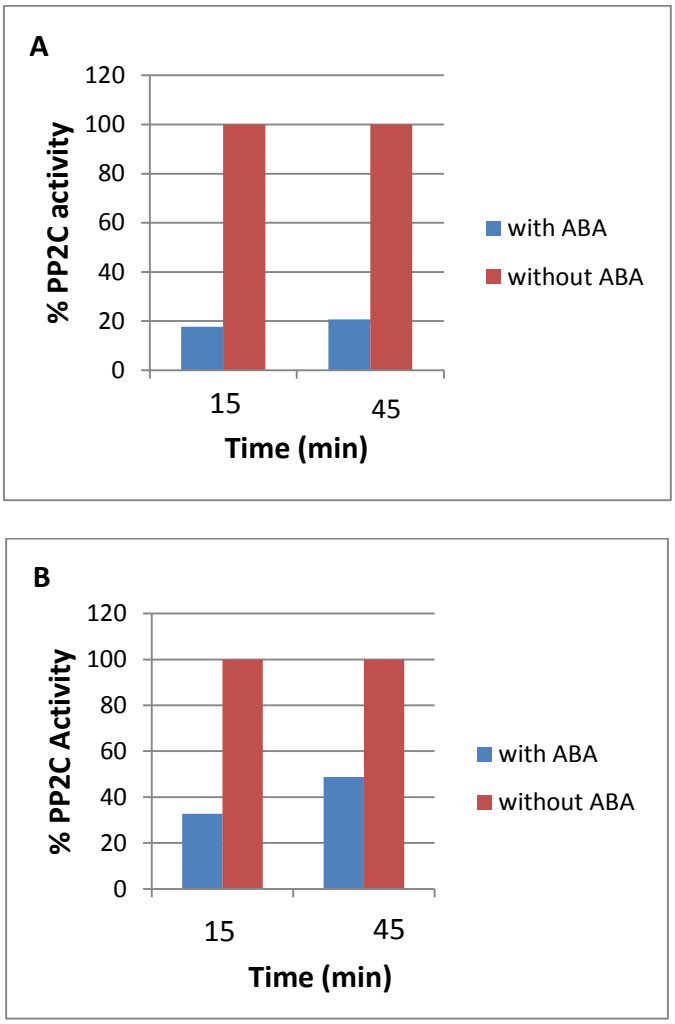

Figure 3.9: Results of the Preliminary PP2C assays. (A) The wheat receptor TaPYL5.1 inhibits wheat PP2C TaABI1 activity in an (+) ABA dependent manor (B) The wheat receptor inhibits *Arabidopsis* phosphatase ABI2. In vitro activity assays were completed with a final ABA concentration of 10 µM. The activity of controls (without ABA) were set to a relative value of 100% while the ABA-treated samples were presented relatively to the controls. Fluorescence activity was measured on a Perkin Elmer Victor 3 V 1420 fluorescent plate reader at 15 and 45 minutes after initiation of the assay. An excitation wavelength of 355 nm, emission wavelength of 460 nm, and measurement time of 0.1 s were used (n=1).

3.4.2 Preliminary ABA Analog Assays

Dr. Suzanne Abrams (The National Research Council) developed a large library of ABA analogs. Of these analogs five showed promise in acting as agonists of ABA *in vitro* (Data not shown). Recently these analogs were used in a study that probed 13 ABA receptors and four PP2Cs from *Arabidopsis* during development and stress response (Benson *et al*., 2014). These five (+) or (S) analogs along with their (-) or (R) enantiomers were chosen for this wheat study (Figure 3.10). The analogs have changes made to the ABA ring. Analogs 352 and 354 are (+) and (-) enantiomers that have the proton of the hydroxyl group replaced with a methyl group. Analogs 413 and 414 are (+) and (-) enantiomers that have the 7' methyl replaced with an aromatic ring attached to the 3' and 2' carbons. Analogs 425 and 426 are (+) and (-) enantiomers that have the 8' methyl group replaced with an acetylene group. Analogs 514 and 515 are (+) and (-) enantiomers that have the 9' methyl group replaced with a propargyl group. Analogs 694 and 695 are (+) and (-) enantiomers that have the 8' methyl group replaced with a cyclpropyl group.

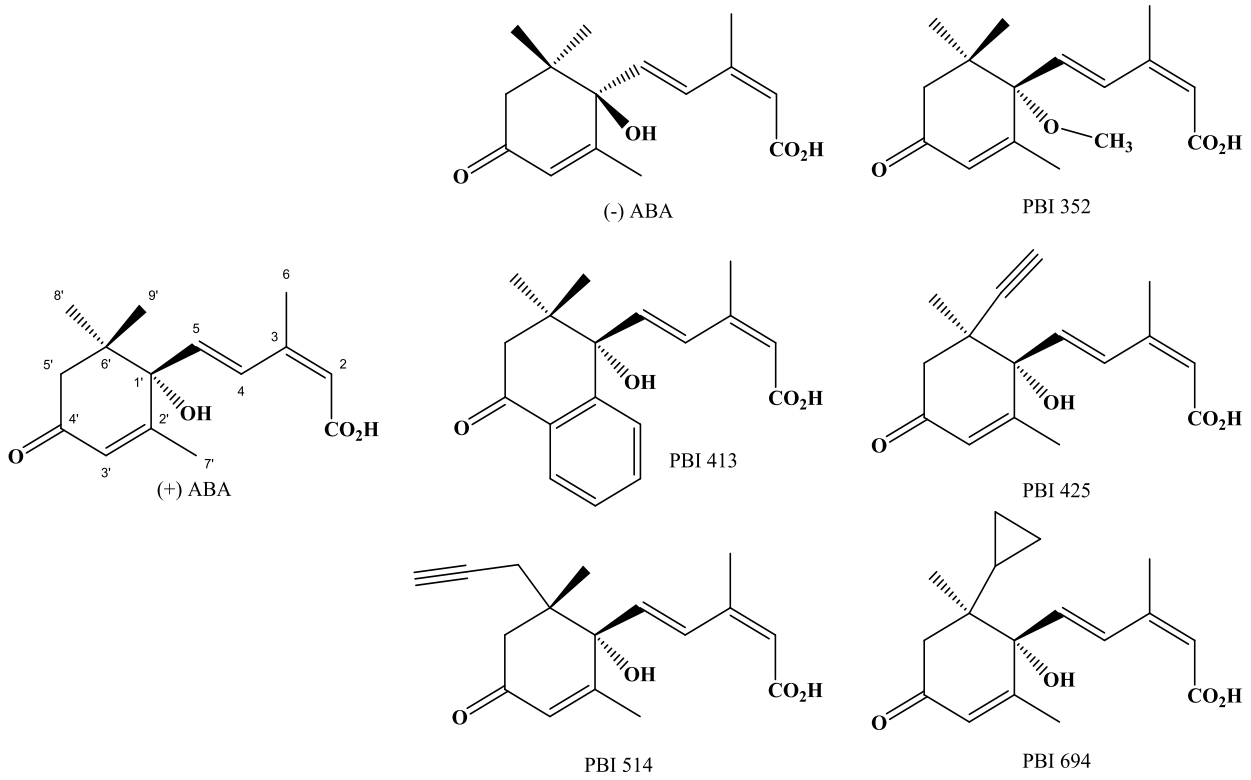

Figure 3.10: Structures of ABA and ABA Analogs. The structures for (+) ABA, (-) ABA, (S)-413, (S)-352, (S)-425, (S)-694, and (S)-514 are shown. The corresponding (R)-analogs (R)-414, (R)-354, (R)-426, (R)-695, and (R)-515 are not shown. Structures are based on structures from Benson *et al.* (2014) and created with Chem Draw

Analysis was carried out using the same phosphatase based enzyme activity assay described previously (Ma *et al*., 2009). These analogs are known agonists of ABA receptors in the *Arabidopsis* ABA signaling pathway and it has been shown in the Loewen lab that the (+) analogs have a more potent inhibition of phosphatase activity than their (-) counterparts. Fraser Ball, a summer student I supervised, worked with assaying the phosphatase against the *Arabidopsis* ABA receptors while I worked on assaying the wheat ABA receptor against the *Arabidopsis* PP2Cs. The preliminary results include the wheat receptor paired with TaABI1 and AtABI2 (Figures 3.11A & 3.11B). Note that the analog order in Figure 3.11 follows a plus-minus or S-R enantiomer pattern. These assays were carried out with a 1.0 µM ABA or ABA analog final concentration as opposed

to the 10 µM concentration used in the previous section (Figure 3.9). A different level of PP2C inhibition could result from the analog binding tighter or looser than ABA within the ABA binding pocket. Also, differences could occur if the analog was somehow interfering with the PP2C binding interface. All the analogs except 352, 354, and 695 were found to have similar results to (+) and (-) ABA with a PP2C inhibition level of more than 80% regardless of whether the wheat receptor was paired with the wheat or *Arabidopsis* PP2C.

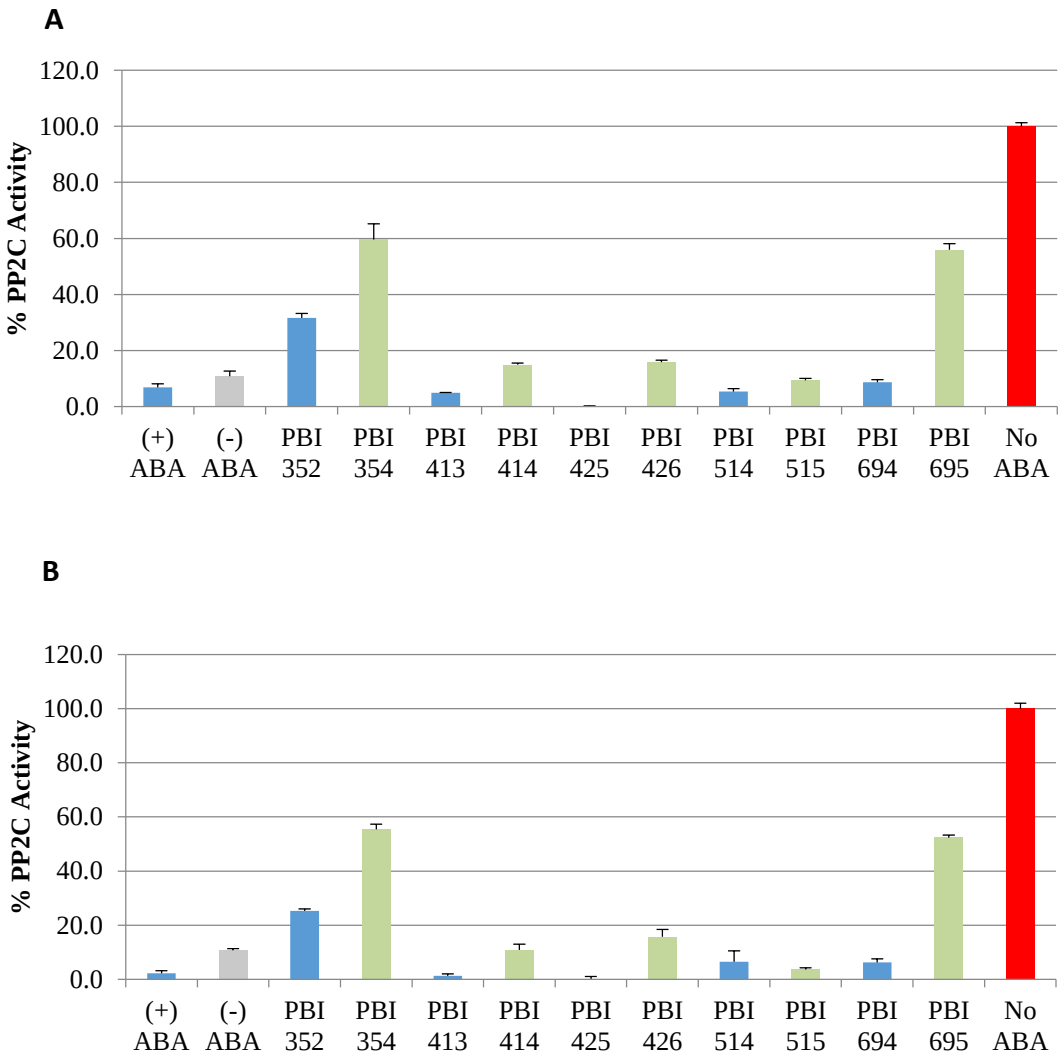

Figure 3.11: In Vitro Activity Assays with 1.0 µM ABA & ABA Analogs. (A) Phosphatase based enzyme activity assay using wheat receptor TaPYL5.1 and wheat phosphatase TaABI1. (B) Phosphatase based enzyme activity assay using wheat receptor TaPYL5.1 and *Arabidopsis* PP2C AtABI2. The concentrations of ABA or ABA analog used were 1.0 µM. The activity of controls (No ABA) were set to a relative value of 100% while the ABA or ABA analog treated samples were presented relative to the controls. Fluorescence activity was measured using a Perkin Elmer Victor 3 V 1420 fluorescent plate reader at 30 minutes after initiation of the assay. An excitation wavelength of 355 nm, emission wavelength of 460 nm, and measurement time of 0.1 s were used. Each bar represents the average of three replicates with standard error shown at the top.

3.4.3 Relative Sensitivity of TaPYL5.1 to Various ABA Analogs

The PP2C activity assays were expanded and redone with a 0.1 μM concentration in order to properly visualize the relative strengths of the activities after ABA/ABA analog binding. When using a 10.0 μM or 1.0 μM ABA/analog concentration it was possible that the receptor binding sites were being saturated and therefore it was difficult to evaluate significant differences between analogs and ABA. It was therefore necessary to lower the ABA/analog concentrations to 0.1 μM, the same concentration used in the Benson *et al*. (2014) study.

TaPYL5.1 was paired with four different PP2Cs for enzyme activity assays using 0.1 μM ABA or ABA analog concentration (Figure 3.12). The lower ABA or ABA analog concentration allowed better visualization of relative PP2C activities when compared to the 1.0 μM assays in the previous section. Generally, the trend of responses to analogs for the receptor TaPYL5.1 remained constant when paired up with the four different phosphatases. When using a (-) enantiomer of a (+)/(-) pair, the resultant activity is always more than when using the (+) enantiomer. The activities when using analog 352 were consistently the highest among all (+) enantiomers in all four assays suggesting that receptor TaPYL5.1 does not bind 352 tightly or that 352 interferes with PP2C binding. Further analysis of this result is carried out in sections 3.3.4 and 3.4.1. The activities when using analog 694 varied depending on the PP2C used suggesting that this analog can produce a response that is more PP2C specific. The other (+) enantiomers (413, 425, and 514) resulted in activities that were similar to (+) ABA suggesting that they could act as ABA in future experiments. The wheat/wheat receptor/PP2C pairing did not produce any unique results when compared to the other three parings (Figure 3.12D).

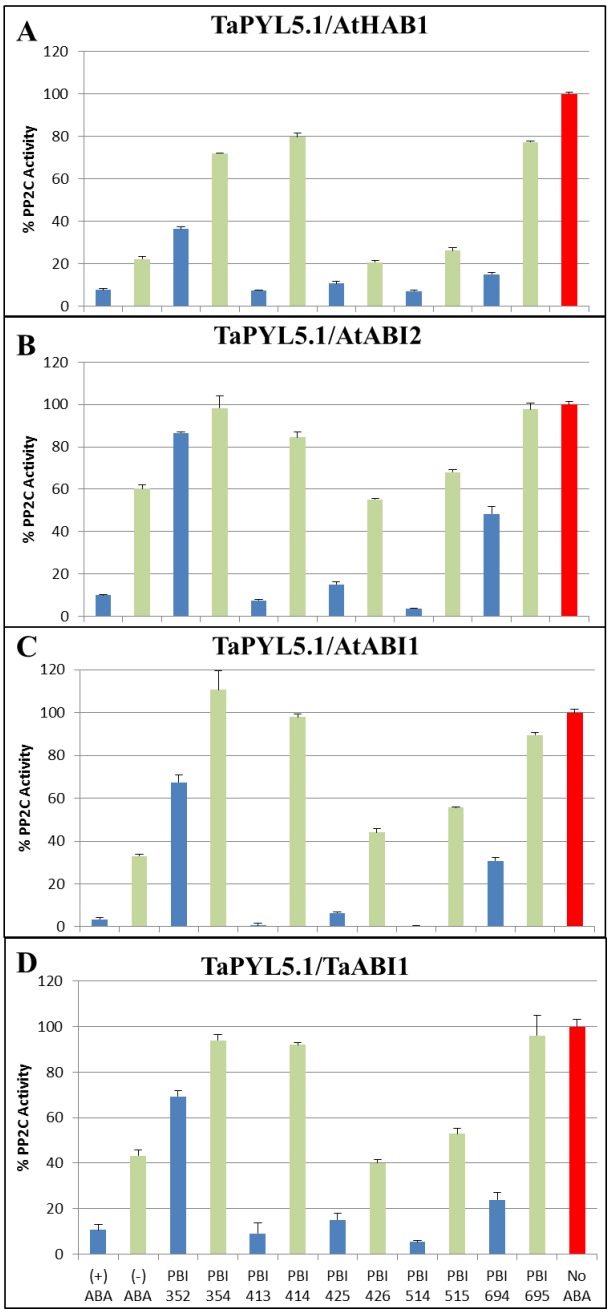

Figure 3.12: Comparison of *Arabidopsis* PP2C Enzyme Activity Assays. Phosphatase based enzyme activity assays using wheat ABA receptor TaPYL5.1 along with PP2Cs AtHAB1 (A), AtABI2 (B), AtABI1 (C), and TaABI1 (D). The concentrations of ABA or ABA analog used were 0.1 µM. The activity of controls (No ABA) were set to a relative value of 100% while the ABA or ABA analog treated samples were presented relatively to the controls. Fluorescence activity was measured using a Perkin Elmer Victor 3 V 1420 fluorescent plate reader at 30 minutes after initiation of the assay. An excitation wavelength of 355 nm, emission wavelength of 460 nm, and measurement time of 0.1 s were used. Each bar represents the average of three replicates with standard error shown at the top.

TaABI1 was paired with three different ABA receptors in enzyme activity assays completed with Fraser Ball (a summer co-op student). The wheat PP2C was assayed for activity with *Arabidopsis* ABA receptors PYL5 (Clade II), PYL6 (Clade II), and PYR1 (Clade III) (Figure 3.13). The overall activity trend remains the same as in Figure 3.12A with the TaABI1/AtPYL5 pairing when using ABA, 414, 425, 514, and 694. AtPYL5 had a stronger analog response to 352 and 694 than TaPYL5.1 (Figures 3.12D & 3.13A). The response to analogs 426, and 514 were the only responses under 20% with the TaABI1/AtPYL6 pairing and even the response to (+) ABA only showed a 34.2% of the maximum PP2C activity (Figure 3.13B). There is no increase in activity with AtPYR1 plus any of the analogs therefore AtPYR1 has no inhibitory effect on TaABI1 activity in the presence of ABA analogs (Figure 3.13C). The best inhibition of PP2C activity with this pairing is with ABA and analog 413 at 45.5 % and 47.1% respectively. This result could be explained by the finding that AtPYR1 forms a dimer and is less effective than other receptors at forming a complex with a PP2C (Cutler et al, 2012) or because TaABI1 does not interact strongly enough with AtPYR1 to fully inhibit the phosphatase activity of TaABI1. TaABI1 may not be able to form a proper complex with AtPYR1, a Clade III receptor, which only has a 54% identity to AtPYL5, a Clade II receptor.

These results suggest that although the wheat receptor TaPYL5.1 is able to interact with and inhibit multiple PP2Cs with a variety of ABA analogs and ABA, the opposite is not true; TaABI1 may not be inhibited well by receptors that do not have a high sequence identity to TaPYL5.1 at the important active site residues.

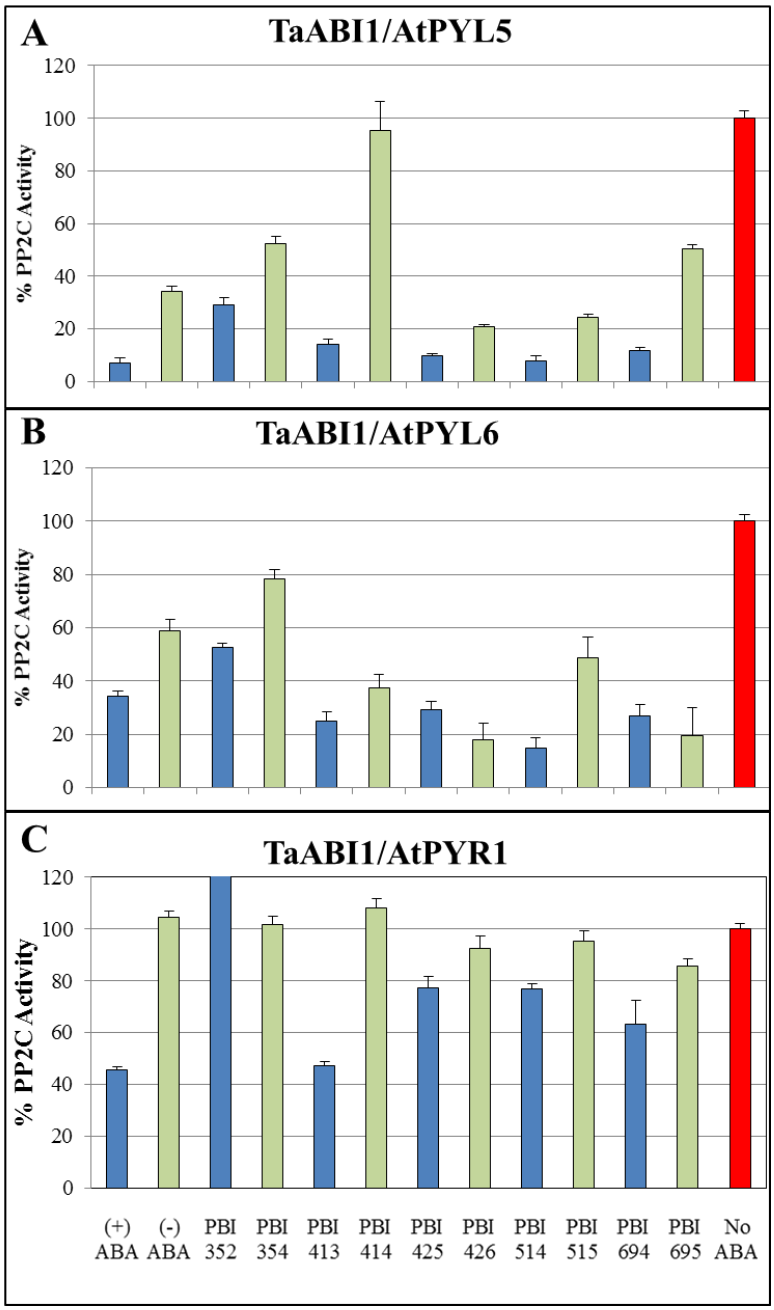

Figure 3.13: Comparison of *Arabidopsis* ABA Receptor Enzyme Activity Assays. Phosphatase based enzyme activity assays using wheat PP2C TaABI1 along with ABA receptors AtPYL5 (A), AtPYL6 (B), and AtPYR1 (C). The concentrations of ABA or ABA analog used were 0.1 µM. The activity of controls (No ABA) were set to a relative value of 100% while the ABA or ABA analog treated samples were presented relatively to the controls. Fluorescence activity was measured using a Perkin Elmer Victor 3 V 1420 fluorescent plate reader at 30 minutes after initiation of the assay. An excitation wavelength of 355 nm, emission wavelength of 460 nm, and measurement time of 0.1 s were used. Each bar represents the average of three replicates with standard error shown at the top.

3.4.4 Comparative Characteristics of TaPYL5.1 & AtPYL5 *in vitro*

The use of the ABA analogs presents a way to determine the similarities and differences in the ABA binding pockets between the characterized wheat ABA receptor TaPYL5.1 and *Arabidopsis* receptor AtPYL5. The data from Section 3.4.3 were re-plotted along with new data from the pairing AtPYL5-AtABI1. The four parings cover all the permutations in which two (one wheat and one *Arabidopsis)* receptors and two (one wheat and one *Arabidopsis*) PP2Cs can be combined, such that any major differences in the results will point towards possible structure/function relationships.

Only three differences between TaPYL5.1 and AtPYL5 protein sequences are noted when the residues known to be involved in ABA and PP2C interactions are considered, and all of these residues are involved in the PP2C receptor complex formation after ABA has already docked (Figure 3.3; (Dorosh *et al*., 2013)). The three changes are S86N, D180E, and V183S (wheat→*Arabidopsis*). Since the changes are not in the ABA pocket itself any changes in the response to ABA or an analog would imply that the analog was somehow creating a conformational change in the binding pocket that is impacting PP2C binding.

To investigate this further, I compared the respective activities for wheat and *Arabidopsis* PYL5's against the ABI1's in the presence or absence of ABA or the ABA analogs (Figure 3.14). Significant differences in PP2C activities were found in the responses to the 352 and 694 analogs. When comparing TaPYL5.1/TaABI1 and TaPYL5.1/AtABI1 to AtPYL5/AtABI1 and AtPYL5/TaABI1 there was ~ 39.5% more inhibition of PP2C activity with the response to 352. When comparing TaPYL5.1/TaABI1 and TaPYL5.1/AtABI1 to AtPYL5/AtABI1 and AtPYL5/TaABI1 there was ~ 15.8% more inhibition of PP2C activity with the response to 694. The analog pairs 352/354 and 694/695 were found to be receptor, but not PP2C, specific. Both

352/354, and 694/695 were less potent towards the wheat receptor than the *Arabidopsis* receptor, regardless of the PP2C that was used. The 352/354 pair differs from ABA in that the proton of the hydroxyl group is replaced with a methyl group and the pair 694/695 differs from ABA by replacing the 8' methyl group with a cyclopropyl group (Benson *et al*., 2014). The modifications in these two analog pairs may be causing steric constraints in the receptor binding site that is translated through allosteric means to the PP2C interface where the variations are located, making this interference specific to the wheat receptor. The (-) enantiomer form analogs are generally less potent than the (+) enantiomer form as is the case with (+)- and (-)-ABA.

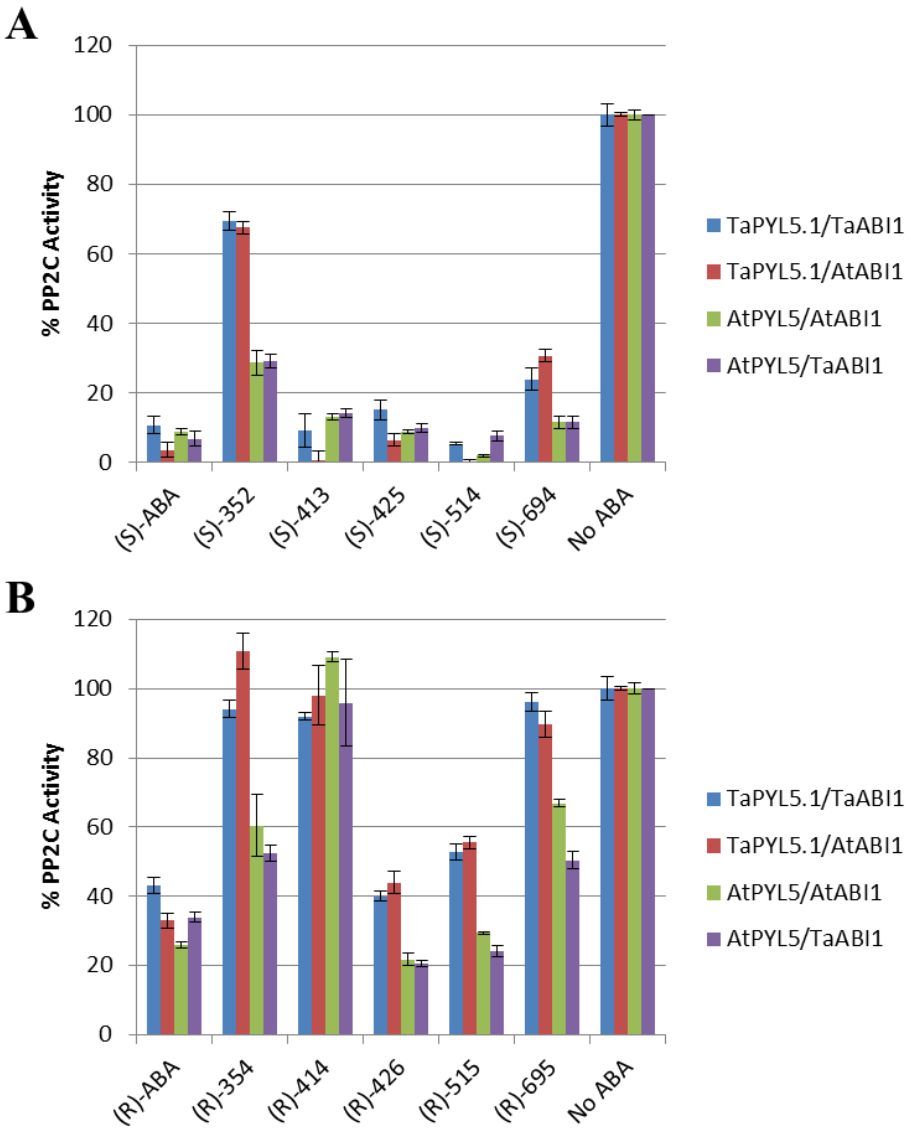

Figure 3.14: Functional differences Between *Arabidopsis* and Wheat ABA receptors and PP2Cs. ABA analogs are described previously in Figure 3.1. S-enantiomer (A) and R-enantiomer (B) forms of ABA and ABA analogs were assayed. Four different combinations of wheat and *Arabidopsis* ABA receptor and PP2C are shown with color legend on the right. Phosphatase based enzyme activity assays using ABA or ABA analog concentrations of 0.1 µM were performed. The activity of controls (No ABA) were set to a relative value of 100% while the ABA or ABA analog treated samples were presented relatively to the controls. Fluorescence activity was measured using a Perkin Elmer Victor 3 V 1420 fluorescent plate reader at 30 minutes after initiation of the assay. An excitation wavelength of 355 nm, emission wavelength of 460 nm, and measurement time of 0.1 s were used. Each bar represents the average of three replicates with standard error shown at the top.

3.5 Protein Modeling

3.5.1 Computer Modeling

Computer modeling was used to look at the differences in the structure of the wheat receptor compared to the *Arabidopsis* receptor in order to explain the differences found in the activity assays. The structure for TaPYL5.1 was modeled and aligned with a structure of AtPYL5 (protein data bank (PDB) 4JDL which supersesedes 3QRZ) with Phyre^2 online software (Kelley and Sternberg, 2009; Zhang *et al*., 2013). At 85% amino acid sequence coverage, TaPYL5.1 has a 58% amino acid identity to AtPYL5. A published structure of receptor AtPYL13 bound to PP2C AtAHG3 (PDB identifier 4NOG) was aligned to the AtPYL5 alignment (Li *et al*., 2013). A published structure of AtPYL9 (PDB identifier 3OQU) bound with ABA was then aligned so ABA would be present in the binding pocket of the model (Zhang et al., 2013). The 352 analog structure was then aligned to the position of ABA. The result is an in *silico* comparison of the two receptors of interest, AtPYL5 and TaPYL5.1, with ABA and 352 in the binding pocket, and a PP2C bound to the interface (Figure 3.15). This model will allow a closer look at the amino acid substitutions in *Arabidopsis* and wheat PYL5s that are involved in ABA docking and PP2C binding.

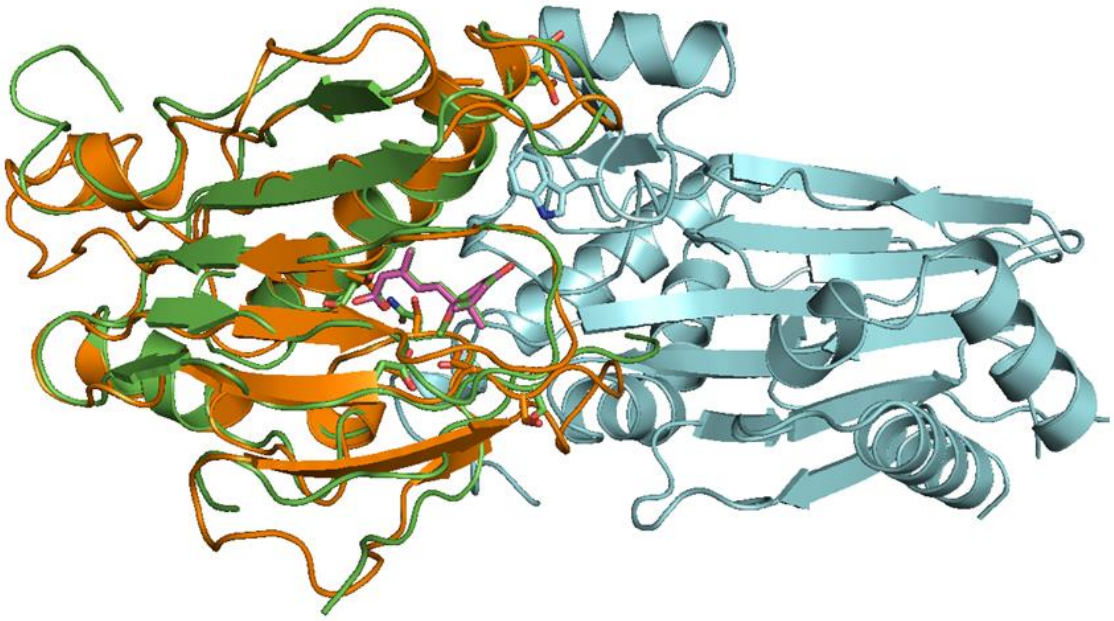

Figure 3.15: Overall Computer Model of ABA Bound Receptors Forming a Complex with PP2C AHG3. Wheat ABA receptor PYL5.1 (orange) aligned with *Arabidopsis* ABA receptor PYL5 (green), and bound to PP2C AHG3 (blue). ABA (pink) and ABA analog 352 (green) are shown in the ABA binding pocket. All structures except TaPYL5.1 and the 352 analog were taken from the protein data bank (Berman *et al*., 2000).

3.5.2 Validation of the TaPYL5.1 Model

It was necessary to validate the TaPYL5.1 protein model. The Phyre^2 online software has a validation function (Kelley and Sternberg, 2009). The model output had a 100% confidence level with a 70% identity to the published AtPYL5 structure 4JDL. The program states that if you have a match with a confidence >90% and an identity >40% you can generally be very confident that your protein adopts the overall fold shown and that the core of the protein is modelled at high accuracy although it does note that surface loops can deviate from the native model. An independent Ramachandran plot was generated through the online software RAMPAGE in order to analyze the distribution of torsion angles in the model (Figure 3.16) (Lovell *et al*., 2003). The

Ramachandran plot outlined the outcome of the Phyre2 analysis which was that 77% of the residues fall into the favored region, 15.7% in the allowable region, and 7.1% in the outlier region.

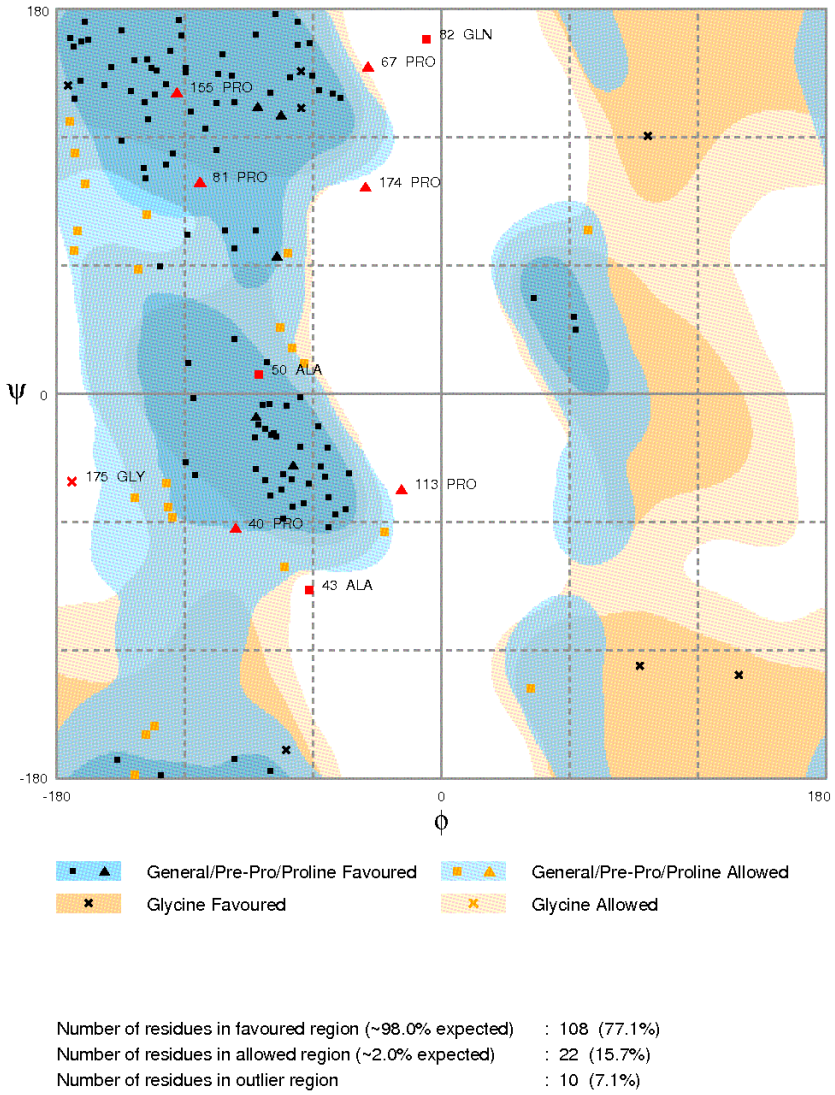

Figure 3.16: A Ramachandran Plot of TaPYL5.1 Protein Model. Plot generated by RAMPAGE online software (Lovell et al., 2003).

The model validation was less than optimal. The Phyre2 software produced an additional model based on AtPYL3, to which TaPYL5.1 had only a 51% amino acid identity. The confidence of this second model was also 100% and it yielded a more acceptable Ramachandran analysis. However, I thought it important to base the model on AtPYL5 because that is the protein used in the PP2C assays and AtPYL5 has the highest sequence homology to TaPYL5.1 (58%). Another PyMOL alignment of the AtPYL5 based model with the AtPYL3 based model showed that they both adopt the same overall fold.

3.6 VIGS of *TaPYL5.2A* in Wheat

3.6.1 Positive & Negative VIGS Controls

Control constructs were used for visual and gene expression comparisons in the VIGS plant trials. A phytoene desaturase (PDS) construct (Appendix 6.2) was used to measure the visual level of knockdown in the heads of the plants and to determine the best time to carry out the VIGS infection. The PDS gene is involved in carotenoid biosynthesis and knocking down the gene results in a bleached phenotype (Qin *et al*., 2007) (Figure 3.17). Two other controls were used as negative controls for the plant trials; empty vector (early plant trials), and GFP. The empty BSMVγLIC-EMPTY vector was first used as the VIGS phenotype control. The viral phenotype was found to be too strong so instead a 180 base pair fragment of GFP was inserted into the LIC cloning site and the BSMVγLIC-GFP construct was used as the viral control instead (Appendix 6.2).

Figure 3.17: Wild Type versus PDS Knock-Down Plants. The wild type head (A) was planted at the same time and grown under the same conditions as the PDS knock-down head (B). PDS knockdown plants were treated with the BSMVγLIC-PDS construct that contained a fragment of the phytoene desaturase gene in order to elicit VIGS. BSMVγLIC-PDS plants have a bleached phenotype and a different texture in areas that have the PDS gene knocked down. Both samples were taken at 14 days past VIGS treatment.

3.6.2 Target Cloning

The receptor fragment was amplified from genomic DNA, while the PP2C was amplified from the previously described expression plasmid as no codon optimization had been performed on the PP2C sequence. The predicted fragment sizes of TaPYL5.1 and TaABI1 were 217 and 245 base pairs respectively. Since the TaPYL5.1 band was faint, a second round of amplification was performed after gel extraction of the band. A 2% agarose gel was used to visualize the VIGS fragments (Figure 3.18). The VIGS fragments were then sub-cloned into the VIGS vector, using two separate cloning strategies; an unpublished/untested Gateway strategy, and the established Ligation Independent Cloning (LIC) system. The resulting Gateway constructs were abandoned after weak results in plant trials and the LIC constructs were used in subsequent experiments (LIC

cloning completed by Dr. Shawn Clark). Correct insertion of the TaPYL5.1 fragment into the BSMVγLIC vector was confirmed by sequencing. With confirmation of the correct proper insertion of the receptor it was identified that the sequence more closely matched that of receptor TaPYL5.2A instead of TaPYL5.1. Further analysis found that the TaPYL5.1 primers would anneal to TaPYL5.2A as well. Since the amplification was completed using a cDNA library from Fielder wheat heads, it is possible that the TaPYL5.2A paralog is more highly expressed than TaPYL5.1. The VIGS construct was subsequently named BSMVγLIC-PYL5.2A. A 217 base pair alignment of the LIC construct and an excerpt from the TaPYL5.2A gene can be found in Figure 3.19. There are 10 differences between the cloned sequence and the genomic sequence. The genomic sequence is from the Chinese Spring cultivar, which would explain some of the differences found in the Fielder cultivar sequence. Other reasons for the differences could be errors produced during two rounds of PCR amplification or sequencing errors. These constructs are close enough to the target gene, and with large stretches of perfect identity that I was confident moving forward with them. The BSMVγLIC-ABI1 VIGS construct was only included in the preliminary plant trials while the BSMVγLIC-PYL5.2A construct was used in the remainder of this study.

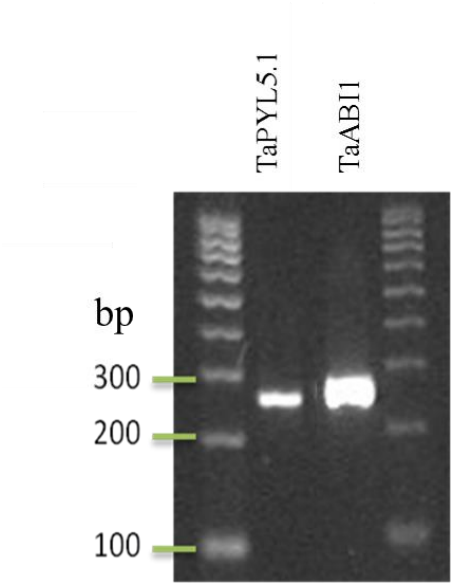

Figure 3.18: A 2% Agarose Gel of VIGS Fragments TaPYL5.1 and TaABI1. The 217 base pair TaPYL5.1 fragment was amplified from genomic wheat head DNA. The 245 base pair TaABI1 fragment was amplified from plasmid DNA. The TaPYL5.1 band is shown after two rounds of amplification. After sequencing, the TaPYL5.1 fragment was found to be a TaPYL5.2A fragment (Figure 3.19).

```
BSMVγLIC-PYL5.2A  GGAAGTTTAAGCTGGAGATCCTGGACGACGAGAGCCACGTGCTCAGTTTCCGCGTCGTCG
TaPYL5.2A         ----------GCTCGAGATCCTGGACGACGAGAGCCACGTGCTCAGCTTCCGCGTCGTCG
                            *** ****************************** *************

BSMVγLIC-PYL5.2A  GTGGCGAGCACCGGCTCAAGAACTACCTCTCCGTCACCACCGTCCACCCGTCCCCAGCCG
TaPYL5.2A         GCGGGGAGCACCGGCTCAAGAACTACCTCTCCGTCACCACCGTGCACCCATCCCCGGCCG
                   * ** ************************************ ***** ***** ****

BSMVγLIC-PYL5.2A CGCCGTCCAGCGCCACCGTCGTCGTGGAGTCCTACGTCGTGGACGTGCCGGCGGGCAACA
TaPYL5.2A        CGCCGTCCAGCGCCACCGTCGTCGTGGAGTCGTACGTCGTGGACGTGCCCGCGGGCAACA
                 ****************************** ***************** **********

BSMVγLIC-PYL5.2A CGATCGAGGACACCCGCGTGTTCATCGACACCATCGTCAAGTGCAACACGGTGGTGGTGG
TaPYL5.2A        CGACCGAGGACACCCGCGTGTTCATCGACACCATCGTCAAGTGCAAC----------
                    *** ****************************************
```

Figure 3.19: Alignment of the Insert Sequence in BSMVγLIC-PYL5.2A with the Corresponding Wheat *TaPYL5.2A* Genomic Sequence. The cDNA used in the LIC cloning reaction was amplified from a Fielder cultivar while the genomic sequencing is from Chinese spring. The TaPYL5.2A fragment is 217 base pairs. The LIC overhangs are underlined. There are 10 differences in the insert sequence when compared to the genomic sequence. The sequencing of the BSMVγLIC vector was carried out by DNA services at the National Research Council in Saskatoon. The alignment was completed with Clustal Omega (Goujon *et al.*, 2010; McWilliam *et al.*, 2013; Sievers *et al.*, 2011).

3.6.3 FHB Infection of VIGS Treated Plants

Plant trials consisted of three sets of plants: wild type control, GFP control, and TaPYL5.2A knock-down. Wild type plants are non-BSMV treated controls. GFP plants are treated with a control BSMV construct that contains a 180 base pair fragment of GFP in the place of the target gene. The TaPYL5.2A knock-down plants are treated with the BSMVγLIC-PYL5.2A construct described in the previous section in order to elicit VIGS. At seven days past *F. graminearum* treatments, the PYL5.2A knock down plants were found to be more resistant to FHB than the GFP control plants (Figure 3.20). This early FHB resistant phenotype was observed in three separate plant trials.

Figure 3.20: FHB Infection in Wheat. The photographs were taken at 7 days past *F. graminearum* treatment (14 days past VIGS treatment). The sample heads are representative of wild type (A and B), GFP (C and D), and PYL5.2A (E and F) plant populations. There are two selected heads from each population to highlight the range of phenotype observed. Plants are either *F. graminearum* infected (A, C, and E) or non-infected (B, D, and F).

3.6.4 Effect of TaPYL5.2A Knockdown on FHB Disease Progression

Further phenotypical quantification was completed (Figure 3.21). When looking at fungal progression within individual spikelets, it was possible to tabulate an average number of infected spikelets per head over a time course of 3, 5, 7, 9, and 13 days past the *F. graminearum* treatments. The larger errors show relatively high variation within treated plants. Overall, all plant populations were found to increase in FHB disease phenotype with time until the disease had killed the head completely which was anywhere from 13 days to 20 days post infection (data not shown). The interesting effects in the receptor knock-down plants occur during the early stages of the disease where they are able to slow down the progression of FHB when compared to the GFP controls (Figure 3.21).

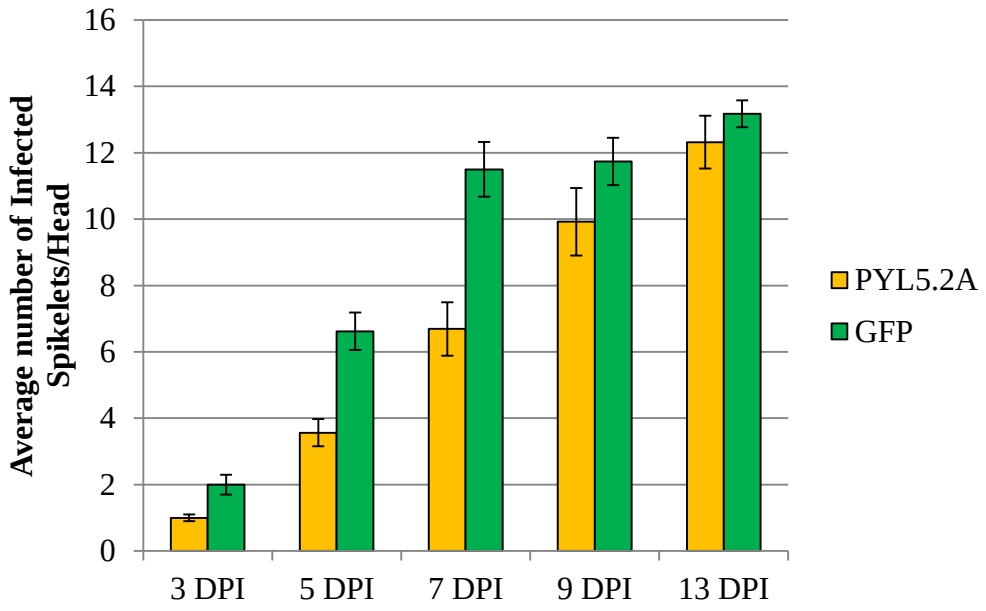

Figure 3.21: FHB Infected Spikelets in PYL5.2A Knock-Down Plants Compared to GFP Control Plants. Data were collected from plants at 3, 5, 7, 9, and 13 days past the FHB infections. The average number of infected spikelets per head of the population were measured. Standard error bars are shown (n=33).

It is also necessary to keep track of the infection in the rachis (the main stem of the head) because infection will spread through the rachis down into the stem. The infection of the rachis was observed and scored at 4 different levels; 25%, 50%, 75%, and 100% infected (Figure 3.22).

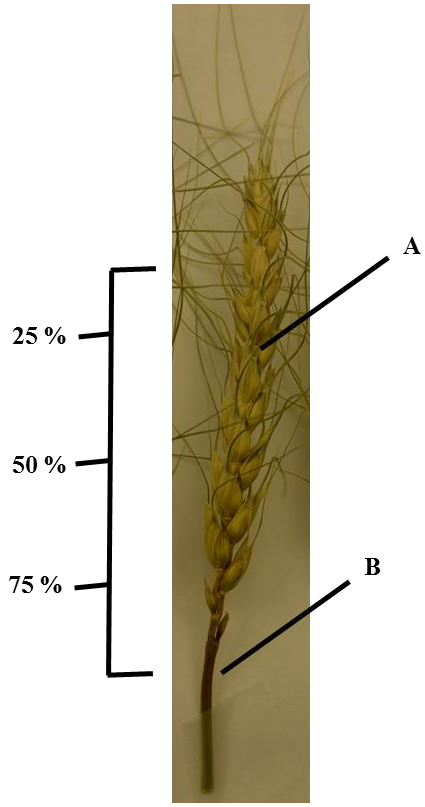

Figure 3.22: Percent Scoring of Rachis in FHB Infected Plants. A GFP plant head 13 days past FHB infection. A 25% infection is representative of an infection around the original inoculation site (A). A 100 % infection is representative of an infection that has spread all the way to main stem of the plant (B). This example head is showing a 100% infected rachis.

The PYL5.2A plants were found to have, on average, a 46.6 % infected rachis seven days post *F. graminearum* treatments while the GFP control plants were found to be 84.6% infected (Figure 3.23).

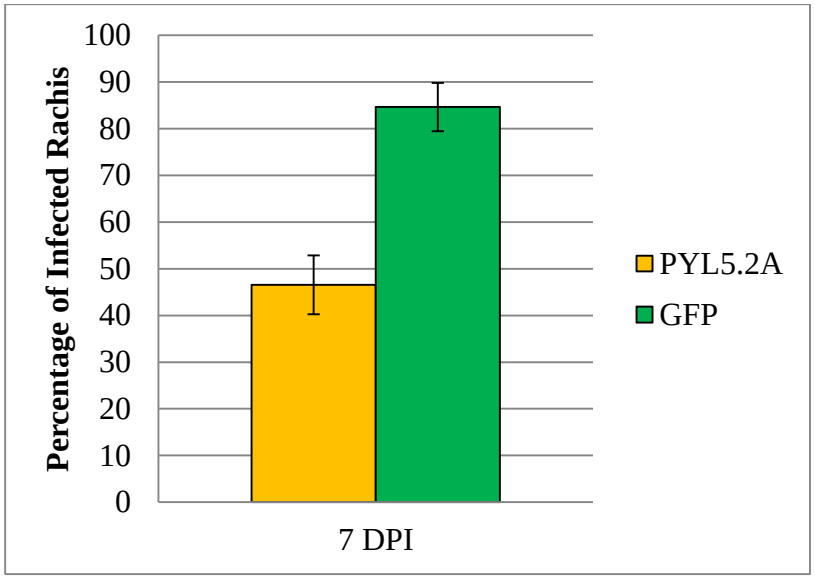

Figure 3.23: Measurement of FHB Disease Progression in Wheat Head Rachis. The average percent of infected rachis within a PYL5.2A population (n=29, orange) versus a GFP control population (n=26, green) seven days past FHB infection. Standard error bars are shown.

These results show that the receptor knock-down plants are able to resist the spread of FHB when compared to control plants up to 7 DPI. Overall the receptor knock-down plants looked healthier than control plants until 9 DPI. At 9 DPI FHB in TaPYL5.2A plants does catch up to infected GFP plant levels (Figure 3.21). This could be because the level of knock-down is not sufficient to maintain the resistance due to the redundancy in ABA signaling pathway, the effectors that the fungus is producing in the later stages of the infection are sufficient enough to overcome the resistance response, or the VIGS construct levels decrease to a level wherein they are no-longer effective.

3.6.5 Quantification of Knockdown by Q-PCR

Relative *TaPYL5.2A* gene expression levels were measured with quantitative real time PCR. Due to high sequence identity between the chromosome four receptors (Appendix 6.3) and beyond, the expression data and observed knockdown of *TaPYL5.2A* is expected to be representative of not just the one receptor but the whole group of receptors with only a few SNP differences between them. Using GFP controls as the reference sample there was a 35% decrease in *TaPYL5.2A* relative expression levels 7 days past *F. graminearum* infections, which is 14 days past BSMV infection (Figure 3.24).

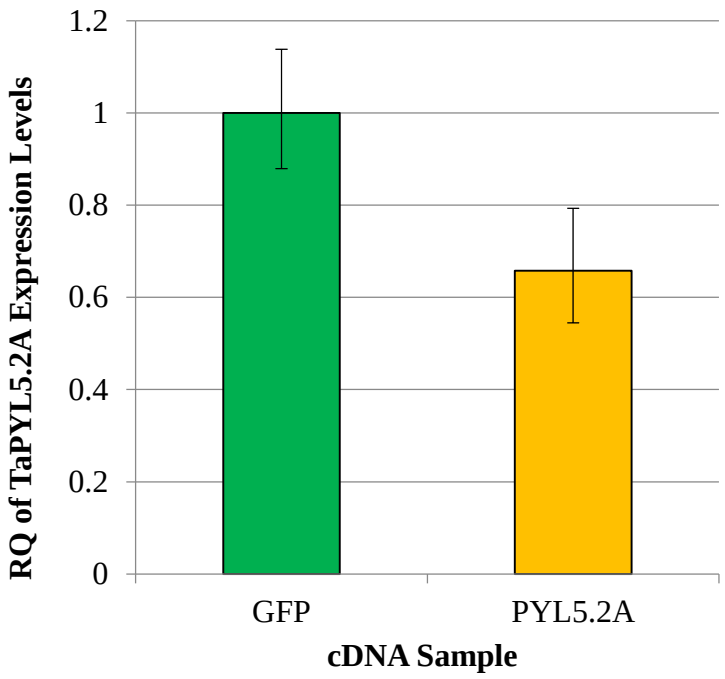

Figure 3.24: Relative *TaPYL5.2A* Gene Expression Levels 14 days past BSMV Infection in Wheat. Quantification of *TaPYL5.2A* gene expression was performed with a StepOne instrument and software (Applied Biosystems) 14 days past VIGS. TaActin was used as an endogenous control. The green GFP bar is representative of the *TaPYL5.2A* expression level in cDNA prepared from GFP control plants. The orange PYL5.2A bar is representative of the *TaPYL5.2A* expression level in cDNA prepared from BSMVγLIC-PYL5.2A treated plants. The expression level of the control (GFP) was set to a relative value of 1 while the PYL5.2A samples were presented relatively to the control (n=3).

The expression levels of TaPYL5.2A were hypothesized to increase during *F. graminearum* infection, which was the basis of the knock-down experiments. Preliminary Q-PCR data from wheat infected with *Fusarium graminearum* showed an induction of a gene with high sequence identity to TaPYL5.1 (data not shown, and personal communication T. Ouellet, AAFC). Relative TaPYL5.2A gene expression levels were measured with quantitative real time PCR on DNA from plants that were infected with FHB. The expression of TaPYL5.2A was found to increase in GFP control samples infected with FHB (Figure 3.25). A similar result was also observed where TaPYL5.2A levels were found to decrease in TaPYL5.2A knock-down plants

versus GFP controls in the non-FHB treated plants (Figure 3.24). The knock-down plants treated with both BSMVγLIC-PYL5.2A and FHB were found to have no increase over the BSMVγLIC-PYL5.2A only plants (Figure 3.25). In conclusion, receptor expression increased more than two fold in GFP plants after *F. graminearum* infection while the VIGS construct reduced expression levels of TaPYL5.2A in both infected and non-infected tissue samples taken at 12 days past VIGS or 5 days past *F. graminearum* infection.

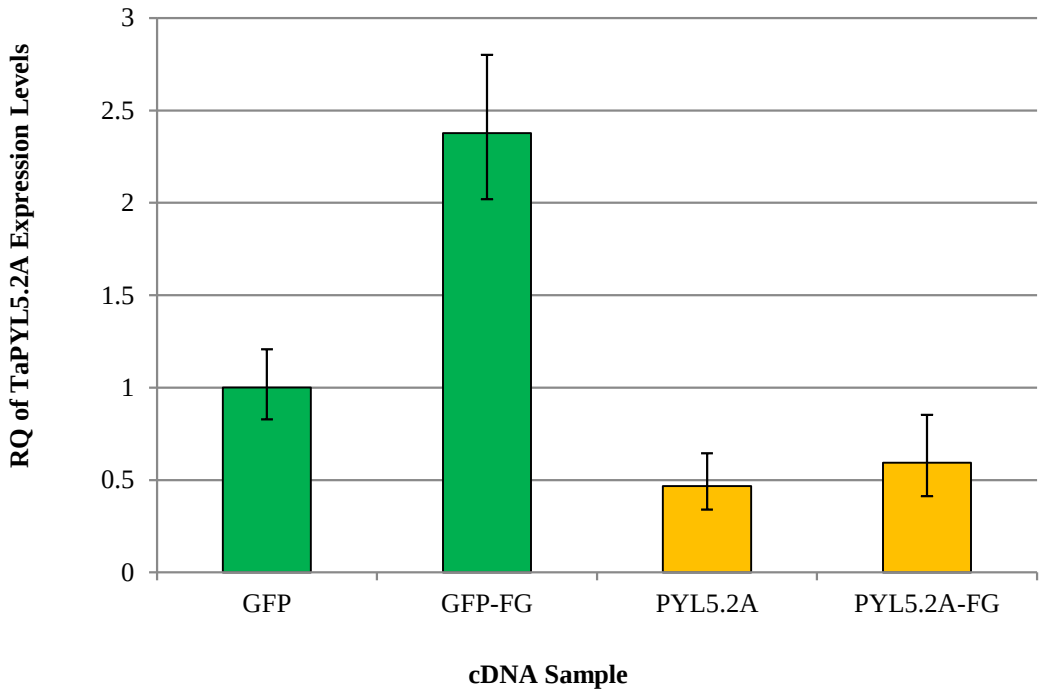

Figure 3.25: Relative *TaPYL5.2A* Gene Expression Levels 12 Days Past BSMV, and Five Days Past Fusarium Infections. Quantification of *TaPYL5.2A* gene expression was performed with a StepOne instrument and software (Applied Biosystems) 12 days past VIGS and 5 days past *Fusarium* treatment. TaActin was used as an endogenous control. The green GFP bars are representative of the *TaPYL5.2A* expression level in cDNA prepared from GFP control plants. The orange PYL5.2A bars are representative of the *TaPYL5.2A* expression level in cDNA prepared from BSMVγLIC-PYL5.2A treated plants. The expression level of the control (GFP) was set to a relative value of 1 while the PYL5.2A samples were presented relatively to the control. Bars labeled with –FG are *Fusarium* treated (n=3).

3.6.6 DON Quantification of FHB Infected Plants

DON quantification analysis was completed with result shown in Figure 3.26. The samples were taken at five and 13 days past *F. graminearum* treatment. The PYL5.2A plants were found to accumulate a significantly lower amount of DON at both time points, which is consistent with the phenotypic data, indicating that the disease was less prevalent in the PYL5.2A knockdown plants (Figure 3.26).

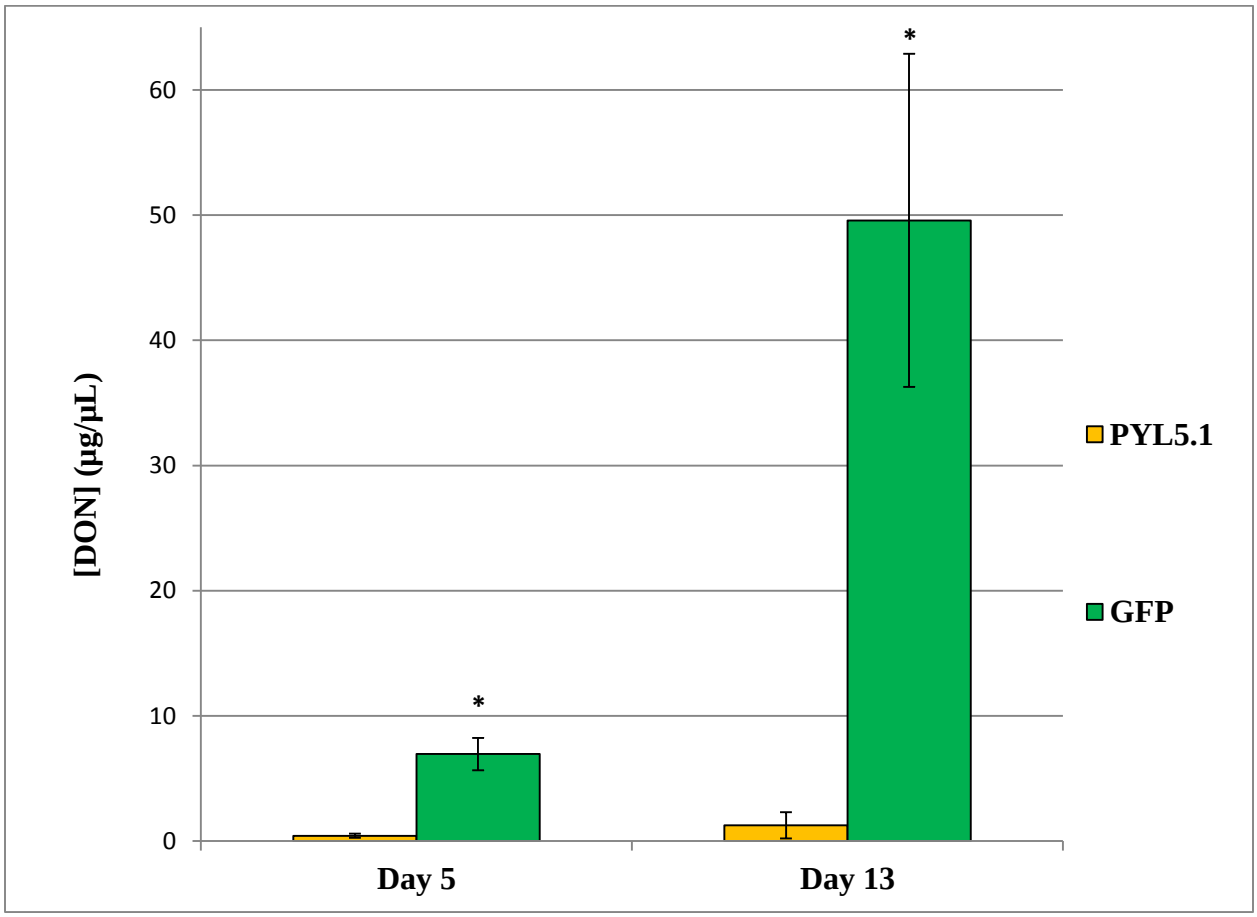

Figure 3.26: DON Analysis of FHB Infected Wheat Head Samples. Samples were analyzed with LC/MS. GFP VIGS control samples (green) were compared to PYL5.2A VIGS knockdown samples (orange) at 5 and 13 days past *F. graminearum* infection (n=3). Error bars are standard error. Data was analyzed with a t-test and found to be significant between control and knock-down samples ($p = 0.05$).

4.0 DISCUSSION

4.1 Putative Wheat ABA Receptors

To date 13 putative wheat ABA receptors have been identified using online databases (Appendix). With 14 ABA receptors in *Arabidopsis*, and 13 in rice it would be reasonable in assuming wheat should have around 13 on each subgenome. Taking into account replicates across the wheat subgenomes, the 13 putative receptors becomes nine, which will likely only represent a portion of the total number or receptors in the wheat genome. Recently one of the identified genes, TaPYL2, was annotated in NCBI (gi|669028527) as an "unnamed protein product" (Choulet *et al*., 2014) which suggests that there will be more simplistic searches for ABA receptors in the future. The incomplete online databases created a lot of challenges when searching for ABA receptors. There are many short partial receptor sequences available but the only ones included in this study were those found on a single contig with a complete open reading frame. A preliminary search using more advanced techniques was initiated to identify "hidden" genes across contigs or containing introns and exons, however this search was not successful.

4.2 TaPYL5.1 is an ABA Receptor *In Vitro*

4.2.1 ABA Receptor & PP2C Activities

The high level of protein sequence identity between TaPYL5.1 and AtPYL5 (58% identity at 85% coverage) suggested that TaPYL5.1 was an abscisic acid receptor in wheat. Recombinant TaPYL5.1 was expressed, purified, and tested for enzymatic activity confirming it as a wheat ABA receptor *in vitro* (Figures 3.4, 3.5, 3.9). TaPYL5.1 was also found to interact with *Arabidopsis* PP2Cs, a result that was hypothesized due to the high level of identity between TaPYL5.1 and AtPYL5 at the important active site residues involved in ABA docking and the PP2C interface

(Figure 3.12, 3.13) (Dorosh et al., 2013). TaPYL5.1 interacting with the four PP2Cs in an ABA dependent manner resulted in a strong 90-95% inhibition of PP2C activity (Figure 3.12 A-D). A 90-95% inhibition of a PP2C activity would result in an increase in downstream ABA signaling events in a living plant (Umezawa *et al*., 2009)

The wheat PP2C TaABI1 was also paired with three *Arabidopsis* ABA receptors. The AtPYL5/TaABI1 pairing showed similar results to those discussed above (Figure 3.12 E), while the AtPYL6 and AtPYR1 pairings were less clear (Figure 3.12 F-G). The TaABI1 PP2C has 60% overall identity with AtABI1, with identity in the PP2C interface even higher. As expected, AtABI1 was able to act as a substitute for TaABI1 in enzyme activity assays. When looking at the AtPYL6/TaABI1 pairing there is at least a 38% inhibition of TaABI1, with (+) ABA and the (+) analogs (except 352). The levels of inhibition are not as strong possibly because normally the receptor binds the ligand and forms the PP2C interface, therefore TaPYL6 may not form as compatible a hydrophobic interface as AtPYL5 for association with TaABI1. The lower level of inhibition with the AtPYR1/TaABI1 paring was discussed in section 3.4.3.

4.2.2 ABA Analogs

Many ABA analogs have been designed in an attempt to address various physiological issues. The analogs used in this study were chosen to identify significant functional differences between *Arabidopsis* and wheat ABA receptors and to link those differences to the structure of both the analog and the receptors. The panel of ABA analogs that was chosen had been previously used in other structure/function studies in *Arabidopsis*, and were available for use at the NRC (Benson *et al*., 2014; Zaharia *et al*., 2005). Benson *et al.* (2014) used these ABA analogs in order identify differences in the binding of ABA to receptors as they form complexes with the PP2Cs.

Zaharia *et al.* (2005) suggested that as the structure of binding pockets becomes more readily available, it should be possible to design a structurally defined analog to fit one receptor but not another. The finding that the S-hexyl chain in the antagonist ASN6 blocks PP2C binding by steric hindrance validates that a structure-based approach to the design of a receptor antagonist is possible (Takeuchi *et al.*, 2015; Takeuchi *et al.*, 2014).

The analog assays highlighted that regardless of the PP2C used, when TaPYL5.1 was assayed with most of the (+) or (S) analogs or ABA there was a high level of PP2C inhibition which would represent a high level of increase in downstream SnRK2 kinase activation resulting in ABF transcription factor activation (Figure 3.12 A-D) (Furihata *et al*., 2006; Umezawa *et al*., 2009; Zhao *et al.*, 2013). The exceptions to this would be with analogs 352 and 694 with the most interesting result in these experiments being with analog 352 which is discussed in the next section (4.2.3). Analog 694 resulted in various decreases in PP2C inhibition in comparison to ABA and the other (+) analogs and these differences depended on which PP2C was paired with TaPYL5.1 (Figure 3.12 A-D). A further 694 structural analysis was not completed, however it is known that 694 differs from ABA by replacing the 8' methyl group with a cyclopropyl group. This information could be useful in designing an analog that combines the attributes of 352 and 694 to develop a strong antagonist in the TaPYL5.1 signaling pathway.

4.2.3 Analog 352

Section 3.4.4 showed the results of the comparison of wheat and *Arabidopsis* PYL5 enzymatic activity. The aim was to look at differences in enzymatic activities only changing one variable at a time thereby pointing towards possible important interactions in wheat ABA signaling. The ABA analog 352 assay produced interesting results that needed to be analyzed

further. It was found that regardless of the PP2C used there was a 50% decrease in inhibitory activity when TaPYL5.1 was used instead of AtPYL5 (Figure 3.14 A). Since the same decrease was found regardless of PP2C the mode of the decrease must be in the ABA receptor. It was necessary to use the model of the receptor to work out which residues are responsible for this unique response in wheat.

A major interaction between ABA and the receptor is a salt-bridge formed between lysine 85 (K85) and ABA, and this residue is highly conserved across all receptors including TaPYL5.1. The carboxyl of ABA forms a salt bridge with the amine group of lysine as well as a water-mediated hydrogen bond network with several side chains of polar residues (Zhang *et al*., 2015). The structural difference between ABA and analog 352 is that 352 has the proton of the hydroxyl group replaced with a methyl group (Figure 3.10). There are no direct interactions from the receptor to the 1'OH group on ABA but normally there are two hydrogen bonds formed through two separate water mediated interactions (Dorosh *et al*., 2013). N192 is a hydrogen bond donor and E119 is a hydrogen bond acceptor (Figure 4.1). The replacement of the 1'OH group with a methyl group would disrupt this hydrogen bonding and shift 352 within the pocket. The addition of a bulky methyl group would also affect binding. V135 has a hydrophobic interaction with the 6' methyl groups on ABA. The presence of another methyl group in the proximity of the 6' groups would potentially shift 352 within the pocket as well (Figure 4.1).

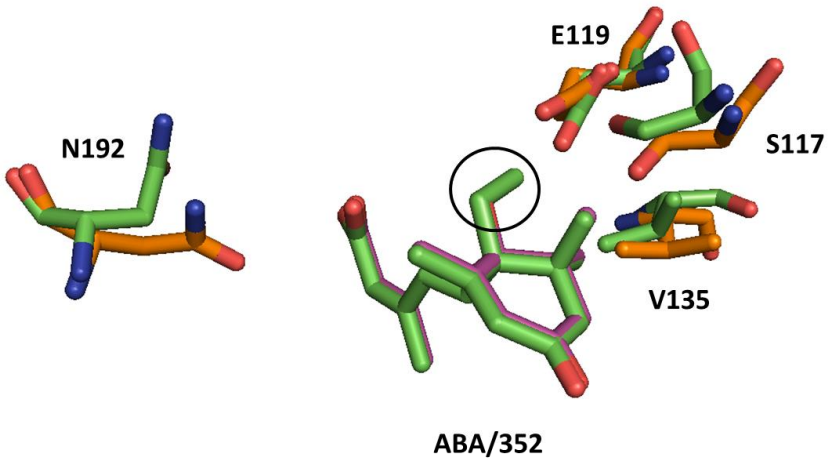

Figure 4.1: Interactions Between the 1' Hydroxyl Group of ABA and the Receptors. The hydroxyl group of ABA (pink) substituted for a methyl group on 352 (green) is highlighted with a black circle. TaPYL5.1 model residues are shown in orange and AtPYL5 (PDB 4JDL) in green.

The differences in the binding of 352 relative to ABA in the pocket could be affecting the activity of the TaPYL5.1 and AtPYL5, and AtPYL5 is able to accommodate the differences and remain biologically active while TaPYL5.1 is not (Figure 3.14 A). The residues in the receptors that are involved in ABA interaction are highly conserved. The wheat receptor TaPYL5.1 and *Arabidopsis* AtPYL5 show 100% identity in the ABA pocket. The only differences in residues that are involved in activity are found in the receptor/PP2C interface. The three differences at the TaPYL5.1/PP2C binding surface when compared to AtPYL5 are N86S, E180D, and S183V (*Arabidopsis* to Wheat) (Figure 3.3, 4.2). There is a highly conserved tryptophan residue in the phosphatase that interacts directly with ABA through a water molecule to the 4' ketone group (Melcher et al., 2009). This residue in AHG3 (or PP2CA) is W280. W280 is termed the "lock" and there could be problems with this residue's mode of action if there is a shift in the pocket during 352 binding in wheat (Figure 4.2). Receptor residues 180 and 183 are in close proximity and would be able to interact with the W280 containing loop. A serine to a valine is a hydrophilic to hydrophobic change. S183 would repel I278 and form a bond with R276 whereas V183 would

want to interact with the hydrophobic, non-polar I278 and repel R276 (Figure 4.3). Because of the proximity of these residues to W280 the S183V substitution could act to shift W280 in a way that is less desirable for complex formation. Mosquna *et al.* (2011) screened a wide selection of active site and PP2C interface residue mutations in the *Arabidopsis* receptor PYR1. In this earlier study, the mutation M158V (M183V in this thesis) was shown to increase the activation of the receptor giving evidence that a valine residue at that position is important for stronger signaling which gives evidence against the wheat residue V183 being the cause of the decrease in activity (Mosquna *et al*., 2011). The E180D substitution is the one with potentially the least affect. Aspartate and glutamate are very similar and vary only in glutamate having one extra carbon in the R group. However, the glutamate is longer, and has been shown to be involved in PP2C interaction (Dorosh *et al*., 2013) therefore it is possible that the shorter aspartate residue is less able to interact with the PP2C which causes a decrease in activity.

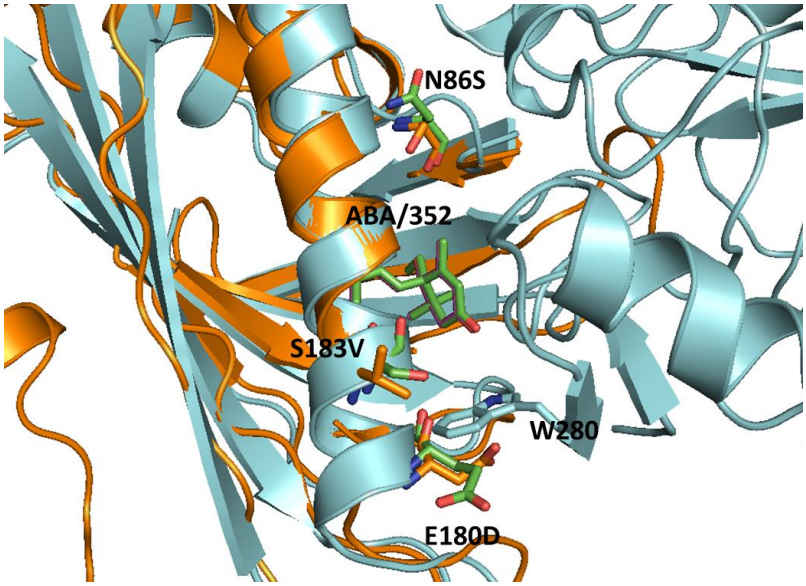

Figure 4.2: Three Residue Substitutions in the PP2C Interface. The TaPYL5.1 model (orange) aligned with PYL13 bound to AHG3 (blue). AtPYL5 residues are shown in green. Tryptophan 280 the "lock" residue is shown in close proximity to residues at the 180 and 183 positions.

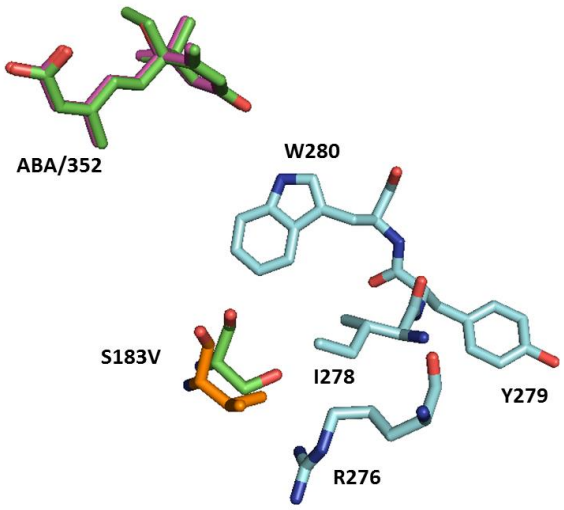

Figure 4.3: Receptor Residue 183 Interactions with PP2C Loop Containing W280. TaPYL5.1 residue is shown in orange, AtPYL5 in green, and AHG3 in blue.

Serine is less bulky than asparagine and has one less group that could be involved in hydrogen bonding but both amino acids are polar and hydrophilic. The asparagine and serine residues are the closest residues to the 352 methyl substitution at approximately 9 angstroms. It is therefore possible that these residues will feel the shift within the binding pocket more than the other substitutions and the less bulky and bondable serine residue in the wheat receptor will not be able to bind the PP2C as tightly thereby decreasing the inhibition activity. The carboxamide functional group of Asn86 in AtPYL5 is in close proximity to two loops on AHG3 (Figure 4.4). The loops contain several potential hydrogen bonding partners; Arg209, Gln216, Cys217, Asp218, and Tyr299.

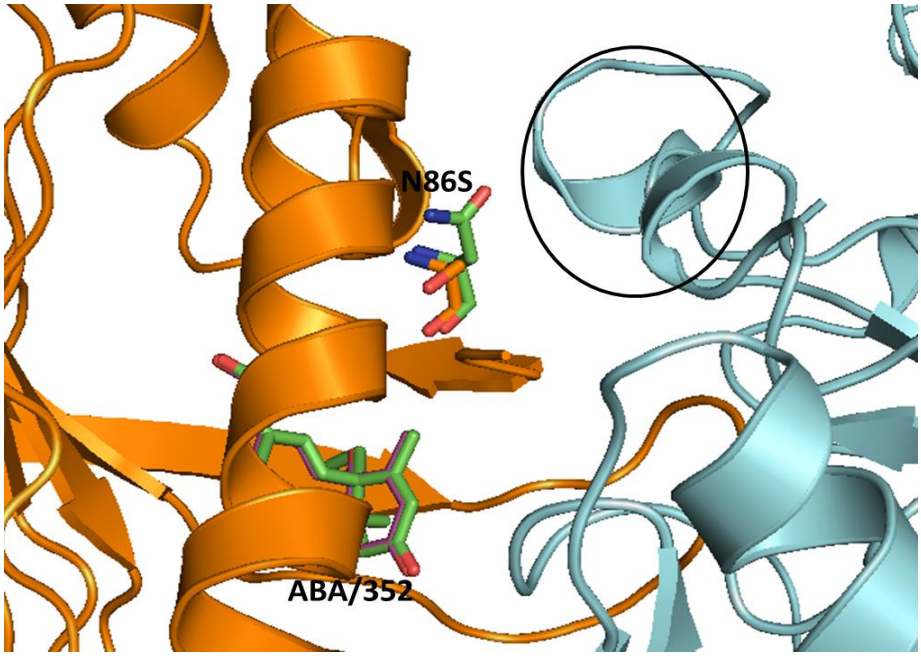

Figure 4.4: Asparagine 86 is Able to Bind to PP2C Loops. There are several polar hydrophilic residues in the loop marked with the black circle that could more readily hydrogen bond to asparagine 86 than serine 86.

Overall, the modelling suggests two residues that could be involved in the significant decrease in PP2C inactivation when analog 352 is used with wheat. The wheat residues S86 and V183 are potentially involved in a wheat specific response to analog 352 where it acts as an antagonist instead of an agonist in *Arabidopsis*. These results suggest a future direction of development of plant species specific analogs. It would be a powerful tool to be able to enhance ABA signaling in one plant and not another, or to be able to antagonize ABA signaling during times of biotic stress. A recent review of ABA signaling during biotic/abiotic stress term the chemical signaling "a double edged sword" (Spence and Bais, 2015). Spence & Bais (2015) discus how although plants use ABA as a positive effector in times of abiotic stress, it is also crucial in times of biotic stress where it plays a role in disease susceptibility to fungal and bacterial pathogens.

4.3 TaPYL5.2A Plays a Role in FHB Disease Progression

The role that the wheat ABA receptor TaPYL5.2A plays in the disease response is unknown but, this receptor does in some way contribute to early disease susceptibility, witnessed through the early disease resistance phenotype in multiple plant trials (Figure 3.20). The VIGS knock-down trials are not conclusive proof of what is happening in this complex pathway, but is evidence that the wheat ABA signaling pathway does play a role in fungal disease susceptibility.

Type II is resistance to fungus spread in the host and a Type II resistance was shown in the head during the initial stages of FHB infection (Figure 3.21). Resistant plants had a decrease in TaPYL5.2A expression levels (Figure 3.24 & 3.25). Type V resistance is characterized by a decrease in DON levels and evidence of decreased DON levels in knock-down plants versus control plants was also found (Figure 3.26). These results suggest that there is a resistant response in the knock-down plants, and this response correlates to a decrease in TaPYL5.2A levels and DON accumulation. These quantification results were taken from a single plant trial. Even though there was a reproducible phenotype during the plant trials, it took several trials to obtain the quantification results. Putting aside problems with equipment and non-target disease, the VIGS system was at times too strong of an infection to co-infect with FHB. The control plants were a way to mitigate this, but during some trials is was difficult to distinguish between FHB and the viral phenotype. I believe the VIGS system described within this thesis to be a reliable way to knockdown target genes in wheat, however, when coupled with FHB it can be too potent to the plant.

Another issue with the quantification data was that it did not all pass the Student's t-test. All the data was statistically significant when using standard error (Standard Deviation (s) / $\sqrt{n}$)

but only the DON data was significant with the Student's t-test. This was due to a large variation in disease between plants in the different sample populations.

4.4 Conclusions

The goals of this project were to identify and confirm wheat ABA receptors, analyze the ABA binding pocket using an ABA analog approach, and to determine if decreased ABA receptor levels correlates to a decrease in severity of FHB. In conclusion, this study led to the following three main results; i) TaPYL5.1 is a wheat ABA receptor that is likely part of a larger family of ABA receptors, ii) analog 352 has a selective effect between TaPYL5.1 and AtPYL5 suggesting evidence to develop wheat specific ABA analogs that could modulate biotic and abiotic stress responses, and iii) the TaPYL5.2A gene, a paralog of TaPYL5.1, is up-regulated during FHB infection and the knock-down of this gene using a VIGS system confers an early Type II FHB resistance and a decrease in the levels of DON, however, the phenotypical results obtained could be questionable due to the potency of the VIGS system coupled with FHB infections.

4.5 Future Directions

It will be necessary to continue mining the online databases to find the rest of the wheat ABA receptors, and other signaling pathway members, once the genomic databases become more complete. The ABA signaling pathway is well explored in *Arabidopsis* and other food crops such as rice so the same principles that were applied to find receptors could also be applied to find players in the wheat ABA biosynthesis pathways and signaling network. Some preliminary RNA seq and Q-PCR on known ABA signaling pathway members was completed but much more work is needed as it will be necessary to look at which genes are being up and down regulated during

the stress response on wheat plants that are infected with *Fusarium graminearum* in non-VIGS treated plants.

There are a combination of different point mutations that will need to be carried out to verify what was found in the activity assays and subsequent modeling. There are three residues of interest in TaPYL5.1; S86, D180, and V183. If these three residues are mutated to the corresponding residue in the *Arabidopsis* PYL5 and activity is restored than those three residues will be shown to be involved in a wheat specific response to analog 352.

5.0 REFERENCES

AAFC (2013). 2013 Annual Review of Agroclimate Conditions Across Canada.

Altschul, S.F., Gish, W., Miller, W., Myers, E.W., and Lipman, D.J. (1990). Basic local alignment search tool. Journal of Molecular Biology *215*, 403-410.

Anderson, J.P., Badruzsaufari, E., Schenk, P.M., Manners, J.M., Desmond, O.J., Ehlert, C., Maclean, D.J., Ebert, P.R., and Kazan, K. (2004). Antagonistic interaction between abscisic acid and jasmonate-ethylene signaling pathways modulates defense gene expression and disease resistance in Arabidopsis. Plant Cell *16*, 3460-3479.

Artimo, P., Jonnalagedda, M., Arnold, K., Baratin, D., Csardi, G., de Castro, E., Duvaud, S., Flegel, V., Fortier, A., Gasteiger, E., *et al.* (2012). ExPASy: SIB bioinformatics resource portal. Nucleic acids research *40*, W597-603.

Benson, C.L., Kepka, M., Wunschel, C., Rajagopalan, N., Nelson, K.M., Christmann, A., Abrams, S.R., Grill, E., and Loewen, M.C. (2014). Abscisic acid analogs as chemical probes for dissection of abscisic acid responses in *Arabidopsis thaliana*. Phytochemistry *113*, 96-107.

Benson, D.A., Karsch-Mizrachi, I., Lipman, D.J., Ostell, J., and Sayers, E.W. (2010). GenBank. Nucleic Acids Research *38*, D46-51.

Berman, H.M., Westbrook, J., Feng, Z., Gilliland, G., Bhat, T.N., Weissig, H., Shindyalov, I.N., and Bourne, P.E. (2000). The Protein Data Bank. Nucleic Acids Research *28*, 235-242.

Bol, J.F., Linthorst, H.J.M., and Cornelissen, B.J.C. (1990). Plant pathogenesis-related proteins induced by virus infection. Annual Review of Phytopathology *28*, 113-138.

Boneh, U., Biton, I., Zheng, C., Schwartz, A., and Ben-Ari, G. (2012). Characterization of potential ABA receptors in *Vitis vinifera*. Plant Cell Reports *31*, 311-321.

Boursiac, Y., Leran, S., Corratge-Faillie, C., Gojon, A., Krouk, G., and Lacombe, B. (2013). ABA transport and transporters. Trends in Plant Science *18*, 325-333.

Bowden, R.L., and Leslie, J.F. (1992). Nitrate-nonutilizing mutants of *Gibberella zeae* (*Fusarium graminearum*) and their use in determining vegetative compatibility. Experimental Mycology *16*, 308-315.

Bradford, M.M. (1976). A rapid and sensitive method for the quantitation of microgram quantities of protein utilizing the principle of protein-dye binding. Analytical Biochemistry *72*, 248-254.

Browse, J. (2009). Jasmonate passes muster: A receptor and targets for the defense hormone. Annual Review of Plant Biology *60*, 183-205.

Buerstmayr, H., Ban, T., and Anderson, J.A. (2009). QTL mapping and marker-assisted selection for *Fusarium* head blight resistance in wheat: a review. Plant Breeding *128*, 1-26.

Canadian Grain Commission (2014). *Fusarium* head blight in western Canada.

Cao, F.Y., Yoshioka, K., and Desveaux, D. (2011). The roles of ABA in plant-pathogen interactions. Journal of Plant Research *124*, 489-499.

Cao, M., Liu, X., Zhang, Y., Xue, X., Zhou, X.E., Melcher, K., Gao, P., Wang, F., Zeng, L., Zhao, Y., *et al.* (2013). An ABA-mimicking ligand that reduces water loss and promotes drought resistance in plants. Cell Research *23*, 1043-1054.

Chai, Y.M., Jia, H.F., Li, C.L., Dong, Q.H., and Shen, Y.Y. (2011). FaPYR1 is involved in strawberry fruit ripening. Journal of Experimental Botany *62*, 5079-5089.

Choulet, F., Alberti, A., Theil, S., Glover, N., Barbe, V., Daron, J., Pingault, L., Sourdille, P., Couloux, A., Paux, E., *et al.* (2014). Structural and functional partitioning of bread wheat chromosome 3B. Science *345*, 1249721.

Christmann, A., Moes, D., Himmelbach, A., Yang, Y., Tang, Y., and Grill, E. (2006). Integration of abscisic acid signalling into plant responses. Plant Biology *8*, 314-325.

Coordinators, N.R. (2014). Database resources of the National Center for Biotechnology Information. Nucleic Acids Research.

Cutler, S.R., Rodriguez, P.L., Finkelstein, R.R., and Abrams, S.R. (2010). Abscisic acid: emergence of a core signaling network. Annual Review of Plant Biology *61*, 651-679.

De Vleesschauwer, D., Höfte, M., and Xu, J. (2014). Making sense of hormone-mediated defense networking: from rice to *Arabidopsis*. Frontiers in Plant Science *5*, 611.

De Wolf, E.D., Madden, L.V., and Lipps, P.E. (2003). Risk assessment models for wheat *Fusarium* head blight epidemics based on within-season weather data. Phytopathology *93*, 428-435.

Deller, S., Hammond-Kosack, K.E., and Rudd, J.J. (2011). The complex interactions between host immunity and non-biotrophic fungal pathogens of wheat leaves. Journal of Plant Physiology *168*, 63-71.

Deng, W., Nickle, D.C., Learn, G.H., Maust, B., and Mullins, J.I. (2007). ViroBLAST: a stand-alone BLAST web server for flexible queries of multiple databases and user's datasets. Bioinformatics *23*, 2334-2336.

Dorosh, L., Kharenko, O.A., Rajagopalan, N., Loewen, M.C., and Stepanova, M. (2013). Molecular mechanisms in the activation of abscisic acid receptor PYR1. PLoS Computational Biology *9*, e1003114.

Finkelstein, R.R., Gampala, S.S., and Rock, C.D. (2002). Abscisic acid signaling in seeds and seedlings. Plant Cell *14 Suppl*, S15-45.

Finkelstein, R.R., and Rock, C.D. (2002). Abscisic acid biosynthesis and response. The Arabidopsis Book / American Society of Plant Biologists *1*, e0058.

Foroud, N.A., and Eudes, F. (2009). Trichothecenes in cereal grains. International Journal of Molecular Sciences *10*, 147-173.

Foroud, N.A., Ouellet, T., Laroche, A., Oosterveen, B., Jordan, M.C., Ellis, B.E., and Eudes, F. (2012). Differential transcriptome analyses of three wheat genotypes reveal different host response pathways associated with *Fusarium* head blight and trichothecene resistance. Plant Pathology *61*, 296-314.

Fu, Z.Q., and Dong, X. (2013). Systemic acquired resistance: Turning local infection into global defense. Annual Review of Plant Biology *64*, 839-863.

Furihata, T., Maruyama, K., Fujita, Y., Umezawa, T., Yoshida, R., Shinozaki, K., and Yamaguchi-Shinozaki, K. (2006). Abscisic acid-dependent multisite phosphorylation regulates the activity of a transcription activator AREB1. Proceedings of the National Academy of Sciences of the United States of America *103*, 1988-1993.

Gautam, P., and Macky, R.D. (2011). Type I host resistance and trichothecene accumulation in *Fusarium*-infected wheat heads. American Journal of Agricultural and Biological Sciences *6*, 231-241.

Gill, U.S., Lee, S., and Mysore, K.S. (2015). Host versus nonhost resistance: Distinct wars with similar arsenals. Phytopathology *105*, 580-587.

Glazebrook, J. (2005). Contrasting mechanisms of defense against biotrophic and necrotrophic pathogens. Annual Review of Phytopathology *43*, 205-227.

Godfray, H.C., Beddington, J.R., Crute, I.R., Haddad, L., Lawrence, D., Muir, J.F., Pretty, J., Robinson, S., Thomas, S.M., and Toulmin, C. (2010). Food security: the challenge of feeding 9 billion people. Science *327*, 812-818.

Goujon, M., McWilliam, H., Li, W., Valentin, F., Squizzato, S., Paern, J., and Lopez, R. (2010). A new bioinformatics analysis tools framework at EMBL-EBI. Nucleic Acids Research *38*, W695-699.

Government of Saskatchewan (2007). *Fusarium* head blight. Agriculture, ed.

He, Y., Hao, Q., Li, W., Yan, C., Yan, N., and Yin, P. (2014). Identification and characterization of ABA receptors in *Oryza sativa*. PLoS One *9*, e95246.

Holzberg, S., Brosio, P., Gross, C., and Pogue, G.P. (2002). Barley stripe mosaic virus-induced gene silencing in a monocot plant. Plant Journal *30*, 315-327.

Inoue, H., Nojima, H., and Okayama, H. (1990). High efficiency transformation of *Escherichia coli* with plasmids. Gene *96*, 23-28.

International Wheat Genome Sequencing, C. (2014). A chromosome-based draft sequence of the hexaploid bread wheat (*Triticum aestivum*) genome. Science *345*, 1251788.

Jansen, C., von Wettstein, D., Schafer, W., Kogel, K.H., Felk, A., and Maier, F.J. (2005). Infection patterns in barley and wheat spikes inoculated with wild-type and trichodiene synthase gene disrupted *Fusarium graminearum*. Proceedings of the National Academy of Sciences of the United States of America *102*, 16892-16897.

Jefferys, B.R., Kelley, L.A., and Sternberg, M.J. (2010). Protein folding requires crowd control in a simulated cell. Journal of Molecular Biology *397*, 1329-1338.

Kang, J., Hwang, J.U., Lee, M., Kim, Y.Y., Assmann, S.M., Martinoia, E., and Lee, Y. (2010). PDR-type ABC transporter mediates cellular uptake of the phytohormone abscisic acid. Proceedings of the National Academy of Sciences of the United States of America *107*, 2355-2360.

Kanno, Y., Hanada, A., Chiba, Y., Ichikawa, T., Nakazawa, M., Matsui, M., Koshiba, T., Kamiya, Y., and Seo, M. (2012). Identification of an abscisic acid transporter by functional screening using the receptor complex as a sensor. Proceedings of the National Academy of Sciences of the United States of America *109*, 9653-9658.

Kelley, L.A., and Sternberg, M.J. (2009). Protein structure prediction on the Web: a case study using the Phyre server. Nature Protocols *4*, 363-371.

Kharenko, O.A., Boyd, J., Nelson, K.M., Abrams, S.R., and Loewen, M.C. (2011). Identification and characterization of interactions between abscisic acid and mitochondrial adenine nucleotide translocators. Biochemical Journal *437*, 117-123.

Kim, H., Hwang, H., Hong, J.W., Lee, Y.N., Ahn, I.P., Yoon, I.S., Yoo, S.D., Lee, S., Lee, S.C., and Kim, B.G. (2012). A rice orthologue of the ABA receptor, OsPYL/RCAR5, is a positive regulator of the ABA signal transduction pathway in seed germination and early seedling growth. Journal of Experimental Botany *63*, 1013-1024.

Koga, H., Dohi, K., and Mori, M. (2004). Abscisic acid and low temperatures suppress the whole plant-specific resistance reaction of rice plants to the infection of *Magnaporthe grisea*. Physiological and Molecular Plant Pathology *65*, 3-9.

Koressaar, T., and Remm, M. (2007). Enhancements and modifications of primer design program Primer3. Bioinformatics *23*, 1289-1291.

Kuromori, T., Miyaji, T., Yabuuchi, H., Shimizu, H., Sugimoto, E., Kamiya, A., Moriyama, Y., and Shinozaki, K. (2010). ABC transporter AtABCG25 is involved in abscisic acid transport and responses. Proceedings of the National Academy of Sciences of the United States of America *107*, 2361-2366.

Kushiro, M. (2008). Effects of milling and cooking processes on the deoxynivalenol content in wheat. International Journal of Molecular Sciences *9*, 2127-2145.

Lackman, P., Gonzalez-Guzman, M., Tilleman, S., Carqueijeiro, I., Perez, A.C., Moses, T., Seo, M., Kanno, Y., Hakkinen, S.T., Van Montagu, M.C., *et al.* (2011). Jasmonate signaling involves the abscisic acid receptor PYL4 to regulate metabolic reprogramming in Arabidopsis and tobacco. Proceedings of the National Academy of Sciences of the United States of America *108*, 5891-5896.

Lacomme, C. (2015). Strategies for altering plant traits using virus-induced gene silencing technologies. Methods in Molecular Biology *1287*, 25-41.

Li, G., Xin, H., Zheng, X.F., Li, S., and Hu, Z. (2012). Identification of the abscisic acid receptor VvPYL1 in *Vitis vinifera*. Plant Biology *14*, 244-248.

Li, G., and Yen, Y. (2008). Jasmonate and ethylene signaling pathway may mediate *Fusarium* head blight resistance in wheat. Crop Science *48*, 1888-1896.

Li, W., Wang, L., Sheng, X., Yan, C., Zhou, R., Hang, J., Yin, P., and Yan, N. (2013). Molecular basis for the selective and ABA-independent inhibition of PP2CA by PYL13. Cell Research *23*, 1369-1379.

Lovell, S.C., Davis, I.W., Arendall, W.B., de Bakker, P.I., Word, J.M., Prisant, M.G., Richardson, J.S., and Richardson, D.C. (2003). Structure validation by Calpha geometry: phi,psi and Cbeta deviation. Proteins *50*, 437-450.

Lu, R., Martin-Hernandez, A.M., Peart, J.R., Malcuit, I., and Baulcombe, D.C. (2003). Virus-induced gene silencing in plants. Methods *30*, 296-303.

Ma, Y., Szostkiewicz, I., Korte, A., Moes, D., Yang, Y., Christmann, A., and Grill, E. (2009). Regulators of PP2C phosphatase activity function as abscisic acid sensors. Science *324*, 1064-1068.

Makandar, R., Nalam, V.J., Lee, H., Trick, H.N., Dong, Y., and Shah, J. (2012). Salicylic acid regulates basal resistance to *Fusarium* head blight in wheat. Molecular Plant-Microbe Interactions *25*, 431-439.

McMullen, M., Jones, R., and Gallenberg, D. (1997). Scab of wheat and barley: A re-emerging disease of devastating impact. Plant Disease *81*, 1340-1348.

McWilliam, H., Li, W., Uludag, M., Squizzato, S., Park, Y.M., Buso, N., Cowley, A.P., and Lopez, R. (2013). Analysis tool web services from the EMBL-EBI. Nucleic Acids Research *41*, W597-600.

Mesterhazy, A. (1995). Types and components of resistance to Fusarium head blight of wheat. Plant Breeding *114*, 377-386.

Mosquna, A., Peterson, F.C., Park, S.Y., Lozano-Juste, J., Volkman, B.F., and Cutler, S.R. (2011). Potent and selective activation of abscisic acid receptors in vivo by mutational stabilization of their agonist-bound conformation. Proceedings of the National Academy of Sciences of the United States of America *108*, 20838-20843.

Nakamura, S., Komatsuda, T., and Miura, H. (2007). Mapping diploid wheat homologues of Arabidopsis seed ABA signaling genes and QTLs for seed dormancy. Theoretical Applied Genetics *114*, 1129-1139.

Nambara, E., and Marion-Poll, A. (2005). Abscisic acid biosynthesis and catabolism. Annual Review of Plant Biology *56*, 165-185.

Ng, L.M., Melcher, K., Teh, B.T., and Xu, H.E. (2014). Abscisic acid perception and signaling: structural mechanisms and applications. Acta Pharmacologica Sinica *35*, 567-584.

Nussbaumer, T., Warth, B., Sharma, S., Ametz, C., Bueschl, C., Parich, A., Pfeifer, M., Siegwart, G., Steiner, B., Lemmens, M., *et al.* (2015). Joint transcriptomic and metabolomic analyses reveal changes in the primary metabolism and imbalances in the subgenome orchestration in the bread wheat molecular response to *Fusarium graminearum*. Genes Genomes Genetics *5*, 2579-2592.

Oh, S.K., Lee, S., Chung, E., Park, J.M., Yu, S.H., Ryu, C.M., and Choi, D. (2006). Insight into Types I and II nonhost resistance using expression patterns of defense-related genes in tobacco. Planta *223*, 1101-1107.

Okamoto, M., Peterson, F.C., Defries, A., Park, S.Y., Endo, A., Nambara, E., Volkman, B.F., and Cutler, S.R. (2013). Activation of dimeric ABA receptors elicits guard cell closure, ABA-regulated gene expression, and drought tolerance. Proceedings of the National Academy of Sciences of the United States of America *110*, 12132-12137.

Pfeifer, M., Kugler, K.G., Sandve, S.R., Zhan, B., Rudi, H., Hvidsten, T.R., International Wheat Genome Sequencing, C., Mayer, K.F., and Olsen, O.A. (2014). Genome interplay in the grain transcriptome of hexaploid bread wheat. Science *345*, 1250091.

Plattner, R.D., and Maragos, C.M. (2003). Determination of deoxynivalenol and nivalenol in corn and wheat by liquid chromatography with electrospray mass spectrometry. Journal of AOAC International *86*, 61-65.

Purkayastha, A., and Dasgupta, I. (2009). Virus-induced gene silencing: a versatile tool for discovery of gene functions in plants. Plant Physiology and Biochemistry *47*, 967-976.

Qin, G., Gu, H., Ma, L., Peng, Y., Deng, X.W., Chen, Z., and Qu, L.J. (2007). Disruption of phytoene desaturase gene results in albino and dwarf phenotypes in *Arabidopsis* by impairing chlorophyll, carotenoid, and gibberellin biosynthesis. Cell Research *17*, 471-482.

Rensink, W.A., and Buell, C.R. (2004). *Arabidopsis* to rice. Applying knowledge from a weed to enhance our understanding of a crop species. Plant Physiology *135*, 622-629.

Rost, B., Yachdav, G., and Liu, J. (2004). The PredictProtein server. Nucleic Acids Research *32*, W321-326.

Saitou, N., and Nei, M. (1987). The neighbor-joining method: a new method for reconstructing phylogenetic trees. Molecular Biology and Evolution *4*, 406-425.

Sambrook, J., and Rusell, D. W. (2001). Molecular cloning : A laboratory manual. Cold Spring Harbor Laboratory Press *3*.

Sanchez-Vallet, A., Lopez, G., Ramos, B., Delgado-Cerezo, M., Riviere, M.P., Llorente, F., Fernandez, P.V., Miedes, E., Estevez, J.M., Grant, M., *et al.* (2012). Disruption of abscisic acid signaling constitutively activates *Arabidopsis* resistance to the necrotrophic fungus *Plectosphaerella cucumerina*. Plant Physiology *160*, 2109-2124.

Schoonbeek, H.J., Wang, H.H., Stefanato, F.L., Craze, M., Bowden, S., Wallington, E., Zipfel, C., and Ridout, C.J. (2015). Arabidopsis EF-Tu receptor enhances bacterial disease resistance in transgenic wheat. The New Phytologist *206*, 606-613.

Schroeder, H.W., and Christensen, J.J. (1963). Factors affecting resistance of wheat to scab cause by *Gibberella zeae*. Phytopathology *53*, 831-838.

Scofield, S.R., Huang, L., Brandt, A.S., and Gill, B.S. (2005). Development of a virus-induced gene-silencing system for hexaploid wheat and its use in functional analysis of the Lr21-mediated leaf rust resistance pathway. Plant Physiology *138*, 2165-2173.

Sheard, L.B., and Zheng, N. (2009). Plant biology: Signal advance for abscisic acid. Nature *462*, 575-576.

Sievers, F., Wilm, A., Dineen, D., Gibson, T.J., Karplus, K., Li, W., Lopez, R., McWilliam, H., Remmert, M., Soding, J., *et al.* (2011). Fast, scalable generation of high-quality protein multiple sequence alignments using Clustal Omega. Molecular Systems Biology *7*, 539.

Snijders, C.H.A. (1990). *Fusarium* head blight and mycotoxin contamination of wheat, a review. Netherlands Journal of Plant Pathology *96*, 187-198.

Sobrova, P., Adam, V., Vasatkova, A., Beklova, M., Zeman, L., and Kizek, R. (2010). Deoxynivalenol and its toxicity. Interdisciplinary Toxicology *3*, 94-99.

Soding, J. (2005). Protein homology detection by HMM-HMM comparison. Bioinformatics *21*, 951-960.

Spence, C., and Bais, H. (2015). Role of plant growth regulators as chemical signals in plant-microbe interactions: a double edged sword. Current Opinions in Plant Biology *27*, 52-58.

Sperschneider, J., Gardiner, D., Taylor, J., Hane, J., Singh, K., and Manners, J. (2013). A comparative hidden Markov model analysis pipeline identifies proteins characteristic of cereal-infecting fungi. BMC Genomics *14*, 807.

Statistics Canada (2014). Table 001-0017 - Estimated areas, yield, production, average farm price and total farm value of principal field crops, in imperial units, annual, CANSIM (database). (accessed: 2014-12-29) (http://www.statcan.gc.ca/start-debut-eng.html).

Szostkiewicz, I., Richter, K., Kepka, M., Demmel, S., Ma, Y., Korte, A., Assaad, F.F., Christmann, A., and Grill, E. (2010). Closely related receptor complexes differ in their ABA selectivity and sensitivity. The Plant Journal *61*, 25-35.

Takeuchi, J., Ohnishi, T., Okamoto, M., and Todoroki, Y. (2015). Conformationally restricted 3'-modified ABA analogs for controlling ABA receptors. Organic and Biomolecular Chemistry *13*, 4278-4288.

Takeuchi, J., Okamoto, M., Akiyama, T., Muto, T., Yajima, S., Sue, M., Seo, M., Kanno, Y., Kamo, T., Endo, A., *et al.* (2014). Designed abscisic acid analogs as antagonists of PYL-PP2C receptor interactions. Nature Chemical Biology *10*, 477-482.

Tamura, K., Stecher, G., Peterson, D., Filipski, A., and Kumar, S. (2013). MEGA6: molecular evolutionary genetics analysis version 6.0. Molecular Biology and Evolution *30*, 2725-2729.

Trail, F. (2009). For blighted waves of grain: *Fusarium graminearum* in the postgenomics era. Plant Physiology *149*, 103-110.

Umezawa, T., Sugiyama, N., Mizoguchi, M., Hayashi, S., Myouga, F., Yamaguchi-Shinozaki, K., Ishihama, Y., Hirayama, T., and Shinozaki, K. (2009). Type 2C protein phosphatases directly regulate abscisic acid-activated protein kinases in *Arabidopsis*. Proceedings of the National Academy of Sciences of the United States of America *106*, 17588-17593.

Untergasser, A., Cutcutache, I., Koressaar, T., Ye, J., Faircloth, B.C., Remm, M., and Rozen, S.G. (2012). Primer3--new capabilities and interfaces. Nucleic Acids Research *40*, e115.

Wicker, T., Mayer, K.F., Gundlach, H., Martis, M., Steuernagel, B., Scholz, U., Simkova, H., Kubalakova, M., Choulet, F., Taudien, S., *et al.* (2011). Frequent gene movement and

pseudogene evolution is common to the large and complex genomes of wheat, barley, and their relatives. Plant Cell *23*, 1706-1718.

Wilkinson, P.A., Winfield, M.O., Barker, G.L., Allen, A.M., Burridge, A., Coghill, J.A., and Edwards, K.J. (2012). CerealsDB 2.0: an integrated resource for plant breeders and scientists. BMC Bioinformatics *13*, 219.

Xu, Y., Chang, P., Liu, D., Narasimhan, M.L., Raghothama, K.G., Hasegawa, P.M., and Bressan, R.A. (1994). Plant defense genes are synergistically induced by ethylene and methyl jasmonate. The Plant Cell *6*, 1077-1085.

Yuan, C., Li, C., Yan, L., Jackson, A.O., Liu, Z., Han, C., Yu, J., and Li, D. (2011). A high throughput barley stripe mosaic virus vector for virus induced gene silencing in monocots and dicots. PLoS One *6*, e26468.

Zaharia, L.I., Walker-Simmon, M., Rodríguez, C., and Abrams, S. (2005). Chemistry of abscisic acid, abscisic acid catabolites and analogs. Journal of Plant Growth Regulation *24*, 274-284.

Zhang, J.Z., Creelman, R.A., and Zhu, J.K. (2004). From laboratory to field. Using information from Arabidopsis to engineer salt, cold, and drought tolerance in crops. Plant Physiology *135*, 615-621.

Zhang, X., Jiang, L., Wang, G., Yu, L., Zhang, Q., Xin, Q., Wu, W., Gong, Z., and Chen, Z. (2013). Structural insights into the abscisic acid stereospecificity by the ABA receptors PYR/PYL/RCAR. PLoS One *8*, e67477.

Zhang, X.L., Jiang, L., Xin, Q., Liu, Y., Tan, J.X., and Chen, Z.Z. (2015). Structural basis and functions of abscisic acid receptors PYLs. Frontiers in Plant Science *6*, 88.

Zhao, Y., Chan, Z., Xing, L., Liu, X., Hou, Y.-J., Chinnusamy, V., Wang, P., Duan, C., and Zhu, J.-K. (2013). The unique mode of action of a divergent member of the ABA-receptor protein family in ABA and stress signaling. Cell Research *23*, 1380-1395.

Zhu, S.Q., Chen, M.W., Ji, B.H., Jiao, D.M., and Liang, J.S. (2011). Roles of xanthophylls and exogenous ABA in protection against NaCl-induced photodamage in rice (*Oryza sativa L*) and cabbage (*Brassica campestris*). Journal of Experimental Botany *62*, 4617-4625.

Zhuang, Y., Gala, A., and Yen, Y. (2012). Identification of functional genic components of major *Fusarium* head blight resistance quantitative trait loci in wheat cultivar Sumai 3. Molecular Plant-Microbe Interactions *26*, 442-450.

Zuckerkandl, E., and Pauling, L. (1965). Molecules as documents of evolutionary history. Journal of Theoretical Biology *8*, 357-366.

6.0 Appendix

6.1 Putative Wheat ABA Receptors

>TaPYL5.1 (gi|241988461)

ATGCCGACGCCGTACAGCGCGGCGGCGCTGCAGCAGCACCAGCGTCTGGTCTCCTC

CTCCGGCGGCCTGGCGGCGACGGGGGCCCACAGGTGCGGCGAGCACGACGGGACG

GTGCCGCCGGAGGTGGCGCGGCACCACGAGCACGCGGCGCCGGGGGGGCGCTGCTG

CTGCTCGGCGGTGGTGCAGCGCGTGGCGGCGCCGGCGGCGGACGTGTGGGCCGTGG

TCCGGCGCTTCGACCAGCCGCAGGCGTACAAGAGCTTCGTGCGCAGCTGCGCGCTG

CTGGACGGCGACGGCGGCGTGGGCACGCTGCGCGAGGTGCGCGTGGTGTCGGGCCT

CCCCGCGGCGTCCAGCCGGGAGCGGCTGGAGATCCTGGACGACGAGCGGCACGTGC

TGAGCTTCAGCGTGGTGGGCGGCGAGCACCGGCTCCGCAACTACCGGTCGGTGACC

ACGGTGCACCCGGCGCCGGGGGAGAGCGCGTCGGCGACGCTGGTGGTGGAGTCGTA

CGTGGTGGACGTGCCCCCCGGGAACACGCCCGAGGACACCCGCGTCTTCGTGGACA

CCATCGTCAAGTGCAACCTCCAGTCCCTCGCCCGCACCGCCGAGAAGCTCGCCGGCC

GGGGGGCGGCCTACGGCGCGCTGCCGTGA

>TaPYL5.1D

GTGGGCGGCGAGCACCGGCTCCGCAACTACCGGTCGGTGACCACGGTGCACCCGGC

GCCGGGGGAGAGCGCGTCGGCGACGCTGGTGGTGGAGTCGTACGTGGTGGACGTGC

CCCCCGGGAACACGCCCGAGGACACCCGCGTCTTCGTGGACACCATCGTCAAGTGC

AACCTCCAGTCCCTCGCCCGCACCGCCGAGAAGCTCGCCGGCCGGGGGGCGGCCTA

CGGCGCGCTGCCGTGA

>TaPYL5.1B

GATCACGGCAGCGCGCCGTAGGCCGCCCCTCGGCCGGCGAGCTTCTCGGCGGTGCG

GGCGAGGGACTGGAGGTTGCACTTGACGATGGTGTCCACGAACACGCGGGTGTCCT

CGGGGGTGTTCCCGGGGGGCACGTCCACCACGTACGACTCCACCACCAGCGTGGCC

GACGCGCTCCCCCCCGGCGCCGGGTGCACCGTGGTCACCGACCGGTAGTTGCGGAG

CCGGTGCTCGCCGCCCACCACGCTGAAGCTCAGCACGTG

>TaPYL5.2A

ATGCCGTGCATCCCGGCGTCCAGCCCCAGCATCCAGCACCACAACCACCACCACAG

AGTCCTAGCAGGCGTCGGCATGGGGTGCGGCGCGGAGGCGGTCGTGGCCGCGGCCG

GGACGGCAGGGATGAGGTGCAGGGAGCACGACTGCGAGGTCCCGGCGGAGGTGGC

GCGGCACCACGAGCACGCGGAGCCGGGGTCCGGCCAGTGCTGCTCCGCGGTGGTGC

AGCACGTGGCGGCGCCCGCGGCGGCGGTGTGGTCCGTGGTGCGCCGGTTCGACCAG

CCGCAGGCGTACAAGCGGTTCGTCCGCAGCTGCGCCCTGGTGGCCGGTGACGGCGG

CGTGGGCACGCTCCGCGAGGTGCACGTCGTGTCGGGCCTCCCCGCGGCGTCCAGCC

GCGAGCGGCTCGAGATCCTGGACGACGAGAGCCACGTGCTCAGCTTCCGCGTCGTC

GGCGGGGAGCACCGGCTCAAGAACTACCTCTCCGTCACCACCGTGCACCCATCCCC

GGCCGCGCCGTCCAGCGCCACCGTCGTCGTGGAGTCGTACGTCGTGGACGTGCCCGC

GGGCAACACGACCGAGGACACCCGCGTGTTCATCGACACCATCGTCAAGTGCAACC

TCCAGTCGCTGGCCAAGACCGCCGAGAAGGTCGCCGCCGTGTCGTGA

>TaPYL5.2B

ATGCCGTGCATCCCGGTGTCCAGCCCCAGCATCCAGCACCACAACCACAACCACCA

CCACCGAGTCCTAGCAGGCGTCGGCGTCGGCATGGGGTGCGGCGCGGAGGCGGTCG

TTGCCGCGGCCGGGACGGCAGGGATGAGATGCAGGGAGCACGACTGCGAGGTCCCG
GCGGAGGTGGCGCGGCACCACGAGCACGCGGAGCCGGGGTCCGGCCAGTGCTGCTC
CGCGGTGGTGCAGCACGTGGCGGCGCCCGCGGCGGCGGTGTGGTCCGTGGTGCGCC
GGTTCGACCAGCCGCAGGCGTACAAGCGGTTCGTGCGCAGCTGCGCCCTGGTGGCC
GGCGACGGCGGCGTGGGCACGCTCCGCGAGGTGCACGTCGTGTCGGGCCTTCCCGC
GGCGTCCAGCCGCGAGCGGCTCGAGATCCTGGACGACGAGAGCCACGTGCTCAGCT
TCCGCGTCGTCGGTGGCGAGCACCGGCTCAAGAACTACCTCTCCGTCACCACCGTCC
ACCCGTCCCCGGCCGCGCCGTCCAGCGCCACCGTCGTCGTGGAGTCGTACGTCGTGG
ACGTGCCGGCGGGCAACACGATCGAGGACACCCGCGTGTTCATCGACACCATCGTC
AAGTGCAACCTCCAGTCGCTGGCCAAGACCGCCGAGAAGCTCGCCGCCGTGTCGTG
A

>TaPYL5.2D

ATGCCGTGCATCCCGGCGTCCAGCCCCAGCATCCAGCACCACAACCACAACCACCA
CCACCGAGTCCTAGCGGGCGTTGGCGTCGGCATGGGGTGCGGCGCGGAGGCGGTCG
TGGCCGCGGCCGGGACGGCAGGGATGAGGTGCAGGGAGCACGACTGCGAGGTCCC
GGCGGAGGTGGCGCGGCACCACGAGCACGCGGAGCCGGGGTCCGGCCAGTGCTGCT
CCGCGGTGGTGCAGCACGTGGCGGCGCCCGCGGCGGCGGTGTGGTCCGTGGTGCGC
CGGTTCGACCAGCCGCAGGCGTACAAGCGGTTCGTGCGCAGCTGCGCCCTGGTGGC
CGGCGACGGCGGCGTGGGCACGCTCCGCGAGGTGCACGTCGTGTCGGGCCTCCCCG
CGGCGTCCAGCCGCGAGCGGCTCGAGATCCTGGACGACGAGAGCCACGTGCTCAGT
TTCCGCGTCGTCGGTGGCGAGCACCGGCTCAAGAACTACCTCTCCGTCACCACCGTC
CACCCGTCCCCAGCCGCGCCGTCCAGCGCCACCGTCGTCGTGGAGTCCTACGTCGTG
GACGTGCCGGCGGGCAACACGATCGAGGACACCCGCGTGTTCATCGACACCATCGT

CAAGTGCAACCTCCAGTCGCTGGCCAAGACCGCCGAGAAGGTCGCCGCCGTGTCGT
GA

>TaPYL5.3

GAGCACGCGGCCGGCGCGGGGCAGTGCTGCTCGGCCGTGGTGCAGGCGATCGCGGC
GCCCGTGGAGGCGGTGTGGTCGGTCGTGCGGCGCTTCGACCGGCCGCAGGCGTACA
AGCGCTTCATCAAGAGCTGCGCTGTGGA
CGGCGACGGCGGCGCGGTGGGGTCGGTGCGGGAGGTGCGCGTGGTCTCCGGCCTGC
CCGGCACCAGCAGCCGCGAGCGGCTCGAGATCCTGGACGACGAGCGGCGCGTGCTC
AGCTTCCGGATCGTCGGCGGCGAGCACCGCCTCGCCAACTACCGGTCCGTGACCACC
GTGAGCGAGGTGGCGTCGACGGTGGCCGGGGCGCCGCGGGTGACCCTGGTGGTCGA
GTCGTACGTGGTGGACGTGCCGCCGGGGAACACCAGCGACGAGACGCGCCTGTTCG
TGGACACCATCGTGCGGTGCAACCTCCAGTCGCT

>TaPYL5.4

CTCACGACACGGCGGCGACCTTCTCGGCGGTCTTGGCCAGCGACTGGAGGTTGCACT
TGACGATGGTGTCGATGAACACGCGGGTGTCCTCGATCGTGTTGCCCGCCGGCACGT
CCACGACGTACGACTCCACGACGACGGTGGCGCTGGACGGCGCGGCCGGGGACGGG
TGGACGGTGGTGACGGAGAGGTAGTTCTTGAGCCGGTGCTCGCCACCGACGACGCG
GAAGCTGAGCACGTGGCTCTCGTCGTCCAGGATCTCGAGCCGCTCGCGGCTGGACG
CCGCGGGAAGGCCCGACACGACGTGCACCTCGCGGAGCGTGCCCACGCCGCCGTCG
CCGGCCACCAGGGCGCAGCTGCGCACGAACCGCTTGTACGCCTGCGGCTGGTCGAA
CCGGCGCACCACGGACCACACCGCCGCCGCGGGCGCCGCCACGTGCTGCACCACCG

CGGAGCAGCACTGGCCGGACCCCGGCTCCGCGTGCTCGTGGTGCCGCGCCACCTCC

GCCGGGACCTCGCAGTCGTGCTCCCTGCACCTCAT

>TaPYL4.1

CGAAGGTGCGCGTCTCGTCGGCGGTGTTCCCGGGGGGCACGTCCACCACGTACGAC

TCCACCACGACGGCGCCGCCGACGCGGCCTCGTGCACGGTGGTCACCGACCGATAG

TTGGAGAGGCGGTGCTCGCCGCCGACGACGCGGAAGCTGAGCACGCGGCGCTCGTC

GTCGAGGATCTCCAGCCGCTCGCGGCTGCTGGTGGCGGGGAGGCCCGACACCACCC

GCACCTCGCGCACCGACCCCACCGCGCCGCCGTCGCCGTCCACGACGCGGCAGCTC

CGGATGAAGTGCTTGTACGCCTGCGGGCGGTCGAAGCGCCGCACCACGGCCCACAC

CGCGCCCACGGGCGCCTCGATCGCCTGCACCACCGCCGAGCAGCACTGCCCGGTAC

CCGCCGCGTGCTCGTGGTGCCGCGCCACCTCCCCCGGCACCGCCCCGCACGACGCCG

CGTGCGCCGCCGCCTTCCACCCCGCGCCCACCGCGGCGACCGAGCCCGCTGCGGCG

CCGACGGCCGCGATGCCGTGTACGGCATTATACACTCTCGCTGTACC

>TaPYL4.2

ATGCCGACGCCGTACAGCGCGGCGGCGCTGCAGCAGCACCACCGTCTGGTCTCCTCC

TCCGGCGGCCTGGCGACGGCGGCGGCCGCGGGGGCCCACAGGTGCGGCGAGCACG

ACGGGACGGTGCCGCCGGAGGTGGCGCGGCACCACGAGCACGCGGCGCCGGGGGG

CCGCTGCTGCTGCTCGGCGGTGGTGCAGCGCGTGGCGGCGCCCGCGGCGGACGTGT

GGGCCGTGGTCCGGCGCTTCGACCAGCCGCAGGCGTACAAGAGCTTCGTGCGCAGC

TGCGCGCTGCTGGACGGCGACGGCGGCGTGGGCACGCTGCGGGAGGTGCGCGTGGT

GTCGGGCCTCCCCGCGGCGTCCAGCCGGGAGCGGCTGGAGATCCTGGACGACGAGC

GGCACGTGCTGAGCTTCAGCGTGGGCGAGCACCGGCTCCGCAACCGCAAT

>TaPYL1

GCAGCGGAGCCGGAGGTACCGGCGGGGCTTGGGCTGACGGCCGCGGAGTACGCGC

AGCTGCTGCCCACGGTGGAGGCGTACCACCGGTACGCCGTGGGGCCAGGCCAATGC

TCCTCGCTCGTGGCGCAGCGTATCGAGGCGCCGCCAGCCGCCGTCTGGGCCATCGTC

CGCCGCTTTGACTGCCCCCAGGTGTACAAGCACTTCATCCGCAGCTGCGCGCTCCGC

CCGGACCCCGAGGCCGGCGACGAGCTCCGCCCGGGCCGCCTCCGCGAGGTCAGCGT

CATCTCCGGCCTCCCCGCCAGCACCAGCACCGAGCGCCTCGACCTCCTGGACGACGC

GCGCAGGGCCTTCGGCTTCACCATCACCGGCGGCGAGCACCGCCTCCGCAACTACC

GGTCCGTCACCACCGTCTCCGAGCTCTCCCCGGCCGCGCCCGCCGAGATCTGCACCG

TCGTTCTTGAGTCCTACGTCGTCGACGTCCCCGACGGCAACAGCGAGGAGGACACG

CGCCTCTTCGCGGACACCGTCGTCAGGCTCAACCTCCAGAAGCTCAAGTCCGTCGCC

GAGGCCAACGCCGCCGCCGCCGCGGCCACGCCCGCGCCGCCGGCAGAATAA

>TaPYR1

GCCGTCTGGGCCATCGTCCGCCGCTTCGACTGCCCCCAGGTGTACAAGCACTTCATC

CGCAGCTGCGCGCTCCGCCCGGACCCCGAGGCCGGCGACGAGCTCCGCCCGGGCCG

CCTCCGCGAGGTCAGCGTCATCTCCGGCCTCCCCGCCAGCACCAGCACCGAGCGCCT

CGACCTCCTCGACGACGCGCGCAGGGCCTTCGGCTTCACCATCACCGGCGGCGAGC

ACCGCCTCCGCAACTACCGGTCCGTCACCACCGTCTCCGAGCTCTCCCCGGCCGCGC

CCGCCGAGATCTGCACCGTCGTTCTTGAGTCCTACGTCGTCGACGTCCCCGACGGCA

ACAGCGAGGAGGACACGCGCCTCTTCGCGGACACCGTCGTCAGGCTCAACCTCCAG
AAGCTCAAGTCCGTCGCCGAGGCCAACGCCGCCGCCGCCGCGGCCACGCCCGCGCC
GCCGGCAGAATAA

>TaPYL2 (gi|669028527)

ATGGAGCCCCACATGGAGAGCGCGCTCCGTCAAGGGTTGACGGAGCCGGAGCGGAG
GGAGGTGGAGGGCGTGGTGGAGGAGCACCACACATTCCCTGGGCGCGCCAGCGGG
ACGTGCACATCGCTGGTCACACAGCGCGTGCAGGCGCCTCTCGCCGCCGTGTGGGA
CATCGTGCGCGGCTTCGCCAATCCGCAGCGCTACAAGCACTTCATCAAGTCCTGTGC
TCTCGCCGCCGGCGACGGCGCCACCGTGGGCAGCGTCCGCGAGGTCACCGTCGTCT
CCGGCCTCCCCGCCTCCACCAGCACCGAGCGCCTCGAGATCCTCGACGACGACCGCC
ACATCCTCAGCTTCCGCGTCGTCGGCGGCGAGCACCGCCTCCGCAACTACCGCTCCG
TCACCTCCGTCACCGAGTTCACGGACCAGCCTTCAGGCCCGTCCTACTGCGTCGTTG
TCGAGTCCTACGTCGTCGACGTACCGGAGGGCAACACCGAGGAGGACACCCGCATG
TTCACCGACACCGTGGTCAAGCTCAACCTCCAGAAACTCGCCGCCATCGCTACCACC
ACCACCACCTCTTCCCCACCGCCGTCGGATGAGCAAAGCTGA

6.2 VIGS Control Construct Sequences

>GFP

GACGACGGCAACTACAAGACCCGCGCCGAGGTGAAGTTCGAGGGCGACACCCTGGT
GAACCGCATCGAGCTGAAGGGCATCGACTTCAAGGAGGACGGCAACATCCTGGGGC
ACAAGCTGGAGTACAACTACAACAGCCACAACGTCTATATCATGGTCGACAAGCAG
AAGAACGGCATCAAGGTGAACTTCAAGATCCGCCAC

>PDS

TTTCTCCAGGAGAAGCATGGCTCGAAAATGGCATTCTTGGATGGTAATCCTCCTGAA

AGGCTATGCATGCCTATTGTTAACCACATTCAGTCTTTGGGTGGTGAGGTCCGGCTG

AATTCTCGTATTCAGAAAATTGAACTGAACCCTGACGGAACAGTGAAGCACTTTGCA

CTTACTGATGGGACTCAAATAACTGGAGA

6.3 Alignment of VIGS Sequence with Genomic Targets

```
BSMVγLIC-PYL5.2A      ----------------------------------------GGAAGTTTAAGCTGGAGATC
TaPYL5.2A             CGCGAGGTGCACGTCGTGTCGGGCCTCCCCGCGGCGTCCAGCCGCGAGCGGCTCGAGATC
TaPYL5.2B             CGCGAGGTGCACGTCGTGTCGGGCCTTCCCGCGGCGTCCAGCCGCGAGCGGCTCGAGATC
TaPYL5.2D             CGCGAGGTGCACGTCGTGTCGGGCCTCCCCGCGGCGTCCAGCCGCGAGCGGCTCGAGATC
                                                       *         *** ******

BSMVγLIC-PYL5.2A      CTGGACGACGAGAGCCACGTGCTCAGTTTCCGCGTCGTCGGTGGCGAGCACCGGCTCAAG
TaPYL5.2A             CTGGACGACGAGAGCCACGTGCTCAGCTTCCGCGTCGTCGGCGGGGAGCACCGGCTCAAG
TaPYL5.2B             CTGGACGACGAGAGCCACGTGCTCAGCTTCCGCGTCGTCGGTGGCGAGCACCGGCTCAAG
TaPYL5.2D             CTGGACGACGAGAGCCACGTGCTCAGTTTCCGCGTCGTCGGTGGCGAGCACCGGCTCAAG
                      ************************* ************** ** ***************

BSMVγLIC-PYL5.2A      AACTACCTCTCCGTCACCACCGTCCACCCGTCCCCAGCCGCGCCGTCCAGCGCCACCGTC
TaPYL5.2A             AACTACCTCTCCGTCACCACCGTGCACCCATCCCCGGCCGCGCCGTCCAGCGCCACCGTC
TaPYL5.2B             AACTACCTCTCCGTCACCACCGTCCACCCGTCCCCGGCCGCGCCGTCCAGCGCCACCGTC
TaPYL5.2D             AACTACCTCTCCGTCACCACCGTCCACCCGTCCCCAGCCGCGCCGTCCAGCGCCACCGTC
                      ********************** ***** ***** ************************

BSMVγLIC-PYL5.2A      GTCGTGGAGTCCTACGTCGTGGACGTGCCGGCGGGCAACACGATCGAGGACACCCGCGTG
TaPYL5.2A             GTCGTGGAGTCGTACGTCGTGGACGTGCCCGCGGGCAACACGACCGAGGACACCCGCGTG
TaPYL5.2B             GTCGTGGAGTCGTACGTCGTGGACGTGCCGGCGGGCAACACGATCGAGGACACCCGCGTG
TaPYL5.2D             GTCGTGGAGTCCTACGTCGTGGACGTGCCGGCGGGCAACACGATCGAGGACACCCGCGTG
                      *********** ***************** ************* ****************

BSMVγLIC-PYL5.2A      TTCATCGACACCATCGTCAAGTGCAACACGGTGGTGGTGG--------------------
TaPYL5.2A             TTCATCGACACCATCGTCAAGTGCAACCTCCAGTCGCTGGCCAAGACCGCCGAGAAGGTC
TaPYL5.2B             TTCATCGACACCATCGTCAAGTGCAACCTCCAGTCGCTGGCCAAGACCGCCGAGAAGCTC
TaPYL5.2D             TTCATCGACACCATCGTCAAGTGCAACCTCCAGTCGCTGGCCAAGACCGCCGAGAAGGTC
                      *************************     *  * ***
```

6.4 Percent Identity Matrix of Clade II ABA Receptors

	CaPYL4.4*	TaPYL5.1B*	TaPYL5.1	TaPYL5.1D*	OsPYL6	TaPYL5.2A*	TaPYL5.2B*	TaPYL5.2D*	AtPYL4	SlPYL6*	VvPYL4.2*	SlPYL4*	StPYL4*	VvPYL4*	CaPYL4.3*	FvPYL4*	AtPYL6	AtPYL5	CaPYL4.2*	CaPYL4*	GmPYL4*	FvPYL6.2*	OsPYL5	BdPYL5*	OsPYL4	TaPYL5.3*	TaPYL5.4*	AtPYL13	AtPYL11	AtPYL12	VvPYL6*	GmPYL6*	GmPYL12*	FvPYL6*	FvPYL11*	FvPYL11.2*
CaPYL4.4*	100.0	67.9	53.5	64.9	53.4	54.0	53.7	53.7	61.3	60.6	61.7	61.0	62.1	61.3	71.0	59.8	52.5	59.8	60.0	60.1	58.8	59.5	53.0	49.8	66.7	64.8	54.1	49.4	51.3	50.3	48.6	46.1	45.6	51.5	52.2	45.0
TaPYL5.1B*	67.9	100.0	98.8	98.7	79.8	78.5	79.8	78.5	67.1	64.6	72.8	68.8	68.8	69.1	71.8	67.9	63.3	69.4	69.3	72.2	76.1	69.2	70.4	64.7	76.7	72.7	70.4	52.0	53.3	57.9	43.4	43.9	43.9	53.8	53.4	54.0
TaPYL5.1	53.5	98.8	100.0	100.0	75.9	75.4	74.4	73.9	58.3	55.4	59.8	60.2	59.7	58.7	67.6	57.7	51.5	58.1	60.6	56.7	62.4	57.9	66.0	60.6	74.0	74.5	64.8	50.0	54.4	54.1	44.7	44.4	44.4	49.7	51.6	45.6
TaPYL5.1D*	64.9	98.7	100.0	100.0	79.2	77.8	79.2	77.8	65.3	62.5	68.9	67.1	67.1	66.2	71.8	66.2	61.1	69.2	67.7	69.2	73.4	64.8	68.9	65.4	78.8	74.6	71.6	52.9	54.3	60.9	42.1	42.7	44.0	54.8	54.6	56.5
OsPYL6	53.4	79.8	75.9	79.2	100.0	86.8	86.2	86.2	57.1	53.5	56.9	57.7	57.2	56.1	65.9	56.1	51.9	54.8	53.3	53.0	57.2	55.2	63.8	60.4	76.0	75.2	63.8	53.9	55.1	54.8	46.3	44.4	45.0	50.3	52.8	42.8
TaPYL5.2A*	54.0	78.5	75.4	77.8	86.8	100.0	98.6	99.6	59.7	54.1	59.7	56.8	56.3	57.7	65.9	56.6	53.4	54.8	54.7	55.6	59.4	58.0	64.0	62.1	74.0	73.8	63.6	52.6	56.1	54.8	48.6	46.9	46.9	51.2	54.1	43.7
TaPYL5.2B*	53.7	79.8	74.4	79.2	86.2	98.6	100.0	99.1	59.1	53.0	59.5	56.3	55.8	57.1	65.9	57.0	52.9	54.3	54.4	54.5	58.7	57.4	63.6	61.4	74.7	73.8	62.9	52.6	55.4	54.8	48.6	46.9	46.9	51.2	54.1	43.8
TaPYL5.2D*	53.7	78.5	73.9	77.8	86.2	99.6	99.1	100.0	59.1	53.0	59.0	56.3	55.8	57.1	65.3	56.5	52.9	54.3	54.4	55.0	58.7	57.4	63.1	61.4	74.0	73.8	62.9	52.6	56.1	54.8	48.6	46.9	46.9	51.2	54.1	43.8
AtPYL4	61.3	67.1	58.3	65.3	57.1	59.7	59.1	59.1	100.0	67.0	66.5	67.9	67.4	69.6	76.5	69.4	60.7	60.1	64.2	66.8	68.8	63.8	56.9	55.3	68.0	68.8	59.5	51.3	56.3	55.4	48.9	46.0	46.6	54.5	55.1	48.7
SlPYL6*	60.6	64.6	55.4	62.5	53.5	54.1	53.0	53.0	67.0	100.0	65.8	76.4	76.9	70.7	74.7	66.2	58.7	58.3	67.8	64.4	66.0	65.1	55.1	52.3	65.3	66.7	54.9	48.7	56.3	55.4	47.2	46.9	46.9	52.7	52.2	47.1
VvPYL4.2*	61.7	72.8	59.8	68.9	56.9	59.7	59.5	59.0	66.5	65.8	100.0	68.4	68.4	73.6	73.6	68.2	56.7	61.4	66.0	65.3	67.2	70.0	58.3	56.0	68.0	68.1	59.7	51.9	55.7	56.7	48.6	46.9	46.9	53.9	55.4	50.3
SlPYL4*	61.0	68.8	60.2	67.1	57.7	56.8	56.3	56.3	67.9	76.4	68.4	100.0	97.2	73.1	76.4	68.3	58.9	58.4	65.6	66.3	67.0	68.0	57.1	57.1	68.7	70.1	60.7	47.8	53.9	52.6	47.5	46.0	46.0	53.6	51.6	45.2
StPYL4*	62.1	68.8	59.7	67.1	57.2	56.3	55.8	55.8	67.4	76.9	68.4	97.2	100.0	73.1	77.0	68.3	59.9	58.4	65.6	66.3	67.0	68.5	56.2	57.1	68.0	70.1	60.2	47.8	53.9	53.2	48.1	46.6	46.6	51.8	50.3	45.2
VvPYL4*	61.3	69.1	58.7	66.2	56.1	57.7	57.1	57.1	69.6	70.7	73.6	73.1	73.1	100.0	79.9	73.1	60.1	59.3	65.6	66.5	68.8	69.5	58.4	56.1	68.7	70.1	59.7	51.3	55.7	54.1	47.9	46.9	46.9	55.1	53.5	50.3
CaPYL4.3*	71.0	71.8	67.6	71.8	65.9	65.9	65.9	65.3	76.5	74.7	73.6	76.4	77.0	79.9	100.0	79.4	63.3	64.3	68.7	71.7	73.8	70.5	65.1	62.0	68.0	68.5	64.3	51.3	55.1	54.8	49.7	51.1	51.1	51.5	52.2	52.0
FvPYL4*	59.8	67.9	57.7	66.2	56.1	56.6	57.0	56.5	69.4	66.2	68.2	68.3	68.3	73.1	79.4	100.0	58.5	57.6	64.2	63.4	67.4	64.0	56.1	53.4	66.2	66.2	57.6	51.6	55.4	55.1	48.1	47.5	48.1	53.6	54.4	48.2
AtPYL6	52.5	63.3	51.5	61.1	51.9	53.4	52.9	52.9	60.7	58.7	56.7	58.9	59.9	60.1	63.3	58.5	100.0	55.8	60.9	60.5	60.6	58.3	53.5	52.9	66.0	64.2	57.2	54.1	56.9	56.6	52.0	49.4	48.9	51.2	53.1	46.6
AtPYL5	59.8	69.4	58.1	69.2	54.8	54.8	54.3	54.3	60.1	58.3	61.4	58.4	58.4	59.3	64.3	57.6	55.8	100.0	60.4	59.9	61.2	60.4	55.9	56.0	68.3	66.4	58.7	49.4	54.0	54.6	49.1	46.4	47.0	53.1	50.3	43.9
CaPYL4.2*	60.0	69.3	60.6	67.7	53.3	54.7	54.4	54.4	64.2	67.8	66.0	65.6	65.6	65.6	68.7	64.2	60.9	60.4	100.0	74.6	75.3	66.2	56.2	57.5	66.7	69.0	61.3	45.5	52.9	51.0	49.1	47.0	48.2	50.3	49.4	44.3
CaPYL4*	60.1	72.2	56.7	69.2	53.0	55.6	54.5	55.0	66.8	64.4	65.3	66.3	66.3	66.5	71.7	63.4	60.5	59.9	74.6	100.0	81.8	65.5	56.6	54.6	66.7	66.9	60.1	48.7	55.3	54.7	50.3	49.4	49.4	53.2	53.0	44.2
GmPYL4*	58.8	76.1	62.4	73.4	57.2	59.4	58.7	58.7	68.8	66.0	67.2	67.0	67.0	68.8	73.8	67.4	60.6	61.2	75.3	81.8	100.0	68.3	59.4	60.9	71.2	69.7	62.3	50.0	56.6	55.3	54.1	49.4	50.6	56.5	55.8	49.2
FvPYL6.2*	59.5	69.2	57.9	64.8	55.2	58.0	57.4	57.4	63.8	65.1	70.0	68.0	68.5	69.5	70.5	64.0	58.3	60.4	66.2	65.5	68.3	100.0	59.4	57.4	66.9	68.3	61.3	51.6	55.4	56.3	51.1	50.3	50.9	56.9	55.1	50.3
OsPYL5	53.0	70.4	66.0	68.9	63.8	64.0	63.6	63.1	56.9	55.1	58.3	57.1	56.2	58.4	65.1	56.1	53.5	55.9	56.2	56.6	59.4	59.4	100.0	72.8	85.0	85.7	79.5	47.5	54.4	53.5	48.9	45.0	45.0	47.9	51.9	45.5
BdPYL5*	49.8	64.7	60.6	65.4	60.4	62.1	61.4	61.4	55.3	52.3	56.0	57.1	57.1	56.1	62.0	53.4	52.9	56.0	57.5	54.6	60.9	57.4	72.8	100.0	81.3	84.0	72.8	50.3	56.3	54.4	48.4	44.8	44.8	46.2	52.5	46.1
OsPYL4	66.7	76.7	74.0	78.8	76.0	74.0	74.7	74.0	68.0	65.3	68.0	68.7	68.0	68.7	68.0	66.2	66.0	68.3	66.7	66.7	71.2	66.9	85.0	81.3	100.0	86.0	84.0	50.7	58.2	56.6	55.9	52.6	52.6	54.2	55.6	56.3
TaPYL5.3*	64.8	72.7	74.5	74.6	75.2	73.8	73.8	73.8	68.8	66.7	68.1	70.1	70.1	70.1	68.5	66.2	64.2	66.4	69.0	66.9	69.7	68.3	85.7	84.0	86.0	100.0	98.7	50.7	56.9	56.6	54.1	50.7	50.0	54.0	55.2	56.2
TaPYL5.4*	54.1	70.4	64.8	71.6	63.8	63.6	62.9	62.9	59.5	54.9	59.7	60.7	60.2	59.7	64.3	57.6	57.2	58.7	61.3	60.1	62.3	61.3	79.5	72.8	84.0	98.7	100.0	48.4	54.0	53.5	49.5	45.5	44.4	49.7	53.1	48.7
AtPYL13	49.4	52.0	50.0	52.9	53.9	52.6	52.6	52.6	51.3	48.7	51.9	47.8	47.8	51.3	51.3	51.6	54.1	49.4	45.5	48.7	50.0	51.6	47.5	50.3	50.7	50.7	48.4	100.0	63.7	65.4	51.9	51.3	51.9	52.8	52.3	57.0
AtPYL11	51.3	53.3	54.4	54.3	55.1	56.1	55.4	56.1	56.3	56.3	55.7	53.9	53.9	55.7	55.1	55.4	56.9	54.0	52.9	55.3	56.6	55.4	54.4	56.3	58.2	56.9	54.0	63.7	100.0	81.1	56.9	56.9	55.6	57.8	59.0	61.4
AtPYL12	50.3	57.9	54.1	60.9	54.8	54.8	54.8	54.8	55.4	55.4	56.7	52.6	53.2	54.1	54.8	55.1	56.6	54.6	51.0	54.7	55.3	56.3	53.5	54.4	56.6	56.6	53.5	65.4	81.1	100.0	55.1	55.7	57.0	59.1	57.4	60.5
VvPYL6*	48.6	43.4	44.7	42.1	46.3	48.6	48.6	48.6	48.9	47.2	48.6	47.5	48.1	47.9	49.7	48.1	52.0	49.1	49.1	50.3	54.1	51.1	48.9	48.4	55.9	54.1	49.5	51.9	56.9	55.1	100.0	59.1	59.1	58.0	59.0	55.7
GmPYL6*	46.1	43.9	44.4	42.7	44.4	46.9	46.9	46.9	46.0	46.9	46.9	46.0	46.6	46.9	51.1	47.5	49.4	46.4	47.0	49.4	49.4	50.3	45.0	44.8	52.6	50.7	45.5	51.3	56.9	55.7	59.1	100.0	93.5	61.0	66.5	59.6
GmPYL12*	45.6	43.9	44.4	44.0	45.0	46.9	46.9	46.9	46.6	46.9	46.9	46.0	46.6	46.9	51.1	48.1	48.9	47.0	48.2	49.4	50.6	50.9	45.0	44.8	52.6	50.0	44.4	51.9	55.6	57.0	59.1	93.5	100.0	61.5	64.6	59.6
FvPYL6*	51.5	53.8	49.7	54.8	50.3	51.2	51.2	51.2	54.5	52.7	53.9	53.6	51.8	55.1	51.5	53.6	51.2	53.1	50.3	53.2	56.5	56.9	47.9	46.2	54.2	54.0	49.7	52.8	57.8	59.1	58.0	61.0	61.5	100.0	73.3	72.5
FvPYL11*	52.2	53.4	51.6	54.6	52.8	54.1	54.1	54.1	55.1	52.2	55.4	51.6	50.3	53.5	52.2	54.4	53.1	50.3	49.4	53.0	55.8	55.1	51.9	52.5	55.6	55.2	53.1	52.3	59.0	57.4	59.0	66.5	64.6	73.3	100.0	76.4
FvPYL11.2*	45.0	54.0	45.6	56.5	42.8	43.7	43.8	43.8	48.7	47.1	50.3	45.2	45.2	50.3	52.0	48.2	46.6	43.9	44.3	44.2	49.2	50.3	45.5	46.1	56.3	56.2	48.7	57.0	61.4	60.5	55.7	59.6	59.6	72.5	76.4	100.0